Session II - B: Nanomaterials properties

Identification of Ductility Function in Titanium Nitride Nanocoating Deposited on Polycarbonate-urethane of Ventricular Assist Device

A. Milenin,[1] M. Kopernik,[1] S. Kąc,[1]
[1]AGH University of Science and Technology, Al. Mickiewicza 30, 30-059, Kraków, Poland

Abstract: The Polish left ventricular assist device (LVAD - RELIGA_EXT) will be made of thermoplastic polycarbonate-urethane (Bionate II) with deposited athrombogenic nano-coatings: gold (Au) and titanium nitride (TiN) (M.Kopernik *et al*.; 2014). The two scale solid numerical model developed in the Polish Artificial Heart Programme in Authors' FEM code was composed of a macro model of blood chamber and a micro model of TiN/Bionate II system (A.Milenin *et al*.; 2009). The input and validation data for the multiscale model was reached in tension test for Bionate II, nanoindentation test and inverse analysis for TiN. Due to the macro model validation, the results of a digital image correlation were compared with the FEM results computed on external surfaces of the blood chamber of LVAD (A.Milenin *et al*.; 2012).
However, a fracture occurrence has been observed on the boundary between the coating and the substrate in the LVAD. The FEA of stress and strain states in a micro and a macro scale models has confirmed the possibility of fracture (Figure 1). Consequently, the fracture criterion must be identified, what is the purpose of the present work. The tensile test in a micro chamber for the SEM has been performed in order to calibrate the fracture model of the TiN/Bionate II system for different thicknesses of deposited coating (Figure 2). Basing on experimental boundary conditions, the micro model of tension test has been developed in the Authors' FE code with implemented fracture criterion. The defined fracture criterion depend on effective strain and critical deformation function. The interpretation of micro tension test results has been done using the inverse algorithm. The FE models of tests were created for determination the conditions of fracture. The variation of values of critical deformation function in the test has been calculated in the stage of the test, in which the initiation of fracture has been occurred. The fracture parameter in each test has been computed. The difference between experimental and computed value of the fracture parameter at the moment of the fracture has been adopted as the objective function. The minimum of the objective function has been reached by a variation of the parameters of critical deformation function.
The micro scale model enriched with the fracture model enables the prediction of fracture and the comparison of different variants of macro and micro parameters of the LVADs.

Keywords: nanocoating, micro tension test, finite element method (FEM), fracture, ventricular assist device (VAD), titanium nitride (TiN).

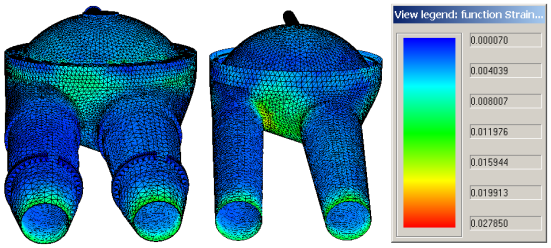

Figure 1: The distribution of strain intensity on external (left) and internal (right) surfaces of POLVAD-EXT chamber (temperature of chamber 25 C, P=37 kPa).

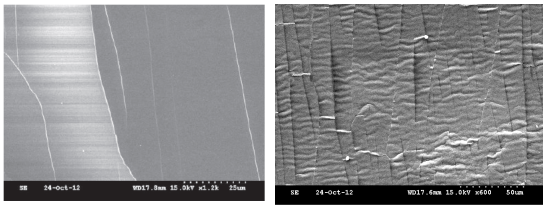

Figure 2: The SEM's image of 50 nm of TiN coating stretched 40 N (left) and 100 nm of TiN coating stretched 60 N (right) with fracture in TiN.

References:

A. Milenin and M. Kopernik, Multiscale FEM model of artificial heart chamber composed of nanocoatings, *Acta of Bioengineering and Biomechanics*, vol. 11, no. 2, pp. 13–20, 2009.

A.Milenin, M.Kopernik, D.Jurkojć, M. Gawlikowski, T. Rusin, M. Darłak, R. Kustosz, Numerical modelling and verification of polish ventricular assist device, *Acta of Bioengineering and Biomechanics*, 14/3 (2012) 49-57.

M. Kopernik, A. Milenin, S. Kąc, M. Wróbel, Stress-Strain analysis in TiN nanocoating deposited on polymer with respect to Au nanointerlayer // *Journal of Nanomaterials*, 2014, ID 813587, 1-12

Acknowledgements: Financial assistance from the Ministry of Science and High Education of Poland, project AGH no. 11.11.110.300 is acknowledged.

Diffusion of Proteins Through and Across Polyelectrolyte Multilayers

S.Pahal,[1] M.Varma,[1,2] A.M.Raichur[3]
[1]Centre for Nanoscience and Engineering, Indian Institue of Science, India
[2]Electrical Communication Engineering, Indian Institue of Science, India
[3]Materials Engineering, Indian Institue of Science, India

Abstract: Layer-by-layer assembly of polyelectrolytre multilayers (PEMs) is the most versatile approach for modifying surface as well as bulk properties of various substrates.This work explores the understanding of diffusion (lateral as well as transverse) of proteins across PEMs and how it can be modified by varying post assembly conditions. A weak PEM system has been selected as the model for these studies. Lateral diffusion studies are visualized by performing Florescence Recovery after Phtobleaching (FRAP) on these PEMs. FITC-labeled proteins have been used for these studies and lateral diffusion is measured by the bleached "hole filling" process as function of time. Transverse diffusion has also been studied by measuring the trasverse protein concentration distribution by using distance dependent fluorescence from fluorophores close to metal surfaces (Figure 1). Although Confocal laser scanning microscopy (CSLM) (Picart *et al.*, 2002) has been employed for diffusion studies across PEMs for the films having thickness in the range of micrometers, it is not suitable for probing PEMs thinner than around 500 nm. Therefore, X-ray photoelectron spectroscopy (XPS) (Jonathan *et al*, 2013) was recently utilized as a tool get transverse concentration profile of diffusing species in ultra-thin PEMs. Our protocol provides a simpler alternate approch to study the lateral diffusion as well as to extract the transverse concentration distribution in ultra-thin PEMs. This can be used a tool to understand the reservoir properties of PEMs and to get the detailed knowledge about the distribution and mobility of molecules acoss PEMs.

Keywords: Polyelectrolyte multilayers, layer-by-layer assembly, Fluorescence Recovery after Photobleaching (FRAP)

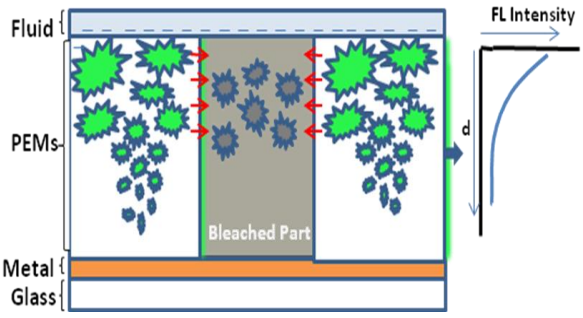

Figure 1: Schematic representing the overall approch for getting the detailed understanding of lateral as well as transverse diffusion across PEMs. Lateral diffusion is shown by movement of fluorphores from unbleached to bleached portion of PEMs and tranverse diffusion by the distance dependent fluorescence from FITC-labeled proteins in the PEM deposited on a metal surface. The temporal variation of fluorescnece intentsity can be fitted to extract the transverse distribution of fluorophores.

References:

Picart, C., Mutterer, J., Richert, L., Luo, Y., Prestwich, G. D., Schaaf, P., Voegel, J. C., Lavalle, P. (2002) Molecular basis for the explanation of the exponential growth of polyelectrolyte multilayers, *Proc. Natl. Acad. Sci. U.S.A.* 99, 12531-12535.

Jonathan, B. G., Michael, F. R., Robert, E. C.(2013) Depth-profiling X-ray photoelectron spectroscopy (XPS) analysis of interlayer diffusion in polyelectrolyte multilayers, *Proc. Natl. Acad. Sci. U.S.A*, 110,17, 6651–6656

Synthesis and Characterisation of Conjugated Polymer Nanoparticles for Fluorescence Imaging Applications

G. Redmond,[1,]
[1]University College Dublin, School of Chemistry & Chemical Biology, Dublin, Ireland.

Abstract: Recent developments in materials synthesis, bio-conjugation methods and luminescence techniques have led to a rapid proliferation of novel fluorescence-based approaches to imaging in the life sciences. However, for high-resolution or long-time duration imaging applications, molecular dyes suffer from limitations of low brightness, poor photostability and fluorescence intermittency (blinking). Likewise, emissive nanoparticles, e.g., semiconductor quantum dots (Q-dots) and dye-loaded latex or silica beads, are also un-optimised. Q-dots often require an inorganic shell with a thick encapsulation layer for stability and biocompatibility, and many batches exhibit low emission rates, blinking, and significant fractions of "dark" particles. Dye-loaded beads have relatively large sizes with limited dye-loading concentrations due to problems of aggregation and self-quenching.

Consequently, we are exploring a potentially promising alternative based on highly fluorescent conjugated polymer materials which are already in use as active layers in polymer light-emitting devices, and, in conjugated polyelectrolyte form, as solar cells. Conjugated polymer materials exhibit a range of attractive properties, including high absorption cross-sections, radiative rates, and effective chromophore densities along with minimal levels of aggregation-induced fluorescence quenching. Using conjugated polymers as an emissive nanoparticle material also eliminates small dye molecules or heavy metal ions that could leach out into solution.

We have developed a range of conjugated polymer nanoparticles based on fluorene co-polymers. These polymers are surface functionalized with different molar ratios of polyethylene glycol. By varying the preparation conditions, different sizes of nanoparticles can be prepared, resulting in smaller (20-50 nm) nanoparticles, produced by a reprecipitation method, and larger (90-110 nm) particles, produced by a solvent exchange method. These particles exhibit high absorption cross-sections (10^{-13}-10^{-12} cm^2), high quantum yield (≈ 50%) and well-resolved, size-independent absorption and fluorescence spectra across a broad wavelength range. Single particle fluorescence imaging studies indicate much higher emission rates (≈ 10^8 s^{-1}) and little or no blinking as compared with typical results reported for single dye molecules and Q-dots. Analysis of single nanoparticle photo-bleaching trajectories for some particles indicates excellent photo-stability with almost 10^8 photons emitted per nanoparticle prior to irreversible photo-bleaching. Finally, nanoparticles were incubated with L929 murine aneuploid fibrosarcoma and MCF-7 human breast adenocarcinoma cell lines, fixed, and counter-stained with nuclear dyes. Subsequent fluorescence microscopic imaging indicated that nanoparticles are readily internalized by the cells; see Figure above. Further studies are in progress to understand processes of their trafficking and localization within various cell types.

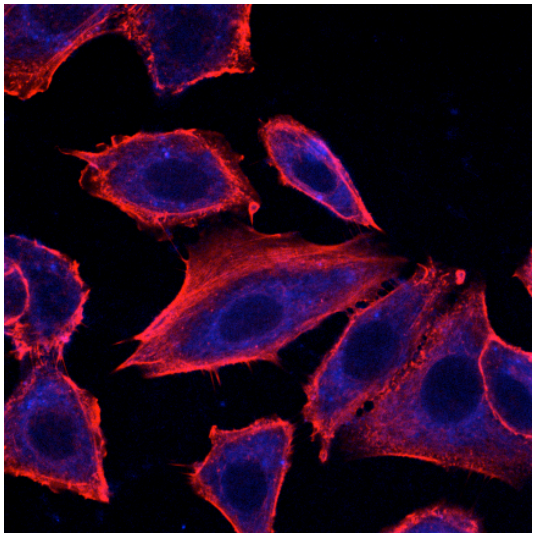

Figure: Polyfluorene nanoparticles (blue) in MCF-7 cells (red / phalloidin-TRITC).

Keywords: nanoparticles, colloidal dispersions, optical spectroscopy, fluorescence, non-blinking, photostability, brightness, cellular uptake.

The Role of DC and PRC Current Densities on the Sliding Wear of Electrodeposited Nickel-Cobalt /CNT Composite Coatings

Ramazan Karslioglu[1], Hatem Akbulut[1]
[1]Sakarya University, Engineering Faculty, Department of Metallurgical & Materials Engineering, Esentepe Campus, 54187, Sakarya/Turkey

Abstract: Surface properties are directly responsible for the performance of engineering materials because most of failures such as friction, wear, corrosion and fatigue often take place on the material surface. Electrodeposition technique is of great interest for industrial usage because it produces functional and protective coatings with low cost and easy control[1, 2]. In the Ni and Ni-Co metal matrix composites, when carbon nanotubes (CNTs) are selected as the third phase, because carbon nanotubes possess many remarkable properties such as high strength and elastic modulus, good flexibility, and unique conductivity[3].

In the present work, Nickel-Cobalt alloys and Nickel-Cobalt /Carbon nanotube composite coatings were prepared under direct current (DC) and pulse reverse current (PRC) methods. The microstructure of coatings was characterized by means of Scanning Electron Microscopy (SEM), X-Ray Diffraction (XRD) analysis and 3D profilometry facilities. One of the example showing co-deposition of MWCNTs with Ni,-Co is shown Fig. 1. The effect of current density and the current type on the co-deposited carbon nanotube content, microstructure and sliding wear properties were investigated. The results showed that the microstructure and performance of the coatings were greatly affected by current density, carbon nanotube content and the electrodeposition current type. Dispersion of the multiwalled carbon nanotubes (MWCNTs) into the Ni-Co matrix structure resulted in improving wear resistance performance of the Ni-Co electrodeposited coatings. This increment was attributed to the unique effect of the MWCNTs on load bearing ability and self lubrication between the friction surfaces. Introducing MWCNT into the Ni-Co matrix by co-electrodeposition resulted in wear mechanism change and decreased the real contact area since MWCNT dispersion causes to increase the surface roughness (Fig. 2). Among the studied electrodeposition techniques, PRC technique showed best features compared with the DC technique.

Keywords: Reverse Pulse electrodeposition; Ni-Co/MWCNT nanocomposites; surface roughness; reciprocating wear; wear mechanisms

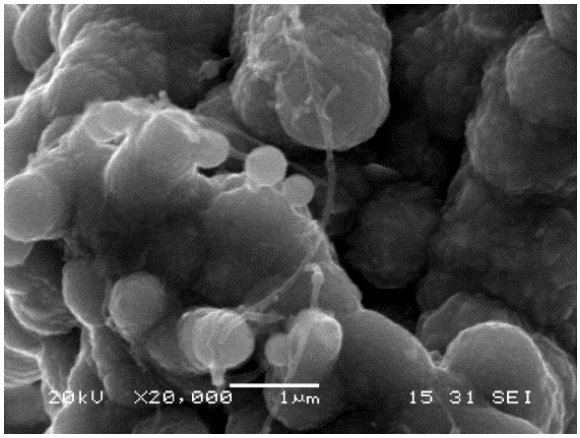

Fig.1. SEM surface structure of co-deposited Ni-Co/MWCNT composite.

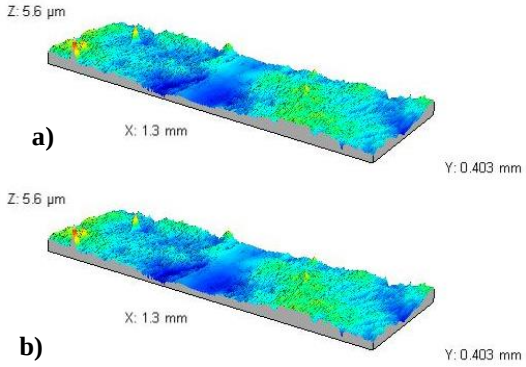

Fig. 2. 3D surface profilometry results of the a) Ni-Co and b) Ni-Co/MWCNT coatings after sliding test.

References:

1. F.Su, C. Liu, J. Guo, and P. Huang, Surface & Coatings Technology, Characterizations of nanocrystalline Co and Co/MWCNT coatings produced by different electrodeposition techniques, (2013), 217, 94-104.
2. L. Kodandarama, M. Krishna, H.N. Narasimha Murthy, and S.C. Sharma, Development and Characterization of Electrocodeposited Nickel-Based Composites Coatings, J. Materials Engineering and Performance, (2012), 21, 105-113.
3. L. Shia, C.F. Suna, P. Gao , F. Zhou, and W.M. Liu, Surface & Coatings Technology, Electrodeposition and characterization of Ni–Co–carbon nanotubes composite coatings, (2006), 200, 4870-4875.

Widely and Rapidly Switchable Wettability Through Short-Range Ordered-Disordered Transition and Redox Reaction

Ya-Huei Chang,[1*] Shien-Ping Feng[1]
[1] Department of Mechanical Engineering, The University of Hong Kong, Pokfulam Rd., Hong Kong

Abstract: As an earth-abundant semiconductor, nickel oxyhydroxide (NiOOH) has mainly been applied for electrochemical, electrochromic and optical devices. Our previous study first achieved its feasibility on wettability control from superhydrophilic to superhydrophobic via anodic plating and post chemical treatment to properly tune the porosity and surface energy.[1] However, the permanently chemical modification results in an irreversible wetting transition, thereby limiting its use for many cutting-edge applications. Some organic and inorganic materials have been found to intrinsically possess switchable nature by the change of composition, conformation, configuration, crystallization, morphology or vacancy recovery.[2] However, these existing wettability switchable materials show a sharp trade-off between the switching range and response time. Specifically, most flat organic materials offer rapid switch within several minutes but only small changes in water contact angles (WCAs < 40°), while smooth inorganic materials have inherently superior switching range (WCAs > 70°) but take several days upon dark storage.[3-5] In this work, without the needs of any chemical treatments, the as-deposited film of nanoporous NiOOH was alternatively exposed to environment chamber and ultraviolet (UV)/ozone, the WCAs could be able to quickly switch between superhydrophobic and superhydrophilic within 70 minutes over ten cycles. The switchable mechanism arises from a chemical redox reaction and short-range ordered-disordered transition (Figure 1) verified by HR-TEM, grazing incidence XRD and XPS. The rewritable two-dimensional (2D) microfluidic channels and wetting-contrast enhanced selective electroplating are demonstrated based on film properties of easily patternable, repairable and switchable wettability.[6]

Keywords: switchable wettability, short-range ordered-disordered transition, micropatterning, selective plating.

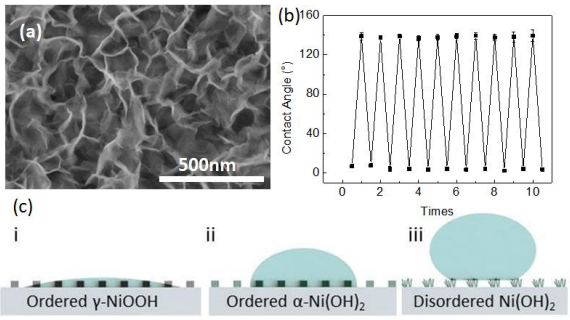

Figure 1: (a) Nanoporous structure of as-deposited NiOOH film through anodic plating. (b) Cycling test of NiOOH film alternatively exposed to environmental chamber and UV/ozone. (c) Schematic of the de-wetting mechanism resulting from the serial reactions of NiOOH/$Ni(OH)_2$ conversion and the defect-driven rearrangement of crystallographic orientation.

References:

1. Y.H. Chang, Y.T. Huang, M. K. Lo, C.F. Lin, C.M. Chen, and S.-P. Feng, "Electrochemical fabrication of transparent nickel hydroxide nanostructures with tunable superhydrophobicity/superhydrophilicity for 2D microchannels application," *J. Mater. Chem. A*, **2**, 1985, 2014.
2. B. Xin and J. Hao, "Reversibly switchable wettability," *Chem. Soc. Rev.*, **39**, 769, 2010.
3. N. Delorme, J. F. Bardeau, A. Bulou, and F. Poncin-Epaillard, "Azobenzene-Containing Monolayer with Photoswitchable Wettability," *Langmuir*, **21**, 12278, 2005.
4. S. Kidoaki, S. Ohya, Y. Nakayama, and T. Matsuda, "Thermoresponsive Structural Change of a Poly(N-isopropylacrylamide) Graft Layer Measured with an Atomic Force Microscope," *Langmuir*, **17**, 2402, 2001.
5. W. Sun, S. Zhou, P. Chen, and L. Peng, "Reversible switching on superhydrophobic TiO_2 nano-strawberry films fabricated at low temperature," *Chem. Commun.*, 603, 2008.
6. Y.H. Chang, N. Y. Hau, C. Liu, Y.T. Huang, C.C. Li, K. Shih, and S.P. Feng, "Short-Range Ordered-Disordered Transition of NiOOH/$Ni(OH)_2$ Pair Induces Switchable Wettability," *Nanoscale*, 2014.

Critical overview of polymer self-assemblies formation and characterization

M. Dionzou[1], C. Roux[1], U. Till[1,2], B. Lonetti[1], J.-D. Marty[1], A.-F. Mingotaud[1], C. Mingotaud[1], P. Joseph[3], D. Goudounèche[4], B. Payré[4], M. Léonetti[5]
[1] Toulouse Unviersity; IMRCP laboratory, CNRS UMR 5623, Toulouse, France
[2] Toulouse University, INPT – EI Purpan, Dpt Sciences Agronomiques et Agroalimentaires, Toulouse, France
[3] LAAS – CNRS, Toulouse, France
[4] Toulouse University, CMEAB, Faculté de Médecine Toulouse Rangueil, Toulouse, France

Abstract: Polymer vesicles, also called polymersomes, are increasingly assessed as drug nanovectors, owing to their ability to transport both hydrophilic and hydrophobic drugs (Messager et al.). A lot of published results in this domain uses an empirical approach to predict the self-assemblies' morphology. However, the rule linking the morphology to the hydrophilic fraction was mainly established on poly(ethyleneoxide-b-butadiene). Linked to our on-going studies on polymer self-assemblies for photodynamic therapy (Gibot et al., Till et al.), the work presented here aimed at cross-examining the methods of formation for polymersomes and pointing out the difficulties of characterization. Thus, a large variety of amphiphilic block copolymers containing first a poly(ethyleneoxide) block for the colloidal stability and the stealth in blood, and secondly various hydrophobic blocks, such as poly(ε-caprolactone), poly(D,L-lactide), poly(styrene), poly(butadiene) or poly(methylmethacrylate), were used, and their self-assembly examined. Different methods of formation will be examined, such as cosolvent addition, film hydration or electroformation. The influence of experimental parameters were assessed and critically compared with literature. This showed that although a general trend of morphology order vesicle – worm-like micelles – micelles is often observed, the limit between each area significantly varied depending on the polymers and for some cases, only micelles could be formed. Also, these self-assemblies being kinetically frozen, the influence of the fabrication method has been observed in some cases, as expected. Thus, selecting the right polymer and the right method of fabrication, either micelles or polymersomes with a size ranging from 15 to 1000 nm can be readily obtained. Regarding their characterizations, the work focused on routinely used dynamic light scattering and electron microscopy which enabled us to highlight difficulties that are often overlooked.

Keywords: Polymer vesicles, self-assemblies, light scattering, electron microscopy

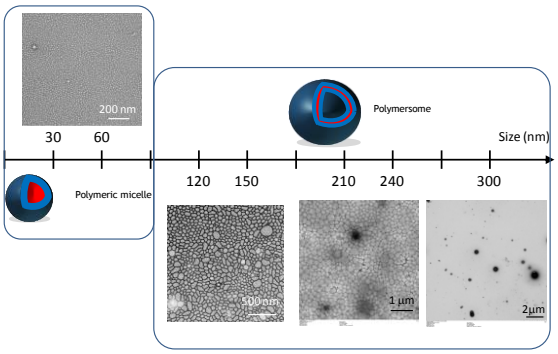

Figure 1: Range of polymer self-assemblies obtained in this study.

References:

L. Gibot, A. Lemelle, U. Till, B. Moukarzel, A.-F. Mingotaud, V. Pimienta, P. Saint-Aguet, M.-P. Rols, M. Gaucher, F. Violleau, C. Chassenieux, P. Vicendo (2014) "Polymeric micelles encapsulating photosensitizer: structure/ photodynamic therapy efficiency relation" *Biomacromolecules*, 15(4), 1443-1455

L. Messager, J. Gaitzsch, L. Chierico, G. Battaglia (2014), "Novel aspects of encapsulation and delivery using polymersomes" *Current Opinion in Pharmacology*, 18 (0), 104-111.

U. Till, M. Gaucher-Delmas, P. Saint-Aguet, G. Hamon, J.-D. Marty, C. Chassenieux, B. Payré, D. Goudounèche, A.-F. Mingotaud, F. Violleau (2014) "Asymmetrical Flow Field-Flow Fractionation with Multi-Angle Light Scattering and Quasi Elastic Light Scattering for characterization of polymersomes: comparison with classical techniques" *Analytical and Bioanalytical Chemistry*, 406(30), 7841-7853

Prediction of photothermal phase signatures from arbitrary plasmonic nanoparticles and experimental verification

O. Blum, N.T. Shaked
Department of Biomedical Engineering, Faculty of Engineering, Tel Aviv 69978, Israel

Abstract: We present a new approach for predicting spatial phase signals originated from photothermally excited metallic nanoparticles of arbitrary shapes and sizes. Heat emitted from the nanoparticle affects the measured phase signal via both the nanoparticle surrounding refractive index and thickness changes. Since these particles can be bio-functionalized to bind certain biological cell components, they can be used for biomedical imaging with molecular specificity, as new nanoscopy labels, and for photothermal therapy. Predicting the ideal nanoparticle parameters requires a model that computes the thermal and phase distributions around the particle, enabling more efficient phase imaging of plasmonic nanoparticles, and sparing trial and error experiments of using unsuitable nanoparticles. For the first time to our knowledge, using the proposed model, one can predict phase signatures from nanoparticles with arbitrary parameters. The proposed nonlinear model is based on a finite-volume method for geometry discretization, and an implicit backward Euler method for solving the transient inhomogeneous heat equation. To validate the model, we correlate its results with experimental results obtained for gold nanorods of various concentrations, which we acquired by a custom-built wide-field interferometric phase microscopy system.

Keywords: interferometric imaging, nanoparticles, digital holographic microscopy, plasmonics, phase measurement

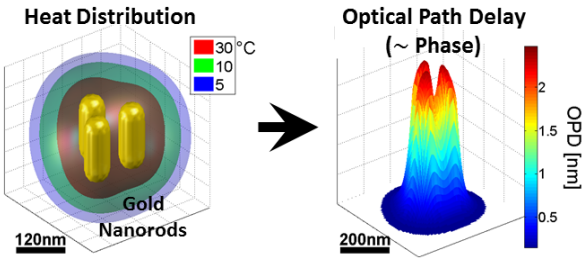

Figure 1: Prediction of Optical Phase Delay (OPD) from heat distribution map created by FVM model of nanoparticle heating

In-Situ Thermally-reduced Graphene Oxide/Epoxy Composites: Thermal and Mechanical Properties

G. B. Olowojoba,[1*] A. C. Taylor,[1] A. J. Kinloch[1]

[1]Mechanics of Materials Division, Department of Mechanical Engineering, Imperial College, London, UK

Abstract:
Graphene has excellent mechanical, thermal, optical, and electrical properties and this has made it a prime target for use as a filler material in the development of multifunctional composites for a variety of applications: electrostatic discharge, electrically conducting, touchscreen display, fire retardant coatings, lightweight materials with good barrier properties, targeted drug delivery applications, etc. However, challenges to overcome in order to take full advantage of the aforementioned properties of graphene include achieving good dispersion and good interfacial properties between filler and matrix. Several approaches aimed at achieving well-dispersed graphene in composites have been reported. In this work we report the thermal and mechanical properties of reduced graphene oxide/epoxy composites prepared via a scalable, environmentally-friendly and commercially-viable method. Transmission and scanning electron micrographs of the composites demonstrate that the reduced graphene oxide is well-dispersed throughout the composite. The composites also show good improvements in thermal conductivity and tensile modulus for relatively low loadings. These properties are compared with those of other commercially available graphene/reduced graphene oxide-based composites.

Keywords: Thermal reduction, graphene oxide, reduced graphene oxide, tensile modulus, thermal conductivity, glass transition temperature, dispersion.

Tribological Behaviors of Yttria-Stabilized Zirconia (YSZ) Nano-particles as Lubricant Additives

A. Sert,[1*] D. Yılmaz Çakta[2]
[1]Eskisehir Osmangazi University, Department of Mechanical Engineering, Eskisehir, Turkey
[2] Eskisehir Osmangazi University, Department of Metallurgical and Materials Engineering, Eskisehir, Turkey

Abstract:
Nanoparticles are used as additives in coatings or lubrication systems in order to prevent friction and wear of materials in industry. The new interest area of nanotribology shows that the lubricants with nano-particles have novel property in tribology, such as wear resistance, low friction coefficient, and high load capacity (Jiao *et al.*, 2011). ZrO_2 is one of the nanoparticles used for tribological consideration such as coatings (Yang *et al.*, 2011) and lubricant additives (Ma *et al.*, 2010). When zirconia doped with yttria, yttria-stabilized zirconia (YSZ) has good mechanical properties at high temperature and good chemical stability up to 1200 °C (Carpio *et al.*, 2015). Due to these properties, YSZ is a current material of choice for thermal barrier coatings.
The aim of this work is to enhance novel lubrication with different amount of YSZ nanoparticles (size<200nm) and characterization of tribological properties of AISI 4140 steel material in the lubricating system. Synthesized YSZ nanoparticles (Figure 1) are dispersed with different concentration (0.1%, 0.5% and 1.0% wt.) in synthetic engine oil (SAE10W40) and tribological test are conducted using ball-on-disc geometry (Figure 2). The morphology of worn surface are studied using scanning electron microscopy (SEM), the elemental analysis on the worn surfaces is also conducted with energy-dispersive X-ray spectroscopy (EDS) and the worn scar lengths are investigated using optical microscopy (OM). When the optimized concentration of nanoparticle additive is 0.5 wt.%, coefficients of friction is decreased about 12.6%. This research has uncovered a novel approach for minimizing energy loss by friction reduction and should benefit many sectors such as automobiles industry.

Keywords: nanoparticles, yttria-stabilized zirconia, lubricant additives, lubricant, friction, wear.

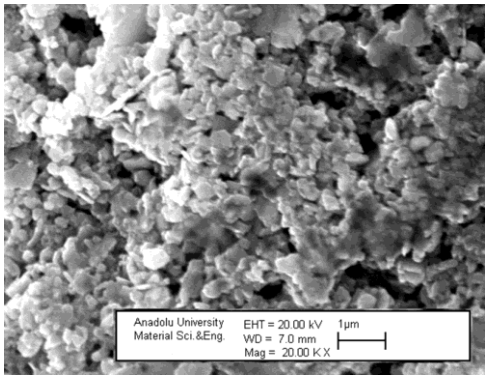

Figure 1: SEM image of the nano YSZ powder.

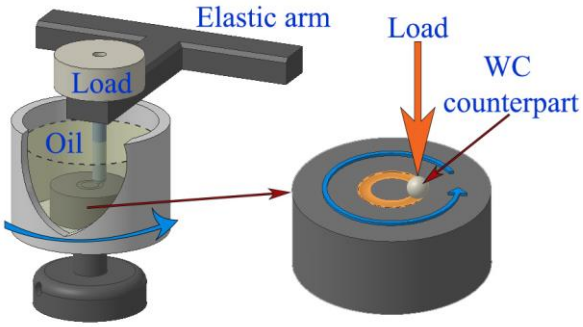

Figure 2: Figure illustrating the wear test device and the wear geometry.

References:
Jiao, D., Zheng, S., Wang, Y., Guan, R., Cao, B. (2011), The tribology properties of alumina/silica composite nanoparticles as lubricant additives, *Appl. Surf. Sci.*, 257, 5720-5725.

Yang, Y., Chen, W., Zhou, C., Xu, H., Gao, W. (2011), Fabrication and characterization of electroless Ni-P-ZrO_2 nano-composite coatings, *Appl. Nanosci.*, 1, 19-26.

Ma, S., Zheng, S., Cao, D., Guo, H. (2010), Anti-wear and friction performance of ZrO_2 nanoparticles as lubricant additive, *Particuology*, 8, 468-472.

Carpio, P., Borrell, A., Salvador, M.D., Gómez, A., Martínez, E., Sánchez, E. (2015), Microstructure and mechanical properties of plasma spraying coatings from YSZ feedstocks comprising nano- and submicron-sized particles, *Ceram. Int.*, 41, 4108-4117.

Calcium phosphate super-balls synthesized in presence of gelatin and chitosan

J. Koetz,* I. Kovach
Universität Potsdam, Institut für Chemie, Potsdam, Germany

Abstract: Calcified tissue of vertebrates can be identified as hybrid material, i.e. inorganic hydroxyapatite crystals bound by polymeric organics, arranged in a hierarchical structure. There are known different strategies to synthesize nanosized hydroxyapatite with diverse morphological structures.

Besides of hydroxyapatite many kinds of calcium phosphates are known. Calcium phosphates are classified by their Ca/P molar ratio. They can be converted into hydroxyapatite or used as Ca^{2+} ion resource.

Various biomineralization processes have been developed to stimulate bone formation in vitro. Here we present a precipitation procedure, where thin calcium phosphate platelets are formed at 90°C in presence of gelatin and chitosan. After heating up the hybridmaterial to 600°C the polymer components are burned out, and supramolecular flower-like ball structures are observed, shown in Figure 1.

By means of FT-IR spectroscopy, powder diffractometric and energy-dispersive X-ray (EDX) analysis in combination with high resolution scanning electron microscopy (HR-SEM) and high resolution transmission electron microscopy (HR-TEM), one can show that dicalcium phosphate and β-tricalcium phosphate (β-TCP) cristallites build up the inner structure of the card house balls.

Additionally experiments, i.e. polyelectrolyte titrations and Differential Scanning Calorimetric (DSC) investigations, show that polymer-polymer interactions between gelatin and chitosan are of special relevance for the formation of such open, porous ball structures. Based on these results one can conclude that electrostatic interactions between the two polymers are of minor importance in contrast to hydrogen bonding.

Keywords: biomineralization, bone formation, cement material in bone repair, β-tricalcium phosphate crystallites, open card house structure, super-balls,

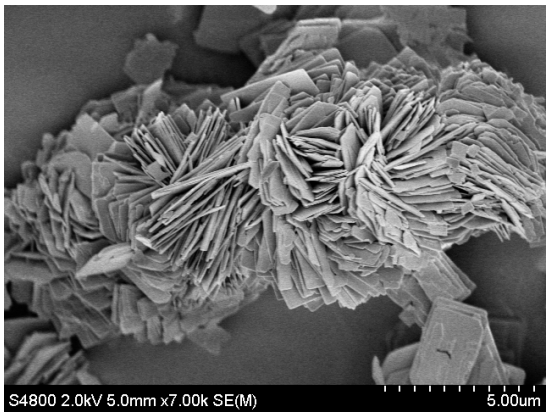

Figure 1: High resolution SEM micrograph of flower-like calcium phosphate balls

References:

Bleek, K., Taubert, A. (2013) New developments in polymer-controlled, bioinspired calcium phosphate meneralization from aqueous solution, *Acta Biometrialia, 9* , 6283-6321.

Sadat-Shojai, M., Khorasani, M-T., Dinpanah-Khoshdargi, E., Jamshidi, A. (2013) Synthesis methods for nanosized hydroxyapatite with diverse structures, *Acta Biometrialia, 9* , 7591-7621.

Nano-Building Blocks based-Hybrid organic-inorganic copolymers with Self-Healing Properties

L. Rozes[1,*], F. Potier[1], A. Guinault[2], S. Delalande[3], C. Sanchez[1], F. Ribot[1]
[1] Sorbonne Universités, UPMC Univ Paris 06, Collège de France, CNRS UMR 7574, Chimie de la Matière Condensée de Paris, F-75005, Paris, France
[2] Arts et Métiers ParisTech, CNRS UMR 8006, Procédés et Ingénierie en Mécanique et Matériaux, F-75013, Paris, France.
[3] PSA Peugeot Citroën, F-78140, Velizy Villacoublay, France.

Abstract: New dynamic materials, that can repair themselves after a strong damage, have been designed by hybridization of polymers with structurally well-defined nanobuilding units.
Hybrid elastomers have been elaborated from a common organic monomer, butyl acrylate, which was co-polymerized, under conventional thermally initiated free radical polymerization, with a difunctional organotin oxo-cluster, $[(BuSn)_{12}O_{14}(OH)_{16}](AMPS)_2$.
This well-defined nano-size cross-linker was selected because of the ionic interactions that the macrocation $[(BuSn)_{12}O_{14}(OH)_{16}]^{2+}$ exchanges with its two polymerizable counter anions (AMPS : Acrylamido-2-methyl-1-propanesulfonate).
The controlled design of cross-linked poly(*n*-butyl acrylate) (pBuA) has been performed by introducing a very low amount of the specific tin oxo-cluster. The non-covalent interactions (*i.e.* ionic bonds) developed at the hybrid interface play a double role. Such interactions are strong enough to cross-link the polymer, which consequently exhibits rubber-like elasticity behavior and labile enough to enable, after a severe mechanical damage, dynamic bond recombination leading to an efficient healing process at room temperature. In agreement with the nature of the reversible links at the hybrid interface, the healing process can be speed up considerably with temperature.
The healing efficiency was measured by a standard stress/strain tensile experiment. Recovery as high as 75% of the original elongation at break was observed. The dynamic nature of the cross-linking, has been studied by measuring the diffusion coefficient of the organotin oxo-clusters inside the swollen material.

Keywords: hybrid materials, polymer nanocomposites, sol-gel processes, DOSY NMR, self-healing properties.

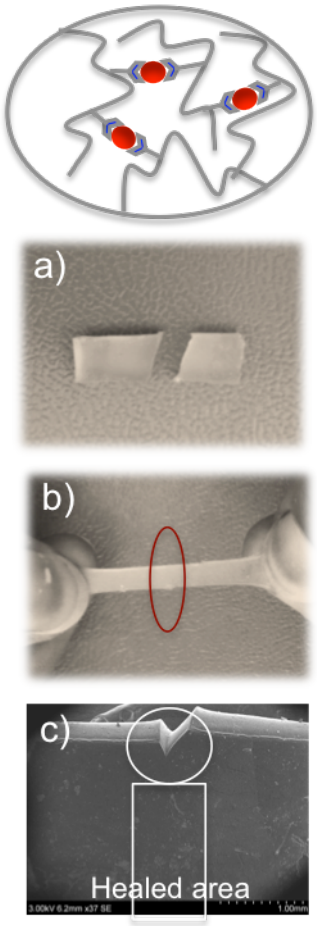

Figure 1: Illustrating of the crosslinking of poly(*n*-butyl acrylate) by nonobuilding blocks : $[(BuSn)_{12}O_{14}(OH)_{16}](AMPS)_2$ a) damaged sample b) healed sample c) healed area by SEM analysis.

References:

F. Potier, A. Guinault, S. Delalande, C. Sanchez, F. Ribot and L. Rozes, *Polymer Chemistry*, 2014, 5, 4474-4479

Hybrid gold nanoparticles modified by oligopeptides for lead (II) ions interaction monitoring

Jane Politi[1,2], Jolanda Spadavecchia[*3,4], Mario Iodice[1], Luca de Stefano[1]

[1]*Institute for Microelectronics and Microsystems, Unit of Naples-National Research Council, Italy*
[2]*Department of Chemical Sciences, University of Naples "Federico II", Naples Italy*
[3]*Sorbonne Universités, UPMC Univ Paris VI, Laboratoire de Réactivité de Surface, Paris, France.*
[4]*CNRS, UMR 7244, Laboratoire de Chimie, Structures et Propriétés de Biomateriaux et d'Agents Therapeutiques, Paris, France*

Abstract: Nanostructured materials have become increasingly popular due to their unique properties in development of novel biosensors. Therefore, more attention should be paid to find efficient synthesis methods to match the enlarging demand of gold nanoparticles. Several different solution synthesis methods have been employed to prepare gold nanoparticles, including biomolecule reduction of $HAuCl_4$, seed mediated synthesis at room temperature and polymer-assisted synthesis. Recently, the utility of nanomaterials for any application is strongly dependent upon their physicochemical characteristics and their interactions with surfaces modifiers (Spadavecchia *et al.*; 2014). Exchange of organic molecules on Au nanoparticles with PEG can indeed be performed to prepare biocompatible PEG-stabilized Au nanoparticles. Gold nanoparticles can interact with specifically sequenced peptides that can self-assemble on their surface. The polypeptides could induce or prevent aggregation of nanoparticles causing consequently the change of absorbance and, moreover, allow to interact with other metal ions i.e. Cd^{2+}, Ni^{2+}, Co^{2+}, Zn^{2+} etc. Lead is a widely used heavy metal in industrial applications (battery manufacture, paint, gasoline, etc.). Lead is toxic by ingestion and inhalation, and can seriously affect the gut and the central nervous system. Phytochelatins (PCs)oligopeptides have been widely studied because of their ability to chelate heavy metal ions in plants and fungi for detoxification mechanisms (Cobbett, 2000). We report here synthesis to prepare polymer-modified gold nanoparticles and gold nanorods using dycarboxylic PEG (DPEG) as stabilizer. A new kind of pegylated gold nanorods based assay to quantify lead-Phytochelatin 6 (PC_6) interactions in aqueous solution by using the proteins as bioprobes was developed (Politi *et al.*, 2015). These hybrids nanocomplexes are stable and biologically active: even if linked by adsorbed-gold interaction on the nanorods surface, the peptides are able to strongly bind the heavy metal ions with an affinity constant in the range of picomolar. The signal changes, i.e. variation of FT-SPR peak position, are important (more than 200 cm^{-1}) even at very low concentration (25 ppb) of metal ions: this result is very promising for development of sensitive and effective nanoparticle-based biosensor for quantifying lead (II) ions concentration in water (see Figure 1).

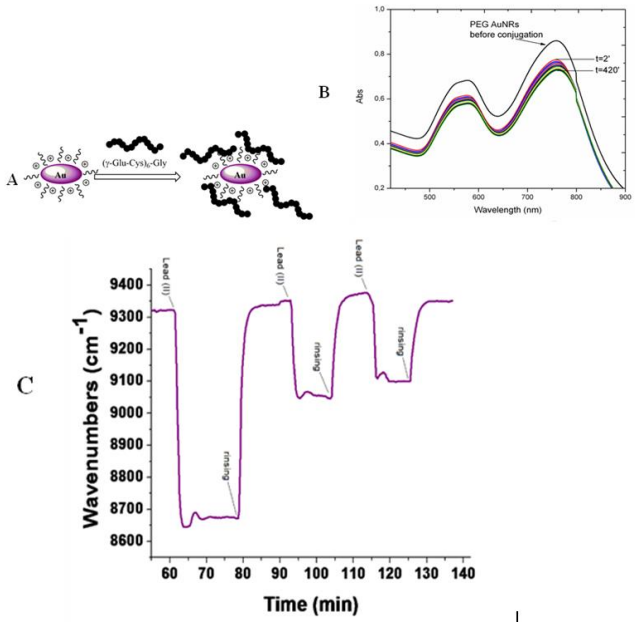

Figure 1. Schematization of oligopeptides self-assemblibg (A); UV-vis spectra of PEG gold nanorods during oligopeptides self-assembling (B); FT-SPR shifts of nanostructured surface as function of time of lead ions interaction (C).

Keywords: oligopeptides self-assembling, gold nanorods, lead ions detection.

References:

Cobbett, C.S.; (2000) Phytochelatin biosynthesis and function in heavy-metal detoxification. Current opinion in plant biology, 3, 211–216.

Politi, J., Spadavecchia, J.; Iodice, M.; De Stefano, L.; (2015**)** Oligopeptide–heavy metal interaction monitoring by hybrid gold nanoparticle based assay, *Analyst*, , 140, 149-155.

Characterization of Ferromagnetic Metal–Carbon NanocompositesPrepared by Solid-Phase Pyrolysis of Metal-Phthalocyanines

A. Manukyan,* A. Mirzakhanyan, H. Gyulasaryan, R. Khachaturyan, E. Sharoyan
Institute for Physical Research, NAS of Armenia, Laboratory of Solid State Physics, Ashtarak-2, Armenia

Abstract: We have synthesized a number of ferromagnetic metal–carbon nanocomposites (M/C, where M = Co, Ni, Fe), using solid-phase pyrolysis of metal-phthalocyanines. This reaction can be represented as (Manukyan *et al.*; 2012)

$$M(C_{32}N_8H_{16}) \xrightarrow[-8H_2,\,-4N_2]{T_{pyr},\,t_{pyr},\,p} M + 32C,$$

Where T_{pyr} is the pyrolysis temperature, t_{pyr} the pyrolysis time, and p_{pyr} the autogenic pressure in a reaction ampoule.

It is evident that the metal concentration in nanocomposites is about 3 at%. Changing the pyrolysis conditions, it is possible to prepare superparamagnetic and ferromagnetic nanoparticles with sizes from 5–10 nm to 200–300 nm in different carbon matrices. The structure, morphology and magnetic characteristics of nanocomposites were investigated by electron microscopy, X-ray diffraction, Raman spectroscopy and magnetometry. In particular, a transmission electron microscope image of Co/C nanocomposite is shown in Figure 1.

As seen, Co nanoparticles are embedded in the walls of multiwalled carbon nanotubes and in their ends, which leads to the bimodal size distribution (around 5 nm and 30 nm). From X-ray diffraction data it follows that Co nanoparticles have the fcc structure and the mean size of 15 nm. Raman spectra of samples contain "graphitic" G- and D-bands specific for carbon nanotubes. Magnetometry data show that Co nanoparticles have the saturation magnetization of 128 emu/g at 300 K, which is about 90% of magnetization of bulk cobalt, and the coercivity 380 Oe.
The structure and magnetic properties of Ni@C and Fe@C nanocomposites essentially differ from these of aforementioned compounds. In this case nanocomposites consist of metal nanoparticles coated by graphite-like shells (Ni@C and Fe@C), which prevent aggregation and oxidation of nanoparticles. The magnetic characteristics such as saturation magnetization and coercivity as well as the specific absorption rate (SAR) make these materials attractive for magnetic hyperthermia applications.

This work was supported by the SCS MES RA, within the framework of joint Armenian–Belarusian research project № 13RB–050 and the FP7 Project of the European Commission with Grant No. 608906 – NANOMAT–EPC.

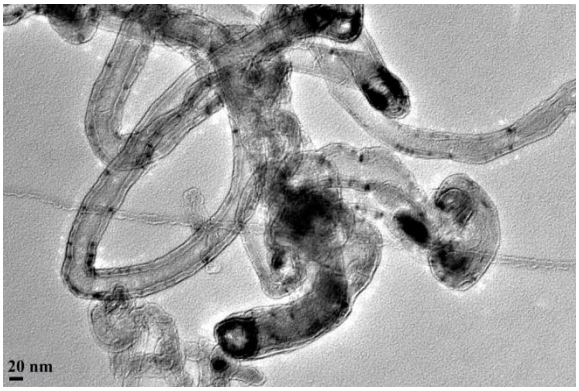

Figure 1: TEM image of cobalt nanoparticles embedded in the walls of multiwalled carbon nanotubes and in their ends.

Keywords: metal–carbon nanocomposites, metal-phthalocyanines, solid-phase pyrolysis, Co, Fe, Ni nanoparticles, ferromagnetism.

References:

Manukyan, A., Mirzakhanyan, A., Badalyan, G., Shirinyan, G., Fedorenko, A., Lianguzov, N., Yuzyuk, Yu., Bugaev, L., Sharoyan, E. (2012) Nickel nanoparticles in carbon structures prepared by solid-phase pyrolysis of nickel phthalocyanine, *J. Nanopart. Res.*, 14, 982-988.

Ambient scalable synthesis of surfactant-free thermoelectric metal chalcogenide nanostructures

C. Han,[1] Z. Li,[1,2,*], W.L. Li, [1] L. J. Zhang, [1] S. X. Dou[1]

[1] Institute for Superconducting and Electronic Materials, Australian Institute for Innovative Materials, University of Wollongong, Squires Way, North Wollongong, NSW 2500, Australia

[2] School of Radiation Medicine and Radiation Protection, Soochow University, 199 Ren Ai Road, Suzhou Industrial Park, Suzhou 215123, China

Email: zhenl@uow.edu.au; Tel: +61-2-42215163; Fax: +61-2-42215731

Abstract: Thermoelectric generators (TEG) / refrigerators (TER) can directly convert heat into electricity or vice versa. It is estimated that around 2/3 of energy produced is wasted as heat, and direct conversion of huge amount of waste heat into electricity by this green technology can significantly save on energy consumption and reduce carbon emissions because of its zero emissions and zero noise, excellent stability and reliability, and robust applicability.(Kraemer *et al.*, 2011) Only niche applications have been achieved, however, due to the limited number of high-performance thermoelectric (TE) materials. Among the different types of TE candidates, metal chalcogenides, especially lead and bismuth based selenides and tellurides, have been extensively investigated and applied in TE devices due to their excellent, reliable performance and lower cost in comparison with other candidates.(LeBlanc *et al.*, 2014) Their performance has been drastically improved through advanced nanoscience and nanotechnology in recent years. (Han *et al.*, 2014) Herein, a robust low-cost and high-efficiency ambient aqueous approach to the scalable synthesis of different surfactant-free nanostructured metal chalcogenides (M_aX_b, M = Cu, Ag, Sn, Pb, Bi; X = S, Se, Te; a = 1 or 2; and b = 1 or 3) has been developed (Figure 1). The effects of different reaction parameters, such as precursor concentration, precursor ratio, and amount of reducing agent, on the composition, size, and shape of the resultant nanostructures have been comprehensively investigated. This environmentally friendly approach is capable of producing large-scale metal chalcogenide nanostructures in a one-pot reaction for investigation of their thermoelectric properties towards conversion of waste heat into electricity. The results demonstrate that the thermoelectric properties of these metal chalcogenide nanostructures are strongly dependent on the types of metal chalcogenides, and their figure of merits are comparable with previous reports on their bulk and nanostructured counterparts. Recently, this roubust approach was extended to prepare CuAgSe ternary thermoelectric nanoparticles in a large scale.(Han *et al.* 2014) The resultant CuAgSe nanoparticles exhibit an interesting temperature-dependent reversible transition of metallic-n-p conductivity, accompanied by the transition of crystal structure from pure tetragonal phase, through a mixture of tetragonal and orthorhombic phases to cubic phase.

Keywords: ambient synthesis, metal chalcogenides, nanostructures, thermoelectric.

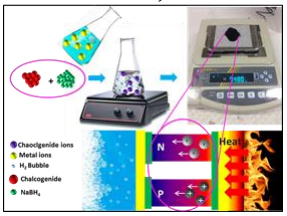

Figure 1: this Figure illustrating the two parts work that we are tempting to do: a general, scalable and low cost synthesized route for different nanostructured metal chalcogenides has been proposed and their thermoelectric performances will be tested.

References:

Kraemer, D., Poudel, B., Feng, H. P., Caylor, J. C., Yu, B., Yan, X., Ma, Y., Wang, X. W., Wang, D. Z., Muto, A., McEnaney, K., Chiesa, M., Ren, Z. F., Chen, G. (2011), High-performance flat-panel solar thermoelectric generators with high thermal concentration, *Nat. Mater.*, 10, 532-538.

LeBlanc, S., Yee, S. K., Scullin, M. L., Dames, C., Goodson, K. E. (2014), Material and manufacturing cost considerations for thermoelectrics, *Renew. Sustainable Energy Rev.*, 32, 313-327.

Han, C., Li, Z., Dou, S. X. (2014), Recent prigress on thermoelectric materials, *Chin. Sci. Bull.*, 59, 2073-2091.

Han, C., Sun, Q., Cheng, Z. X., Wang, J. L., Li, Z., Dou, S. X., Wang, L. Z. (2014), Ambient scalable synthesis of surfactant-Free thermoelectric CuAgSe nanoparticles with reversible metallic-n-p conductivity transition, *J. Am. Chem. Soc.*, 136, 17626-17633.

Acknowledgments

C. Han gratefully acknowledges the Chinese Scholarship Council (CSC) for his scholarship. Z. Li acknowledges support from the Australian Research Council (ARC) through the Discovery Projects DP130102699 and DP130102274. S. Dou is grateful for support from the Baosteel-Australia Research Centre (BARC) through the project BA110011 and from the ARC through the Linkage Project LP120200289.

Efect of Temperature During Composite Materials Synthesis for the use as Gas Separators in Alkaline Water Electrolysers on their Ionic Conductivity and Oxygen Barrier Propreties

J. Stojadinović,[1,*] G. Kasiribidhendi,[1] F. La Mantia,[1]
[1]University of Bochum, Dept. Chemistry and Biochemistry, Center for Electrochemical Sciences, Bochum, Germany

Abstract: Development of materials for the use in alkaline electrolyzers for gas separation has been directed towards surpassing the ionic conductivity, gas tightness, chemical, mechanical and thermal resistivity, life span, and cost effectiveness of the health hazardous asbestos and current state of the art Zirfon® separator [1].

Ionic conductivity of different gas separation membranes can be accurately determined by Electrochemical Impedance Spectroscopy with a four-electrode zero gap cell, while the use of the four-electrode non-zero gap cell coupled with a Mass Spectrometer enables the oxygen permeability assessment [2].

In order to gather better understanding of the separator materials' synthesis process, the interplay of the synthesis parameters and the electrochemical properties of the separator is studied here.

Temperature during synthesis was shown to have a significant influence on the ionic conductivity of developed separators. The effect of temperature on the morphology of the separators was investigated using X-Ray Diffraction and Scanning Electron Microscopy.

The understanding of the synthesis parameters interactions enables tuning of separators' ionic conductivity and oxygen permability, through the optimisation of the material fabrication.

Additionaly, it contributes towards broadening the material's application to systems other than alkaline electrolyzers, such as fuel cells and solar hydrogen generation.

Keywords: gas separation, synthesis temperature, ionic conductivity, oxygen permeability, X-Ray Diffraction.

References:

[1] P. Aerts, S. Kuypers, I. Genne, R. Leysen, J. Mewis, I. F. J. Vankelecom, P. A. Jacobs, Polysulfone-ZrO2 Surface Interactions. The Influence on Formation, Morphology and Properties of Zirfon-Membranes, *J. Phys. Chem.* B 110 (2006) 7425-7430.

[2] J. Stojadinović, S. Weiss, F. La Mantia, Effect of Electrochemical Cell Design on the Ionic Conductivity and Oxygen Permeation Determination of Gas Separators, *Electroch. Acta* 127 (2014) 153–158.

Effect of polystyrene nanocomposite prepared via Pickering emulsion polymerization on the mechanical properties of PP and EVA

A.B. Moustafa,[1] M.E. Abd El-Aziz,[1] A.M Rabie[2], H.A. Essawy[1*]
[1]Department of Polymers & Pigments, National Research Center, Dokki 12311, Cairo, Egypt
[2]Ain Shams University of Annaba, Chemistry Department, Cairo, Egypt

Abstract: Solid nanoparticles can be used as stabilizers for oil/water emulsions instead of the conventional surfactants. Emulsion polymerization of styrene, as an example of polymerizable oil, was started in the current study after ultrasonication of the monomer into the aqueous phase, with the aid of montmorillonite nanoparticles as solid particles stabilizer for the process. The imaging by a field emission scanning electron microscope (FESEM) equipped with energy dispersive X-ray (EDX) unit and transmission electron microscope (TEM) proved the formation of polystyrene/ montmorillonite nanocomposite as hybrid latex particles via Pickering mode of emulsification. The mechanical properties of polypropylene (PP) and ethylene-vinyl acetate copolymer (EVA) were studied after addition of various loadings (2, 4, 8, 12, and 14 wt%) of prepared polystyrene/ montmorillonite nanocomposite hybrids.

Keywords: Pickering emulsion, styrene, montmorillonite, polymerization, ethylene vinylacetate, polypropylene, reinforcement, mechanical properties.

Figure 1: Scheme demonstrates the synthesis of montmorillonite armored polystyrene latex via Pickering emulsion polymerization.

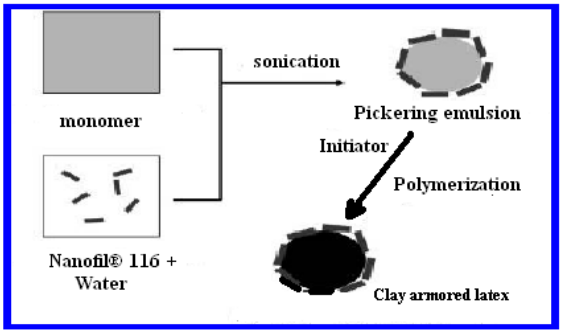

References:

Zhou, H., Shi, T., Zhou, X., (2013) Preparation of polystyrene/SiO_2 microsphere via Pickering emulsion polymerization: Synergistic effect of SiO_2 concentrations and initiator sorts, *Appl. Surf. Sci.*, 266, 33-38.

Moustafa, A.B., Abd El-Aziz, M.E., Emira, H.S., Rabie, A.M., Essawy, H.A. (2014), Emulsion polymerization of styrene using silica nanoparticles as solid stabilizer , *KGK*, 10, 47-53.

Lin, K., Yang, H., Petit, C. Lee, W. (2015), Magnetically controllable Pickering emulsion prepared by a reduced grapheme oxide-iron oxide composite, *J. Coll.Interf. Sci.*, 438,296-305.

Session II - C: Nanomaterials synthesis & properties

Kinetic Study of Functionalization of Carbon Nanomaterials

T.P. Dyachkova, E.N. Tugolukov, I.V. Anosova, A.G. Tkachev
Tambov State Technical University, Department "Technology and Methods of Nanoproducts Manufacturing", Tambov, Russian Federation

Abstract: Carbon-based nanomaterials are highly variable and possess unique physical properties. Presently, multi-walled carbon nanotubes (MWCNTs) and graphene nanoplatelets (GNPs) appear to be one of the most common and available materials. Nevertheless, their use in composite materials is often limited owing to a tendency to agglomerate. To improve the dispersibility in polymers and solvents, the surface of carbon nanomaterials can be functionalized by covalent attachment of various functional groups (Kharitonov *at all*, 2015) (hydroxyl, carboxyl, fluoride, amine, etc.). Functionalization is particularly valuable with respect to multilayered carbon nanostructures based on graphene, because tendency to agglomeration for this materials is especially strong because of large contacting surfaces.

The functional groups provide different kinds of interactions between the carbon nanostructures and polymer molecules: 1) electrostatic interaction; 2) hydrogen bond formation; and 3) covalent bond formation. Sometimes, the formation of composite polymer layers on the carbon nanomaterial surface can be observed due to such interactions. For instance, this may occur when modifying functionalized MWCNTs and GNPs with conducting polymers (polyaniline and polypyrrole).

Owing to the above-mentioned effects, functionalized MWCNTs- and GNPs-based composites are becoming more widely used in the manufacture of structural, building and electrode materials (Kondrashov *et al.*, 2013). This, in turn, raises the problem of obtaining functionalized and modified forms of carbon nanostructures in the industry. However, scaling processes of MWCNT and GNP functionalization requires a detailed study of the laws of their kinetics, determination of optimum technological regimes, providing production of materials with controlled characteristics (Dyachkova et al., 2013).

In this report, we present the results from a study on kinetic regularities of the carbon nanotube functionalization with liquid (nitric acid, potassium permanganate and hydrogen peroxide solutions) and gaseous (ozone, nitric acid and hydrogen peroxide vapors) oxidizing agents. It is shown that the gas-phase oxidation under optimum conditions allows obtaining materials with a high degree of functionalization with minimal consumption of reagents. It is proposed for the first time to use hydrogen peroxide vapor as oxidizing agent. It is demonstrated that in this case, the hydroxyl groups providing interactions with polar polymer matrices are mainly formed on the carbon nanotube surface. The optimum conditions for the carbon nanotube functionalization process in the hydrogen peroxide vapor were determined. The advantages of the proposed methods are the ease of implementation in the industry and the absence of environmentally hazardous waste.

Composites based on carbon nanomaterials modified with polyaniline (PANI) were obtained, and it was shown that preliminary functionalization of carbon surface with oxygen-containing functional groups improves the quality of nanocomposites obtained. With using this method, composites PANI/oxidized GNP and PANI/functionalized MWCNT were synthesized by of oxidative polymerization of aniline in presence of functionalized carbon nanomaterials. The kinetic regularities of the carbon nanostructure modification with polyaniline were studied. Besides, differences in temperature profiles of the oxidative polymerization reaction after modifying the pristine and oxidized MWCNTs and GNPs were disclosed. Influence of the morphology of original carbon nanomaterial, the degree of its pre-functionalization, medium acidity and molar ratio of reagents in the oxidative polymerization on the yield of PANI and electrical, thermal and electrochemical properties of composite materials was investigated. It was found that degree of polymerization and structure of PANI coatings are sensitive to the nature of functional groups on the surface of carbon nanotubes. Specific electrical resistance and capacitance properties of composites based on carbon nanotubes modified with PANI also depend on the conditions of oxidative polymerization.

The work was carried out within the framework of supporting the cooperation between Russian higher education institutions, state scientific institutions and organizations implementing complex projects on creation of high-tech production (RF Government Decree of April 9, 2010 No. 218; Contract of August 14, 2014 No. 02.G25.31.0123).

Keywords: multiwalled carbon nanotubes, graphene nanoplatelets, functionalization, oxidation, oxidative polymerization, nanocomposites.

References:

Kharitonov, A.P., Tkachev A.G., Blohin, A.N., Dyachkova, T.P., Maksimkin, A.A. Chukov, D.I. (2015) Reinforcement of epoxy resin composites with fluorinated carbon nanotubes, *Compos. Sci. Technol.*, 107, 162-168.

Kondrashov, S.V., Dyachkova, T.P., Bogatov, V.A., Mansurova, I.A., Marakhovskii ,P.S., Fokin, A.S. (2013) Utilization of carbon nanotubes for enhancing the heat resistance of epoxy binders, *Inorg. Mater. Appl. Res.*, 5, 394-399.

Dyachkova, T.P., Melezhyk, A.V., Gorsky, S.Yu., Anosova, I.V., Tkachev, A.G. (2013) Some aspects of functionalization and modification of carbon nanomaterials, *Nanosystems: Physics, Chemistry, mathematics*, 5, 605-621.

Single and Biphasic TiO_2 nanotubes by Electrochemical Anodization

R.Savitha,[1,2,*] Kieran Nolan,[2] Anne Morrissey,[3] R.RaviKrishna,[1] P.Selvam,[4] Raghuram Chetty[1]

[1] Department of Chemical Engineering, Indian Institute of Technology (IIT) Madras, Chennai, India.
[2] School of Chemical Sciences, Dublin City University (DCU), Dublin, Ireland.
[3] School of Biotechnology, Dublin City University (DCU), Dublin, Ireland.
[4] Department of Chemistry,IIT Madras, Chennai, India.
(*savitharangasamy@gmail.com)

Abstract: Titania (Titanium dioxide/TiO_2), is one of the most abundant elements and its application spans through various fields because of its chemical stability and specific photo induced properties. Utilization of TiO_2 in applications such as water splitting, solar cells, pollutant mineralization and disinfection needs high photocatalytic activity whereas in paints and cosmetics TiO_2 as a UV absorbent needs controlled photo reactivity (Carp *et al.*; 2004). There are four polymorphs of titania found in nature Anatase, Brookite, Rutile and Monocilinic. Among these Rutile is the most thermodynamically stable and Anatase has the most favourable kinetics. In certain systems, especially in photocatalytic degradation reactions, the presence of two phases (biphasic) for example, Anatase and Rutile, results in visible light activation of the catalyst for the production of reactive hydroxyl radicals. Thus the crystalline nature of TiO_2 decides its fate of utilization. Precise and controlled fabrication of titania nanoforms, to avail of high surface area is a key challenge in developing TiO_2 catalysts. One dimensional structures such as nanotubes and nanowires can be made as a mechanically stable three dimensional assembly with high surface area. Annealing of amorphous nanotubes (up to 500°C) crystallized into Anatase phase, and heat treated beyond 500°C, results in Anatase to Rutile transformation along with collapsing of nanotube morphology (Eder *et al.*; 2006).

In this work a simple and facile route to the synthesis of pure anatase and biphasic (Rutile+Anatase) nanotubes in powder form is proposed. This work focuses on nanotubes formation through rapid breakdown, electrochemical anodization with perchloric acid electrolyte and crystallization of the amorphous nanotubes through heat treatment. The effect of impurities present in the system, which causes early nucleation favoring rutile phase growth by introducing surface defects and oxygen vacancies, was also investigated. The nanotubes are morphologically characterized by Scanning and Transmission Electron Microscope; the crystalline phases are studied by X-ray diffraction pattern; optical properties by Diffusive Reflectance Spectroscopy (UV-DRS). Nitrogen adsorption-desorption (BET) studies were also carried out to estimate the porosity and surface area.

Preliminary experiments were conducted to examine the efficiency of these nanostructures for the photocatalytic degradation of Paracetamol and Famotidine in aqueous solutions.

Keywords: TiO_2 Nanotube, Electrochemical Anodization, Crystallization, Biphasic nanotube, Photodegradation.

References:

Carp, O., Huisman, C.L. & Reller, a., (2004), Photoinduced reactivity of titanium dioxide, *Progress in Solid State Chemistry*, 32, 33–177.

Eder, D., Kinloch, I. a & Windle, A.H., (2006), Pure rutile nanotubes. *Chemical Communications*, 30(13), 1448–50.

3D Printed Hydrophobic and Antimicrobial Nanofunctionalised Surfaces

M. J. Cook,[1*] L. Gilbertson,[2] J. H. Johnston,[1,3] T. Miller[2]
[1] Victoria University of Wellington, School of Chemical and Physical Sciences, New Zealand
[2] Victoria University of Wellington, School of Design, New Zealand
[3] The MacDiarmid Institute for Advanced Materials and Nanotechnology, New Zealand

Abstract: Superhydrophobic surfaces have been widely studied for many years, in order to determine their characteristics and create new surfaces with similar high water repellency. It has been determined that in addition to a chemical hydrophobicity (low surface energy), a surface roughness is also needed (Cassie & Baxter, 1944; Wenzel, 1936). This surface roughness is generally thought to require both a microstructure and an overlying nanostructure as observed on the superhydrophobic surface of the *lotus* leaf (Neinhuis & Barthlott, 1997). This required surface roughness has been produced in existing literature, using many different methods including solid freeform fabrication (Barahman & Lyons, 2011), etching, lithography and sol-gel (Celia *et al.*, 2013). Superhydrophobic surfaces are conventionally described as those with a static water contact angle of greater than 150°.

3D printing is a very useful fabrication method for producing 3D models with finely tuned physical forms. Fused Deposition Modelling (FDM) is the cheapest and easiest 3D printing technology, but has a comparatively low print resolution. It was thought to be unsuitable for printing superhydrophobic surfaces, as the necessary micro-scale dimensions of the surface roughness were difficult to achieve. In addition, the majority of FDM 3D printable materials are chemically hydrophilic or have too low viscosity to print the fine structures. Research by us has shown that by manipulating the build parameters of the 3D printer, carefully selecting the build material and subsequently chemically treating the 3D printed surfaces with a hydrophobic polymer, it is possible to produce close to superhydrophobic surfaces by FDM printing. The surfaces produced in this way have achieved contact angles of greater than 125° with a 10 μL water droplet. This provides a new method of fabricating water repellent surfaces and opens up new applications and possibilities for the design of consumer products.

The hydrophobic nature of such a surface can impart inherent bacteriostatic properties. This effect can be increased by incorporating silver nanoparticles onto the surfaces, as silver nanoparticles have been shown to have high antimicrobial activity (Morones et al., 2005). Using the technology of Johnston & Parry (2014) the 3D printed surface or initial polymer filament can be functionalized with silver nanoparticles to provide an effective antimicrobial surface without destroying the hydrophobicity of the surface. The paper presents the results of this study.

Keywords: surfaces, superhydrophobicity, antimicrobial, 3D printing, silver nanoparticles

References:

Barahman, M., Lyons, A. M. (2011), Ratchetlike slip angle anisotropy on printed superhydrophobic surfaces. *Langmuir*, 27, 9902-9909.

Cassie, A. B. D., Baxter, S. (1944), Wettability of Porous Surfaces. *Trans. Faraday Soc.*, 40, 546–551.

Celia, E., Darmanin, T., Taffin de Givenchy, E., Amigoni, S., Guittard, F. (2013), Recent advances in designing superhydrophobic surfaces. *J. Colloid Interface Sci*, 402, 1–18.

Johnston, J. H., Parry, M. (2014), New Generation Nanogold and Nanosilver Polymer Composites and Their Applications. *Proceedings NSTI-Nanotech 2014*, 1, 358-361. Washington, DC.

Morones, J. R., Elechiguerra, J. L., Camacho, A., Holt, K., Kouri, J. B., Ramírez, J. T., Yacaman, M. J. (2005), The bactericidal effect of silver nanoparticles. *Nanotechnology*, 16, 2346–2353.

Neinhuis, C., Barthlott, W. (1997), Characterization and Distribution of Water-repellent, Self-cleaning Plant Surfaces. *Ann. Bot.*, 79, 667–677.

Wenzel, R. N. (1936), Resistance of solid surfaces to wetting by water. *J. Ind. Eng. Chem.*, 28, 988–994.

Molecular dynamics simulation of glass formation and crystallization in binary PdNi and CuNi alloys.

Muhammad Faruq,[a] Antoine Villesuzanne,[a,b] and Guosheng Shao [a,c]

[a] Institute for Renewable Energy and Environmental Technologies, University of Bolton, Bolton BL35AB, UK

[b] CNRS, ICMCB, University of Bordeaux, F-33600 Pessac, France

[c] UK- China Centre for Multi-functional Nanomaterials, Zhengzhou University, Zhengzhou 450001, P.P. China

Abstract: Molecular dynamics (MD) using Quantum Sutton-Chen potentials were used to obtain an atomistic description of melting, glass formation and crystallization processes for Cu, Ni and Pd metals to study the PdNi and CuNi alloys. The thermodynamic and mechanical properties were calculated in the 0-2000K temperature range from the MD trajectories. The formation of amorphous Cu, Ni and Pd and their equimolar alloys by rapid quenching was investigated from MD at constant pressure and temperature (TPN ensemble). The structural properties were analyzed by means of pair distribution functions and volume *vs* temperature, at cooling rates ranging from 40 K/ps to 0.4K/ps. The relation between the cooling rate and glass transition temperature, or crystallization, was investigated. The radial distribution function agrees well with experimental results for amorphous phases. Upon cooling rates in the range from 5K/ps to 0.4K/ps, Cu, Ni, Pd metals and CuNi alloy form a crystalline structure while the PdNi alloy form a glass. A mismatch in atomic size (1.02 vs 1.134 ratio for CuNi and PdNi, respectively) appears to favor the glass formation.

Keywords: Molecular dynamics, Quantum Sutton-Chen potentials,Cu-Ni alloys, Pd-Ni alloys, Quenching rate,Glass formation.

Graphene mediated synthesis of gold nanoparticles and it nanocomposite and their Applications

P. C. Pandey, Yashashwa Pandey
Department of Chemistry, Indian Institute of Technology (BHU), Varanasi-221005, India

Abstract: The conversion of 3-Aminopropyltrimethoxysilane capped noble metal ions (Au^{3+} , Pd^{2+} , Ag^{+}) into respective nanopartcles in the presence suitable organic reducing agents constitute new route of metal nanoparticle synthesis justifying potential applications in many biomedical applications (Pandey et al, 2011, 2012).[1] The choice of organic reducing reagent precisely govern the dispersibility, nanogeometry, pH and salt tolerance of as synthesized nanoparticles for specific application[2-4]. Some of the organic reducing agent enable the formation of organic –inorganic hybrid during nanoparticle synthesis justifying enhanced catalytic activity of nanomaterial.[5] It was further investigated that the presence of graphene suspension along with reaction mixture facilitate the process of nanopparticles synthesis with significant change in electrocatalytic ability of the material. The presence of graphene allow nucleation site fo nanoparticles and results the formation of hybrid nanomaterial having potentiality for biocompatible thin film formation. This study will also permit us to discuss a new route of nanaoparticles synthesis justifying the micellar behavior of 3-APTMS that precisely control the practical usability of nanomaterial in biomedical applications..

Keywords: nanoparticle synthesis, organic-inorganic hybrid, electrocatalysis, silica-based nanomaterials, biomedical applications.

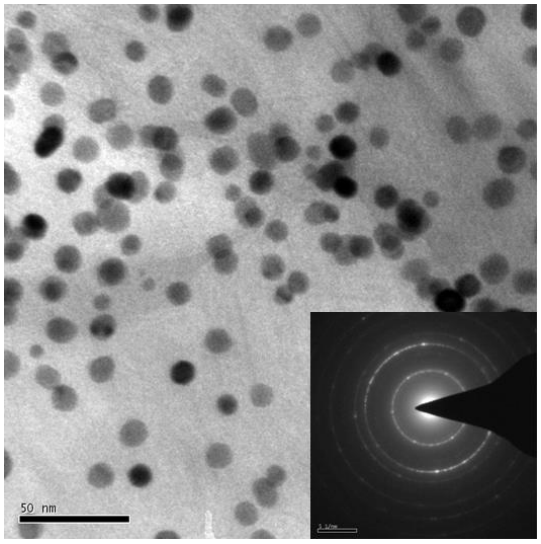

Figure 1: Figure illustrating the TEM image and respective diffraction pattern of graphene sheet that facilitate the 3-aminopropyltrimethoxysilane and formaldehyde mediated synthesis of gold nanoparticles.

References:

1. P. C. Pandey and D. S. Chauhan, *Analyst* 137, 376 **(2012)**.
2. P. C. Pandey, A. Pandey and G. Pandey, J. Nanosci. Nanotech. 14, 6606 **(2014)**
3. P. C. Pandey and G. Pandey, J. Nanosci.. Nanotech**.(2015)** (in press).
4. P. C. Pandey and Richa Singh, J. Nanosci.. Nanotech. 15, 5749 **(2015)**
5. P. C. Pandey and G. Pandey, J. Mater. Chemistry B. 2, 3383, **(2014).**

Preparation, morphological and AC electrical characterization of porous PEG/Polyaniline/Gold Nanowires composite.

M. Celentano[2], R. Vecchione[1], P. A. Netti[1,2]
[1]Center for Advanced Biomaterials for Health Care – IIT@CRIB, Istituto Italiano di Tecnologia – Largo Barsanti e Matteucci, Napoli, Italy
[2]Centro di Ricerca Interdipartimentale sui Biomateriali – CRIB, Università di Napoli Federico II, Napoli, Italy

Abstract: Heterogeneous conducting composites have been object of extensive studies in the last decades. The combination of conducting polymers with inorganic materials having different properties opens up new avenues for the development of innovative hybrid materials with interesting features.[1-4]
Polyanilines have been extensively studied in recent years due to many advantages among other conducting polymers such as low cost, easy synthesis, range of electrical conductivities and unique reversible proton doping-dedoping processes.[5]
At the same time, gold nanoparticles have been applied both in biology and in technology due to their tunable chemical-physical properties. Moreover, they can be easily conjugated with biological molecules.[6] Combination of organic and inorganic materials having biological moieties could be potentially applied in biosensor devices.[7]
We report the preparation of a new type of conducting organic-inorganic composite. In particular, conducting polyaniline in fiber form was dispersed into PEG porous matrix containing gold nanowires in network form.
The composite was characterized by TEM, SEM, ATR-FTIR and XPS. The AC electrical behavior was also studied. The relation among composition, morphology and AC electric response was taken into account.
Morphological and spectroscopic analysis have revealed that the gold nanowires were included only in the pores, while the hydrophobic polyaniline was dispersed in the PEG matrix. It was assumed that the more conductive phase were the pores, while the less conductive was ascribed to the PEG matrix. Results indicated that the PEG porous matrix conductivity was marginally affected if only gold nanowires networks or polyaniline were added. In the first case the pores filled by gold nanowire networks were electrically isolated, while in the second case the contribution to the electrical conductivity of PEG matrix was low due to the low amount and low intrisinc conductivity of polyaniline.
Newertheless, when both these two fillers were present in the matrix, at the same concentration of the previous cases, the percolation threshold was surpassed. Probably, the two fillers exerted a synergic effect on the AC conductivity. Indeed, the pores may be electrically interconnected through the polyaniline chains inside the PEG matrix.
In conclusion, high conductive heterogeneous composite with high porosity has been realized. This composite could be easly functionalizated with biological sensors and potentially applied as transduser in a biosensor device.

Keywords: heterogeneous composites, porous polymer matrix, gold nanoparticles, AC conduction, electron microscopy.

References:

[1] C.G.Wu, D.C. Degroot, H.O. Marcy, J.L. Schindler, C.R. Kannewurf, Y.J. Liu, W. Hirpo, M.G. Kanatzidis, *Chem. Mater.* 8 (1996) 1992.
[2] T.A. Kerr, H. Wu, L.F. Nazar, *Chem. Mater.* 8 (1996) 2005.
[3] E.R. Hitzky, P. Aranda, B. Casal, J.C. Galvan, *Adv. Mater.* 7 (1995)
180.
[4] W.J. Bae, K.H. Kim,W.H. Jo, Y.H. Park, *Macromolecules* 37 (2004) 9850.
[5] Trivedi, D. C., 1997. "Handbook of Conducting Molecules and Polymers", (ed.) by Nalwa, H. S., John Wiley and Sons 2:505.
[6] P. M. Tiwari, K. Vig, V. A. Dennis and S. R. Singh, *Nanomaterials*, 1, 31-63 (2011).
[7] T. A. Kumar , E. Capua , M. Tkachev , S. N. Adler, and R. Naaman, *Adv. Funct. Mater.*, 24(37), 5833-5840 (2014).

Low Pressure Chemical Vapor Deposition of Nickel Oxide Nanospheres as Anode for Lithium-ion Battery

L. Meda,[1*] C. Arnold. A,[1] J. He,[2] A. Dangerfield[3]
[1]Xavier University of Louisiana, Department of Chemistry, New Orleans, LA, USA
[2]Tulane University, New Orleans, LA, USA
[3]University of Texas at Dallas, Department of Materials Science and Engineering, Arlington, Texas, USA

Abstract: Low pressure chemical vapor deposition (LPCVD) of nickel oxide (NiO) nanospheres prepared directly on current collectors is ideal for studying the electrochemical properties because they are no interferences from additives. The direct growth of the materials onto current collectors provides faster mass and electron transport due to the improvement in conductivity across the interfaces and through the materials due to its nanosize. The microstructural characteristics of the as-prepared nanospheres were examined by high resolution transmission electron microscopy which showed that they were arranged randomly on the current collector. Selected area electron diffraction showed that the NiO is polycrystalline with the face-centered cubic crystal structure. The X-ray photoelectron spectroscopy showed that the as-prepared materials are pure NiO.

Aging of NiO electrodes were evaluated by cyclic voltammetry (CV) and charge-discharge measurements up to 140 cycles in the voltage range from 0.1 – 4.0 V versus Li/Li^+. After 140 cycles, a capacity of 1500 mAh/g was still observed. The expected capacity of NiO is 718 mAh/g, therefore 782 mAh/g is excess capacity. Both measurements revealed that the material is intact on the current collector. The LPCVD growth process creates very high surface area NiO which is one of the reasons for the overall improvement in electrochemical performances. However, high surface area introduces new challenges in the use of conversion reaction (equation 1a) for actual rechargeable batteries. This study will highlight the improvement in mass and electron transfer kinetics, but will also address the origin of the excess capacity observed in these systems due the high surface area of the NiO.

$$NiO + 2Li+ + 2e- \leftrightarrow Li_2O + Ni^0 \quad (1)$$

$$Li + LiPF_6/PC/DC/DMC \rightarrow \text{Li-Polymer} + Li_2CO_3 + LiF + LiO_2CO.R \quad (2)$$

$$\text{Li-Polymer} \leftrightarrow \text{Polymer} + Li \quad (3)$$

Keywords: nickel oxide, nanospheres, low pressure chemical vapor deposition, conversion reaction, electrochemical properties

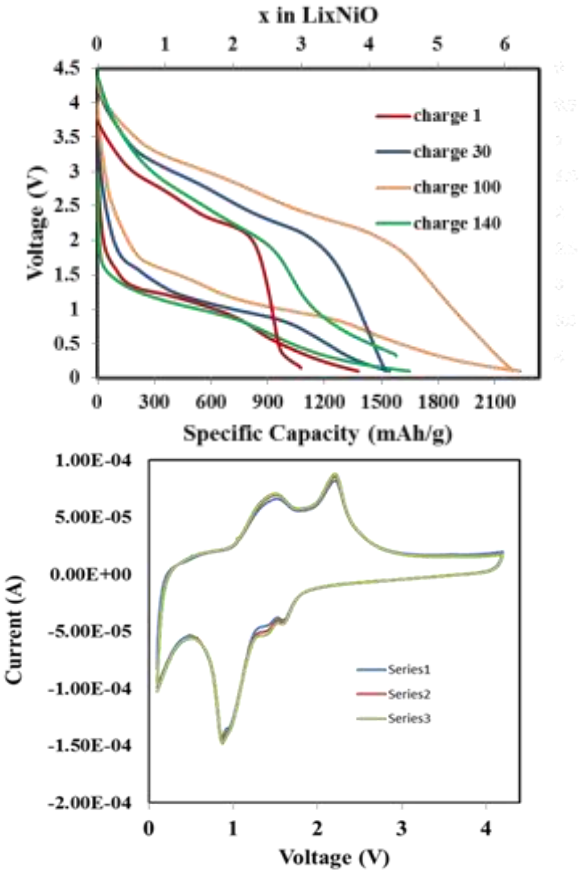

Figure1. (a) The galvanostatic discharge/charge performances of NiO nanospheres for 1st, 30th, 100th, 50th and 140th cycles at 1.5 C rate and (b) the CVs at 2nd and 130th cycles.

References:

Navulla, A., Stevens, G., Kovalenko, I., Meda, L. (2014), Reversible High Capacity in Hierarchical Columnar RuO_2 Nanoplates and Their Improved Performance in Lithium Ion Batteries, *J. Phys. Chem. C.*, 118, 13382−13386.

Varghese, B., Reddy, M. V., Yanwu, Z., Chang, S.L., Hoong, T.C., Rao, Subba, G.V., Chowdari, B.V.R., Wee, A.T.S., Chwee, T.L., Sow, C-R., (2008) Fabrication of NiO Nanowall Electrodes for High Performance Lithium Ion Battery, *Chem. Mater*., 20, 3360-3367.

Morphology, Properties and Electrocatalytic Behaviour of Nanoporous Metals prepared by Electrolytic Dealloying of AgAuPt Alloys

Adrián Vega and Roger C. Newman
University of Toronto, Dept. of Chemical Engineering and Applied Chemistry
200 College St., Toronto, M5S 3E5, Ontario, Canada

Abstract: Nanoporous gold fabricated by electrolytic dealloying (selective dissolution) of Ag from an AgAu solid solution alloy has become a highly fashionable subject of research in the past decade. A high-profile book published by RSC and an inaugural conference held in Germany last summer have brought the subject to an even wider audience. Our own recent research has focused on the dealloying of ternary AgAuPt alloys with a low Pt content (1-3 at%) and systematic variation of the Au/Pt ratio, while maintaining 77 at.% Ag. Our published research, cited below, focused on the fundamental mechanisms of formation of the nanoporous materials and their response to heating in air or inert atmospheres (Pt co-segregates with O to the ligament surfaces in air, but desegregates in inert atmospheres). All ternary alloys gave a much more refined as-dealloyed morphology than the binary AgAu alloy, because Pt enriches at step edges, hindering the surface diffusion of gold. The smallest ligament size observed in our family of alloys is around 4 nm. Like all dealloyed materials, they show a bicontinuous morphology of ligaments and pores, with good mechanical integrity.

More recently, we have been examining the electrocatalytic properties of the dealloyed binary and ternary alloys. Alongside studies of methanol and ethanol oxidation, the Pt coverage of the nanosized ligaments has been probed by underpotential deposition (UPD) of hydrogen and UHV surface analysis. The UPD measurements show interesting variation from what is usually observed, which we attribute to the presence of isolated Pt atoms or very small clusters that do not have hollow sites with 3 Pt neighbours for H adsorption. These data require further analysis using a more sophisticated model than we have been using so far.

The kinetics of methanol and ethanol oxidation on the dealloyed AgAuPt materials are very rapid, and heat treatment in air to cosegregate Pt and O gives even faster kinetics (when expressed as true anodic current density; of course the porosity coarsens by surface diffusion when the material is heated at the necessary temperatures, $\geq$300ºC, so the true surface area is less).

In basic solution, carbonate yields are high for methanol and surprisingly high for ethanol. The latter result is under further investigation using a variety of analytical techniques. Studies in sulfuric acid are in progress.

The air-annealing process to segregate Pt can probably be optimized further, and even lower Pt contents in the starting alloy are of interest; however thermal coarsening of the porosity appears to accelerate below 1% Pt.

Further alloying is of interest in order to further stabilize the porous structure.

Keywords: nanoporous metals, electrolytic dealloying, electrocatalysis, surface segregation.

References:

Adrián A. Vega and Roger C. Newman, Nanoporous Metals Fabricated through Electrochemical Dealloying of Ag-Au-Pt with Systematic Variation of Au:Pt Ratio, *J. Electrochem. Soc. 2014 161(1): C1-C10.*

Adrián A. Vega and Roger C. Newman, Beneficial Effects of Adsorbate-Induced Surface Segregation of Pt in Nanoporous Metals Fabricated by Dealloying of Ag-Au-Pt Alloys, *J. Electrochem. Soc. 2014 161(1): C11-C19.*

Modulation of Active Sites in Supported $Au_{38}(SC_2H_4Ph)_{24}$ Cluster Catalysts: Effect of Atmosphere and Support Material

B.Zhang[1], S.Kaziz[2], H.Li[3], M.G.Hevia[4], D.Wodka[1], C.Mazet[3], T.Bürgi[1*], N.Barrabés[1*]
[1] Department of Physical Chemistry, University of Geneva, Geneva, Switzerland
[2] Department of Industrial Engineering, National High School of Engineers of Tunis, Tunisia
[3] Department of Organic Chemistry, University of Geneva, Geneva, Switzerland
[4] Institute of Chemical Research of Catalonia (ICIQ), Tarragona, Spain

Abstract: Thiolate-protected Au nanoclusters have fascinated chemists by offering well-defined and homogenous surface, which can be applied for catalytic reactions (Yamazoe *et al.;* 2014). Exposure of catalytically active gold sites on the cluster surface by thermal treatment and stabilization by supporting on metal oxides represent two effective methods to balance the catalytic activity and stability of Au nanoclusters in oxidation reactions (Shivhare *et al.;* 2013). $Au_{38}(SR)_{24}$ nanocluster bears intrinsically chiral features due to the arrangement of the protecting ligands on the surface of the cluster (Dolamic *et al.;* 2012), which makes it promising in enantioselective catalysis. We investigate the distinctly different interaction of $Au_{38}(SR)_{24}$ with two support materials Al_2O_3 and CeO_2 (Figure 1). The catalytic surfaces have been heated in different atmospheres and the removal of the thiolate ligands has been studied. Thermogravimetry (TG), Temperature programmed process coupled with mass spectrometer (TPRDO-MS) and X-ray absorption spectroscopy (XAFS) studies were performed to understand the desorption of thiol ligands depending on conditions and support material. Depending on the atmosphere and the support material the fate of the thiol ligands is different upon heating leading to metallic Au in the case of Al_2O_3 and to cationic Au with CeO_2. The thiolate removal seems to be a two-step procedure. The catalytic activity of these Au_{38} supported clusters was studied for the aerobic oxidation of cyclohexane. Conversion was higher for the gold clusters supported on CeO_2. Surprisingly, a significant amount of cyclohexanethiol was found, revealing the active participation of the thiolate ligand in catalytic reactions. The observation also indicates that breaking and formation of C-S bonds can be catalyzed by the gold clusters.

Keywords: Gold Cluster, catalyst, thiol ligand, thermal treatments, oxidation

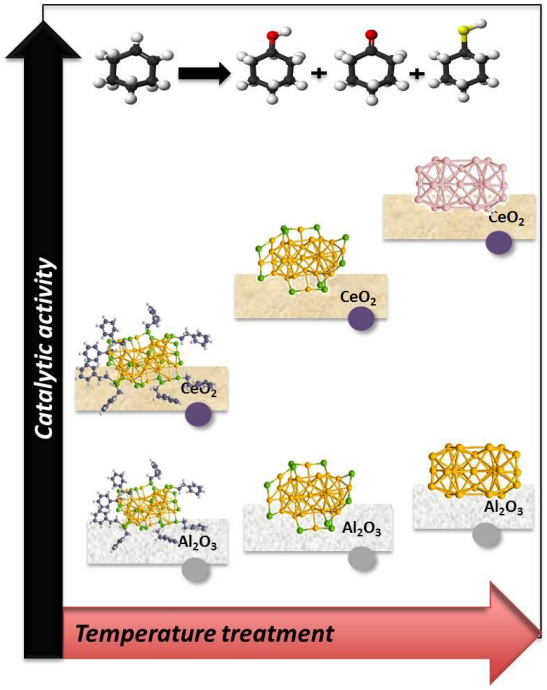

Figure 1: Figure illustrating the support and thermal pre-treatment effect on the modulation of $Au_{38}(SR)_{24}$ catalytic activity for cyclohexane oxidation.

References:

Yamazoe, S., Koyasu, K., Tsukuda, T. (2014) Nonscalable oxidation catalysis of gold clusters, *Acc. Chem. Res.*, 47,816-824.

Shivhare, A., Chevrier, M. D., Purves, W.R., Scott, W.J.R. (2013) Following the thermal activation of $Au_{25}(SR)_{18}$ clusters for catalysis by X-ray absorption spectroscopy, *J. Phys. Chem. C.*, 117,20007-20016.

Dolamic, I., Knoppe, S., Dass, A., Bürgi, T. (2012) First enantioseparation and circular dichroism spectra of Au_{38} clusters protected with achiral ligands, *Nat. Commun*, 3,798

Tuning colloidal stability, MRI relaxivity and bioelimination of functional nanoparticles

A. Walter,[1,2] A. Garofalo,[1] J. Taleb,[3,4] P. Bonazza,[3,4] C. Billotey[3,4], S. Laurent,[5] L. Vander Elst,[5] R. N. Muller[5], D. Felder-Flesch[1],S Begin-Colin,[1]

[1] Institut de Physique et Chimie des Matériaux de Strasbourg (IPCMS), UMR 7504, CNRS, Université de Strasbourg, 23, rue du Loess, BP 43, 67034 Strasbourg Cedex 2 (France).
[2] EPFL, Laboratoire de Technologie des Poudres, EPFL-STI-IMX-LTP Station 12 CH-1015 Lausanne, Suisse
[3] Laboratoire de Physico-Chimie des Matériaux Luminescents, UMR 5620 CNRS-UCBL, Université Claude Bernard Lyon1, 10 rue Ada Byron 69622 Villeurbanne cedex, France.
[4] Hospices Civils de Lyon - Service de Médecine Nucléaire Pavillon B, 5 place d'Arsonval, 69437 Lyon cedex 03, France
[5] General, Organic, Biomedical Chemistry; NMR and Molecular Imaging Laboratory Université de Mons. 19 Avenue Maistriau, B-7000 Mons, Belgium; Center for Microscopy and Molecular Imaging (CMMI), 6041 Gosselies, Belgium

Abstract: Superparamagnetic iron-oxide nanoparticles (SPION) with appropriate functionalized surface have attracted a great deal of attention for their potential biomedical applications including magnetic resonance imaging (MRI) contrast enhancement, hyperthermia treatment, cell sorting, drug delivery, immunoassay and tissue repair. In all these applications, the tailoring of the SPION surface is mandatory not only to improve biocompatibility, solubility and stability but also to ensure a small particle size distribution (below 100 nm) after decoration and to preserve good magnetic properties, e.g. a high saturation magnetization. Furthermore, the steric hindrance of coating can affect the fate of NPs in biological system, such as cellular uptake and accumulation, circulation and clearance from body. Moreover, appropriate surface functionality is the perquisite for conjugating biomolecules to NPs for biomedical applications.

A dendritic approach as a coating strategy for the design of functional NPs is particularly interesting in the field of diagnostics (Figure 1). The appeal of such strategy is due to the unique properties of the dendritic structures which can be chemically tuned to reach ideal biodistribution or highly and efficient targeting efficacies. Indeed, dendrimers are macromolecules consisting of multiple perfectly branched monomers and this architecture makes them versatile constructs for the simultaneous presentation of receptor binding ligands and other biologically relevant molecules.

Keywords: SPION, Dendron, MRI, bioelimination, colloidal stability

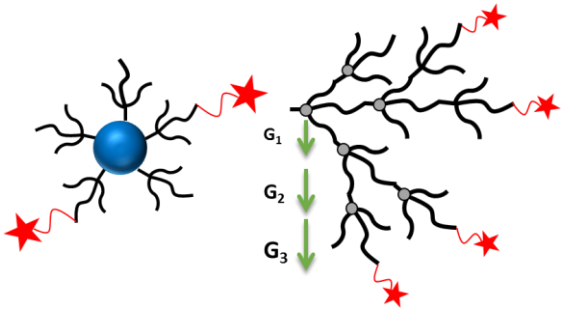

Figure 1: Figure illustrating the dendritic approach to functionalize NPs and dendritic coatings of generation 1(G1), 2 (G2) or 3 (G3)

We propose here to compare the effect of a linear ligand versus a dendritic coating of low generation (generation 1(G1), 2 (G2) or 3 (G3)) on the suspension stability, relaxivity properties and bioelimination of spherical SPION of 10 nm (NS10). NPs were synthesized by thermal decomposition and functionalized via a direct ligand exchange process.

The functionalization yielded nano-objects of 15 to 30 nm in size, stable in physiological media and showing both renal and hepatobiliary elimination.

The colloidal stability of functionalized NS10 has been evaluated in water and in different physiological media. NMRD profiles and relaxivity measurements highlighted the influence of the molecule architecture on the water diffusion close to the magnetic core thus influencing the relaxation properties at low magnetic field. Coupling of a fluorescent dye on the functionalized NS10 allowed investigating their biodistribution and highlighting urinary and hepato-biliary eliminations.

Parametric study on Fiber Bragg Grating for improvement of AE sensitivity

Ishac Kandas[1,2], Nader Shehata[1,2,3], Effat Samir[2], Hatem A. Khater[4]
[1]Department of Engineering Mathematics and Physics, Faculty of Engineering, Alexandria University, Egypt.
[2]Center of Smart Nanotechnology and Photonics (CSNP), Smart Critical Infrastructure (SmartCI) research center, Alexandria University, Egypt.
[3]Bradley Department of Electrical and Computer Engineering, Virginia Tech, United States.
[4]Naval Research & Development Department, Egypt.

Abstract: Recently, Fiber Bragg Gratings (FBGs) are attracting great attention in many applications such as underwater acoustic sensing. In this novel work, it is aimed to improve the sensitivity of FBG through analyzing relationship between the detected light power and the wavelength shift due to the applied pressure of the acoustic signal. The performance of various apodization profiles has been investigated. Among some selected apodization profiles, Cauchy profile has been proved to give the best performance. Then, by applying to different photodetectors, the results show that InGaAs detector type is more suitable than Ge one. At certain index modulation depth, a maximum wavelength shift is calculated for different lengths of FBG, after which there is no change would happen to the curve of light power and wavelength shift. These results could be applied in developing the sensitivity of acoustic sensors.

Fiber Bragg grating (FBGs) are becoming increasingly important in optical communication systems and sensing[1]. Many applications were recorded for FBGs. One of the most vital applications is sensing [2]. Either reflection spectrum or transmission one can be used as a sensing tool. For acoustic emission (AE) detection , Pizo-type sensor (PZT) can be used . Due to its many drawbacks [3], FBG becomes a promising sensor for AE. Simplicity, small size, multiplexing probability , high sensitivity [1, 3] make FBGs being better than PZT in sensing AE. The change on the pressure due to the AE would change the transmission or reflection spectrum. The shift in the FBG wavelength, λ_B is considered an indicator for the pressure change. The operational range and pressure sensitivity are the main targets to enhance the performance of FBG sensor.

First of all, the apodization profiles were tested to see which one will produce maximum sensitivity . The simulation uses uniform FBG of length 0.75 cm , and index modulation depth Δn of value 2×10^{-4}. Constant response of the photodector was
assumed. Also, constant intensity of the incident light (Fig. 1) .

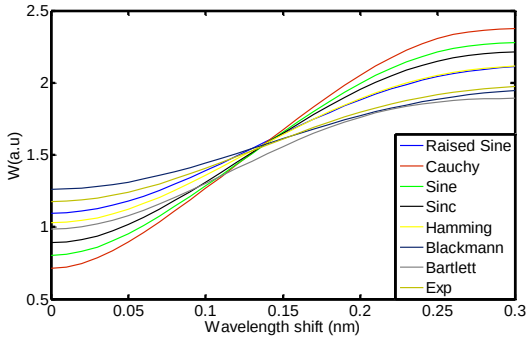

Fig. 1 The received intensity , W for different apodization profiles.

As shown , Cauchy profile is the best one as it provides the maximum slope.

Another analysis were done for different types of photodetectors at 1550 nm range . The used photdetectors are Ge, InGaAs. For all cases, the Cauchy profile is the best one. we compared the performance of the two photodetectors and the case of constant response (Fig.2). InGaAs is much better.

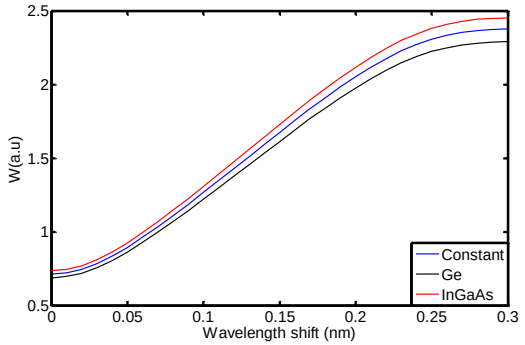

Fig.2 Response of different types of photodetectors.

It is important to calculate the maximum wavelength shift before saturation. Fig.3 shows the reflectivity for different FBG lengths.

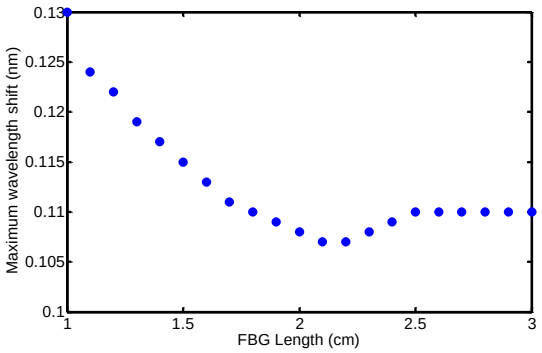

Fig.3 Maximum wavelength shift versus different lengths of FBG.

Keywords: Fiber Bragg Grating, apodization profile, photodetector, Acoustic sensor.

References:

[1] Graham Wild and Steven Hinckely, "Optical Fibre Gratings for Acoustic Sensors" Proceeding of 20th International Congress on Acoustic Sensors, ICA (2010).
[2] Xingjie Ni,Yong Zhao, JianYang, "Research of anovel fiber Bragg grating under water acoustic sensor" Sensors and Actuators A **138**, 76-80 (2007).
[3] Dae-Cheol Seo, Dong-Jin Yoon, IL-Bum Kwon and Seung-Suk Lee, "Sensitivity enhancement of fiber optic FBG sensor for acoustic" Proc. of SPIE Vol. 7294 729415:1-10 (2009).

The Power of Heterogeneity: A Systems Approach to Complex Data in Materials Science

M. Nyden,[1*] N, Williamson[1], M. Röding,[1] T. Nann[1]
[1]The Ian Wark Research Institute, Department of Information technology, engineering and the environment, University of South Australia, Adelaide, Australia

Abstract: Heterogeneity is here to stay – and will influence science even more in the future – partly because future raw materials are likely to originate from natural resources. It is a major challenge to science and technology to the point where it is difficult to consistently meet product quality standards.

We have developed a new method – a systems approach – to unlock the inherent potential of distributed data to create quantitative relationships between inputs/parameters and outputs/performances.

Previous work on quantitative correlation of distributed data is very limited[1]. The systems approach we have developed allows for the first time quantitative relationships from data that come in distributions of P(x), P(y) and P(z), rather than single values of x, y and z. It enables us to predict and optimise processes and materials and increase our fundamental understanding of heterogeneous materials. The goal is a 'grand unified theory' for dealing with distributed data, spectral data, temporal data, spatial data and more in all fields underpinned by distributed data.

Here we address effects of variable quality and heterogeneity of raw materials. More specifically we show the power of the systems approach for manufacturing of polydisperse catalytic particles and understanding relationships between diffusion and molecular weight of polymers in solution.

Keywords: Nanoscience, nanotechnology, material science, advanced manufacturing, processing, distributed data, polydispersity, heterogeneity, polymers, nanoparticles, diffusion, scaling.

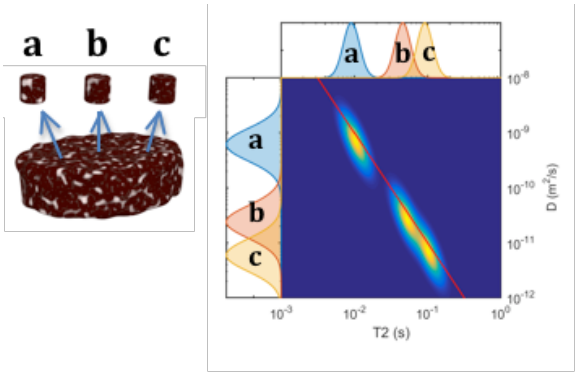

Figure 1 Six independent NMR relaxation and diffusion measurements represented on the x- and y-axes, from three subsamples a,b, and c of the same heterogeneous material, e.g. meat. Combined, the independent measurements are used to find the quantitative relationship (solid red line) between the parameters without performing time-consuming 2-d measurements (unpublished data).

References:

1. Oliva, J., Póczos, B., & Schneider, J. (2013). Distribution to distribution regression. In *Proceedings of The 30th International Conference on Machine Learning*, 1049-1057.

A facile route to synthesize rutile TiO_2 nanorods arrays via hydrothermal method

M. Guo[1, 2], Y. Gao[1], Q. Deng[3], X. Xia[1], G. Shao[2, 3*]
[1]Faculty of Materials Science and Engineering, Hubei University, Wuhan, 430062, P. R. China
[2]Institute for renewable energy and environmental technologies, University of Bolton, Bolton, BL3 5AB, UK
[3]UK-China Centre for Multifunctional Nanomaterials, Zhengzhou University, Zhengzhou 450001, China

Abstract: Hydrothermal method is a well-accepted sysnthesition method for its simple and low-cost procees as well as its rapid growth rate. Here highly-ordered, one-dimensional (1D) nanowires/nanorods arrays of rutile TiO2 were successfully grown on transparent, conductive glass substrate (FTO) by a hydrothermal method. Controllable length, diameter and density of the nanorod arrays (NRAs) were realized by adjusting hydrothermal conditions such as temperature, reaction time, concentration of reactants and type of solvent etc. The effect of these hydrothermal parameters on TiO2 nanofilms growth was discussed in detail. The density of nanorods can be adjusted by varying the volume ratio of ethanol/water, and the orientation and crystallinity of TiO2 nanofilms were enhanced with increasing dosage of ethanol. Samples with only ethanol as solvent displayed the best orientation and maximum thickness. Except for ethanol, other alcohol such as methanol, n-propanol and n-butyl were also used as solvent to investigate the role of alcohol type during hydrothermal process. It turned out that TiO2 nanofilms derived from all these alcohol solvents had the feature of morphology and single-crystal orientation similar to those prepared from ethanol. Furthermore, the areal density and degree of orientation of these samples reduced with decreasing molecular mass of the alcohol solvent. Films using ethanol as solvent possessed the optimal balance between orientation and surface morphology. Highly sensitive hydrogen sensors have been realised using self-assembled TiO_2 films.

Keywords: self-assembly, TiO2 thin films, Hydrogen sensing, hydrothermal synthesis

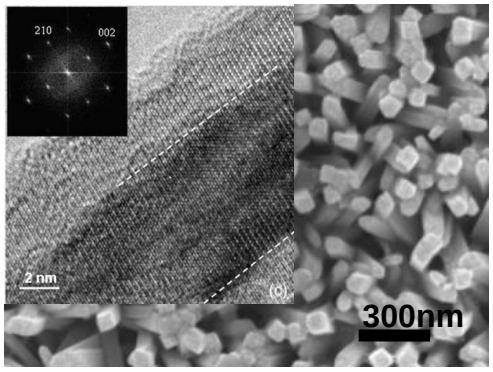

Figure 1: Morphology of typical rutile nanorod. The density of the nanorod varies with the volume ratio of ethano/water. HRTEM image exhibits high crystalinity of the nanorods, which contained clomnar subgrain boundaries. Inset shown corresponding FFT from the top subgrain.

The Effect of pH on Expanding Titanate Nanotubes & Their Use as a High Capacity Lithium-Ion Battery Electrode with High Rate Capability

A. Yürüm[1,*], M. Yarali[2], E. Bicer[3], S. Alkan Gürsel[2]
[1]Sabanci University Nanotechnology Research and Application Center, Istanbul, Turkey
[2]Faculty of Engineering and Natural Sciences, Sabanci University, Istanbul, Turkey
[3]Faculty of Pharmacy, Yeni Yuzyil University, Istanbul, Turkey

Abstract: Improvement of lithium-ion electrodes with high charge and discharge capacities is in high need especially for electronic devices and electric vehicles (Gong *et al.*, 2013). For that reaso, development of ion transport in the crystal structure is needed (Li *et al.*, 2013). The general idea is synthesizing nanometer scale particles. Reducing the particle size helps the ion diffusion in the structure (He *et al.*, 2014). Titanate nanotubes are promising materials because of their special morphology and high specific surface area. The nanotubes are formed by rolling-up of titanate nanosheets (Kasuga *et al.*, 1998). These titanates provide high rate capability and low volume expansion upon lithiation (Ren *et al.*, 2010). More importantly their tubular structure helps the transport of ions through the crystal. In this study, we synthesized titanate nanotubes and modified the interlayer distance by changing the pH. For the characterization XRD, SEM and BET (Figure 1) techniques were used. In addition, the effect of interlayer distance on energy capacity and rate capability was investigated. The shortest interlayer distance was observed at pH 4,5. Getting further away from this point, interlayer distances increased and this also increased the nanotube diameter. Conversely, specific surface area reaches its maximum value at pH 4,5. Potential-capacity profiles of TiO_2 nanoparticles showed distinct potential plateaus. Nevertheless, a very fast capacity drop was observed for TiO_2 particles. On the other hand, for titanates, broad peaks appear in CV measurements. For titanates capacities higher than 700 mAh/g were obtained. More importantly, titanates showed exceptional rate capabilities especially at wider interlayer distances due to higher mobility of ions in the structure (Figure 2). It was found that interlayer distance plays an important role in rate capability. However the material still needs some modifications to stabilize the capacity.

Keywords: expanded titanate nanotubes, pH, high capacity, high rate capability, Li-ion.

Acknowledgement. This study is supported by The Scientific and Technological Research Council of Turkey (TUBITAK): Project No. 113M575.

References:

Gong , Y. J., Yang, S. B., Liu, Z., Ma, L. L., Vajtai, R., Ajayan, P. M. (2013), Graphene-Network-Backboned Architectures for High-Performance Lithium Storage, *Adv. Mater.*, 25, 3979.

Li, L., Raji, A.-R. O., Tour, J. M. (2013), Graphene-Wrapped MnO_2–Graphene Nanoribbons as Anode Materials for High-Performance Lithium Ion Batteries, *Adv.Mater.*, 25, 6298.

He, M., Kravchyk, K., Walter, M., Kovalenko, M. V. (2014), Monodisperse Antimony Nanocrystals for High-Rate Li-ion and Na-ion Battery Anodes: Nano versus Bulk, *Nano Lett.*, 14, 1255.

Kasuga, T., Hiramatsu, M., Hoson, A., Sekino, T., Niihara, K. (1998), Formation of Titanium Oxide Nanotube, *Langmuir*, 14, 3160.

Ren, Y., Hardwick, L. J., Bruce, P. G. (2010), Lithium Intercalation into Mesoporous Anatase with an Ordered 3D Pore Structure, *Angew. Chem. Int. Ed.*, 49, 2570.

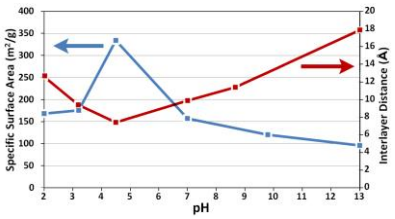

Figure 1: Surface area and interlayer distance values at various pH values: The shortest interlayer distance of 7,4 Å was observed at pH value of 4,5. Getting further away from this point, interlayer distances increased and this also increased the nanotube diameter. However, the highest specific surface area value of 334 m^2/g at was obtained at pH of 4,5.

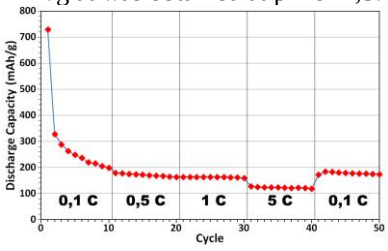

Figure 2: Rate capability test of titanate modified at pH 4,5: Potential-capacity profiles of TiO_2 (anatase) nanoparticles showed distinct potential plateaus at 1.7 and 2.2 V for discharging and charging, respectively. However, the capacity dropped from 254 mAh/g to 87 mAh/g in 10 cycles. Titanates show broad peaks appear in CV measurement. For titanates capacities as high as 750 mAh/g were obtained. More importantly, titanates showed exceptional rate capabilities especially at wider interlayer distances due to higher mobility of ions in the structure.

Preparation of Graphene Encapsulated Silicon Nanoball by CVD using Metal Coating

H. Kim,[1,2] S. Park,[2] I. Kang,[3] H. Huh[1*]
[1]Korea Institute of Industrial Technology, Thermochemical Energy System R&BD Group, Cheonan, Korea
[2]Inha University, Department of Chemistry, Incheon, Korea
[3]PuKyong National University, Division of Mechanical Engineering, Busan, Korea

Abstract: Concerning application of graphene, a lot of efforts have been made to improve performance of nanomaterials in many fields, such as electric and electronic devices. Some examples are preparation of 3-dimentional structure like nanoball or nanobubble by CVD process and hybridizing with silicone. These graphene-based materials are proven to be available for secondary battery, EMI and ACF in electronics. Especially, some research has shown that they were very effective to enhance safety and volumetric capacity when they were used as anode materials of secondary battery. Graphite or its compound with metal has been used as an anode material due to their high stability and reversibility, but it still has lower charge capacity. On the contrary, silicon is known as a material which increases the charge capacity to four times compared with carbon-based materials but it has lower stability and reversibility. For that reason, a few researchers just started to improve the charge capacity by hybridization of carbon-based material with silicon. In this study, we prepared a nanocarbon based material which had a new structure of graphene encapsulated silicon nanoball as an anode material which was applicable to high-capacity secondary battery. In order to form a graphene encapsulated silicon nanoball, metal coated silicon nanoballs was fabricated by electroless plating process. And then graphene was formed on surface of the resulting metal coated silicon nanoballs by CVD process. Finally, metal of the resulting materials was etched by hydrogen chloride. After etching process, the graphene encapsulated silicon nanoballs were formed a space between the silicon particle and the graphene, which can give more safety to volumetric change of anode during lithiation and delitiation when it applies to secondary betteries. Morphology of the graphene encapsulated silicon nanoball was observed by the field emission scanning electron microscope (FESEM) and the field emission transmission electron microscope (FETEM) to find core-shell structured nanoball. Spherical structure of graphene encapsulated silicon nanoball was investigated by the Raman, the X-ray Photoelectron Spectroscopy and the X-ray diffraction spectra to identify graphene layers on the surface of the inner silicon core.

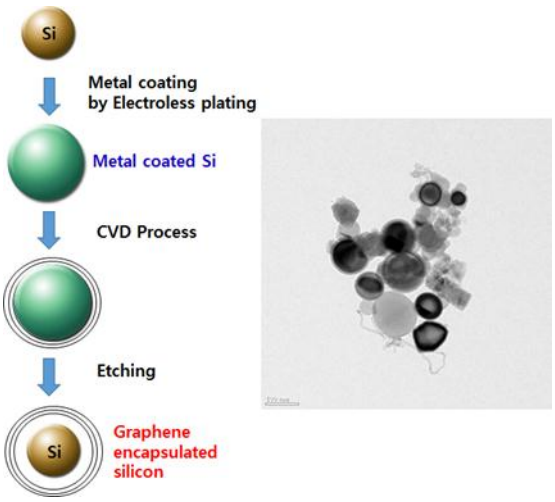

Figure 1. TEM image of graphene encapsulated silicon nanoball

Keywords: graphene, nanoball, silicon, encapsulate, CVD.

References:

Jung-Soo, L., Sun-I, K., Jong-chul, Y., Ji-Hyun, J. (2013) Chemical Vapor Deposition of Mesoporous Graphene Nanoballs for Supercapacitor, *Acs. Nano.* 7, 6047.

Seon-Mi, Y., Won Mook, C., Hionsuck, B., Hyeon-/jin, S., Inyong, S., Moon-Seok, K., Jung Jun, B., Hansu, K., Young Hee, L., Jae-young, C. (2012) Synthesis of Multilayer Graphene Balls by Carbon Segregation from Nickel Nanoparticles, *Acs. Nano.* 6, 6803.

Langli, L., Jinsong, W., Jiayan, L., Jiaxing, H., Vinayak P, D. (2014) Dynamics of Electrochemical Lithiation/Delithiation of Graphene-Encapsulated Silicon Nanoparticles Studied by In-situ TEM, *Scientific Reports*, 4, 3863.

Session III: Nano Electronics

Towards a force-displacement sensor based on vertical ZnO piezoelectric nanowires

E. León Pérez[1*], M. Mouis[2], E. Pauliac-Vaujour[1]
[1]CEA-LETI, Systems Department, F-38054 Grenoble, France
[2]IMEP-LAHC, Minatec, 3 Parvis Néel, 38016 Grenoble, France

Abstract: One-dimensional nanostructures offer a large range of potential applications in nano-electronics devices. For instance, ZnO piezoelectric nanowires (NWs) are promising elements for functionalities enhancement in nanodevices (Wang *et al.*, 2010), The implementation of these structures has been considered for high sensitivity sensors applications (Hichet *et al.*,2012) and the work presented here aims towards the full integration of these NWs within conventionnal silicon technologies in a more-than-Moore approach. In order to do so, a certain number of issues must be addressed: (i) pixel geometry, (ii) optimal pixel response collection, (iii) micro-fabrication and processing of specific materials (ZnO seed-layers) and (iv) controlled growth of NWs on processed chips.

We present the progress on finite element method (FEM) model of the full pixel architecture that provide valuable guidelines for optimal micro-fabrication. We report the parametric study of the piezo-response of one pixel as a function of the seed-layer thickness (t) and the electrode-NW spacing (d). It was found that the collection efficiency, i.e. the ratio of piezo-potentials in the electrodes and the NW, is higher for thinner seed-layers. For a perfect electrode-NW contact (d=0nm), collection efficiencies of about 60% are obtained for realistic seed-layer thicknesses (t~20nm). This value drops from 30% when electrode-NW contact is discontinued (few nm), emphasizing the small tolerance towards the contact spacing related to process variability.This study suggests the importance of fabrication variables and the nature of the seed-layers on the pixel response.
The impact of the seed-layers nature on the NWs features (e.g. average diameter, length and tilt angle) was investigated by carrying out NWs growth by hydrothermal method (Lincot *et al.*,2010) on different polycrystalline layers. We showed that chemical vapor deposited gallium-doped ZnO layers at 450°C are suitable, leading to µm long NWs and to 85 ± 23 nm and 165 ± 40 nm average diameter for template-free and localized growth (through 150nm holes spaced of 750nm), respectively.
It is shown that both FEM simulations and nanowires growth provide valuable insight for device guidelines and micro-fabrication.

Keywords: heterogeneous integration, nanowires, piezoelectricity, zinc oxide, nanodevice, simulation.

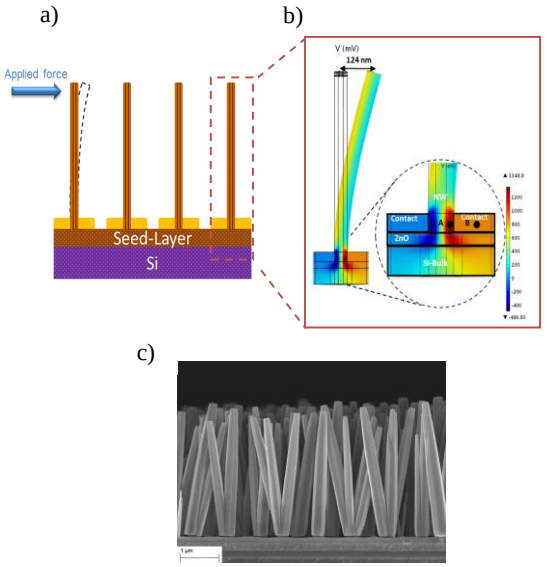

Figure 1: a) Schematic of the NW-based sensor; b) FEM simulation illustrating the mapping of the piezopotential of one pixel including one NW, two electrodes, the underlying ZnO seed-layer and a Si-substrate; and c) ZnO NWs obtained in a localized growth approach (through 150nm holes spaced of 750nm).

References:

Wang, Z. L. (2010), Piezopotential gated nanowire devices: Piezotronics and piezo-phototronics, *Nano Today, vol. 5, no.6, 540-552.*

Hinchet, R., Ferreira, J., Keraudy, J., Ardila, G., Pauliac-Vaujour, E., Mouis, M., Montès, L. (2012), Scaling rules of piezoelectric nanowires in view of sensor and energy harvester integration, *IEDM, 621-624.*

Lincot, D. (2010), Solution growth of functional zinc oxide films and nanostructures, MRS Bull., vol.35, 778-790.

Transport properties of nanoscale TFET by atomic scale simulations

U. Martinez Pozzoni, T. Markussen, A. Blom, K. Stokbro
QuantumWise A/S, Copenhagen, Denmark

Abstract: In this study we describe the transport characteristics of 2D-InAs tunnel field-effect transistors by means of atomic scale simulations. In particular, we compare results from density functional theory (DFT) using the Meta-GGA exchange correlation potential and tight-binding (TB) Hamiltonian. For the first time we show that the two methods give comparable results proving the predictive power of atomic scale simulations for this type of devices. Here, we describe the relevant theory and methodology employed. Moreover, we illustrate how one can easily modify all the important parameters of such nano devices to tune the corresponding transfer characteristic. For example, we can modify, at the atomic level, surface passivation, device geometry, doping concentration and doping regions (see figure 1a where the transfer characteristic of the 60 nm 2D-InAs p-i-n device with a 10-nm underlap region is shown), gate material (through work gate function tuning), and more. Results are analyzed in terms of I-V and transfer characteristics, real space density of states (band bending, see figure 1b), charge transfer, spectral current, effective potential across the device, as well as band structure and effective mass analysis of the nano structures employed. All calculations are performed with state of the art theories and methods as implemented in Atomistic Toolkit [1].
The research leading to these results has received funding from the European Community's Seventh Framework Programme (FP7/2007-2013) under Grant Agreement III–V-MOS Project No. 619326.

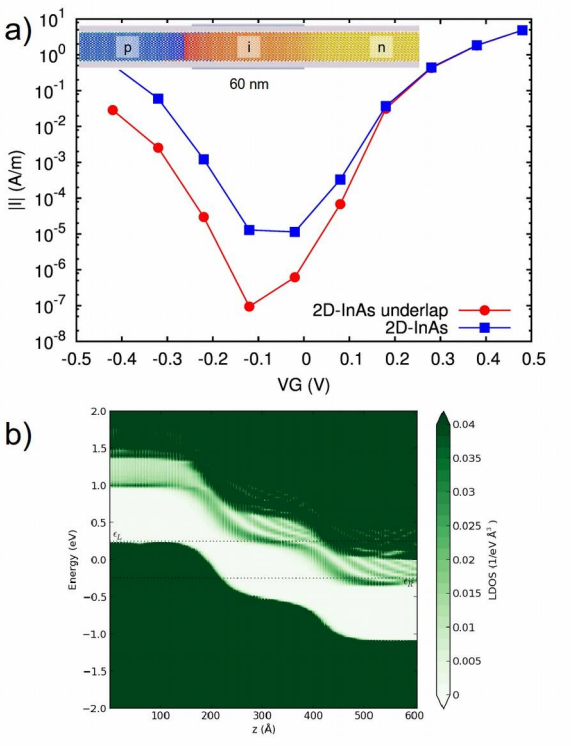

Figure 1: TFET atomistic simulation of a 2D-InAs p-i-n device: a) transfer characteristic of the device with a 20 nm and a 10 nm n-doped region, respectively. The source-drain bias is -0.5 V; b) projected local density of states across the 60 nm device

Keywords: tunnel field-effect transistor; density functional theory; tight binding Hamiltonian; InAs; atomic scale simulations;

References:

[1] Atomistic Toolkit 2015, QuantumWise A/S (www.quantumwise.com)

InAsSb based room temperature Infrared Photodetectors

Jinchao Tong, Peinan Ni and Dao-Hua Zhang*

School of Electrical and Electronic Engineering,
Nanyang Technological University, Nanyang Avenue, Singapore 639798
Email: edhzhang@ntu.edu.sg

Abstract: InAsSb based semiconductors have been attracting more attention in the recent years as they are excellent materials for midwave infrared photodetectors which have wide applications over many areas [1-5]. One of the main features of the materials is the operation at near room temperature. In this paper, we present structural and optical properties of InAsSb epitaxial layers grown on GaSb substrates by molecular beam epitaxy and their photodetection performance. X-Ray Diffraction study shows that the ternary alloys operating at mid-wave infrared range can be made almost lattice-matched to the GaSb substrate. Photoluminescence measurements reveal that the energy band gap of the InAsSb materials follows the Bose-Einstein relation better than the Varshni law. Photoconductors fabricated with this material show spectral responses ranging from NWIR to MWIR at near room temperatures. The measured Johnson-noise limited detectivity is $\sim 1.4\times10^{8}\ \mathrm{cm\cdot Hz^{1/2}W^{-1}}$ at room temperature, and it can reach $\sim 1.1\times10^{9}\ \mathrm{cm\cdot Hz^{1/2}W^{-1}}$ by decreasing the temperature to 38 K.

Keywords: Infrared photodetector, InAsSb based, detectivity.

References:

[1] M. Razeghi, *Opto-Electron. Rev*., **6**, 155 (1998).
[2] D. H. Zhang, W. Shi, *Appl. Phys. Lett*., **73**, 1095 (1998).
[3] D. H. Zhang, W. Liu, Y. Wang, X. Z. Chen, J. H. Li, *Appl. Phys. Lett*. 93 (2008) 131107.
[4] Y. Wang, D. H. Zhang, X. Z. Chen, Y. J. Jin, J. H. Li, C. J. Liu, A.T. S. Wee, Sam Zhang and A. Ramam, *Appl. Phys. Lett*. 101 (2012) 021905.
[5] X. Z. Chen, D. H. Zhang, W. Liu, Y. Wang, J.H. Li, A.T.S. Wee and A. Ramam, *Electronics Letters*, 46 (2010) 787.

Selective preconcentration within a nanoslit: one route for monitoring the biomolecule focusing front line.

F-D. Delapierre,[1,*] A-C. Louër,[1] A. Pallandre,[1] A-M Haghiri-Gosnet[1]
[1]Laboratoire de Photonique et de Nanostructures, LPN/UPR20 CNRS, route de Nozay, 91460 Marcoussis, France

Abstract: Due to the electrical double layer, a nanometric restriction in a glass microchannel acts as a selective filter for ions under specific electric field and ionic strength. The unbalanced transport between anionic and cationic species in the microsystem leads to a polarization of the ionic concentrations (Zangle *et al.*, 2009). This polarization effect provokes variations of the local ionic flow which can be canceled at some specific locations where ions are collected. This phenomenon can be used to preconcentrate biomolecules before a separation step to improve the limit of detection. Numerical simulations (Plecis *et al.*, 2008) have shown that the localization, the intensity and the stability of the preconcentration vary depending on several parameters such as the electrophoretic mobilities, the channel surface charge, the bulk composition, the ionic force, the voltage or the height of the nanochannel etc. Four different preconcentration regimes, stable or unstable, can thus be defined depending on the position of the preconcentration front line. Our experiments have demonstrated the existence of these four regimes and our capabilities to travel in the regime diagram by varying the ionic force or the voltage. Tuning these parameters, preconcentration rates as high as 10^3 have been reached after 5 minutes. Moreover, by adding a hydrodynamic pressure flow (Figure 1) (Louër *et al.*, 2013), we are also able to stabilize unstable preconcentration regimes or adjust the localization of the preconcentration front line either on the anodic or on the cathodic side of the nanochannel (Figure 2) where it is required for further step of analysis.

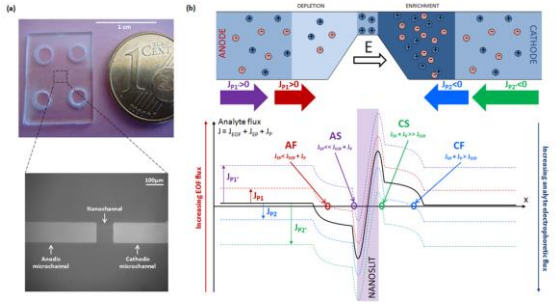

Figure 1: (a) General view of the whole pure-glass chip that integrates a 100µm-long and 150nm-deep nanochannel in a 1µm deep microchannel and (b) The mechanism of pressure-assisted preconcentration and separation. The local transport rate profile is represented in the MNM structure (flux of the analyte vs distance in the structure).

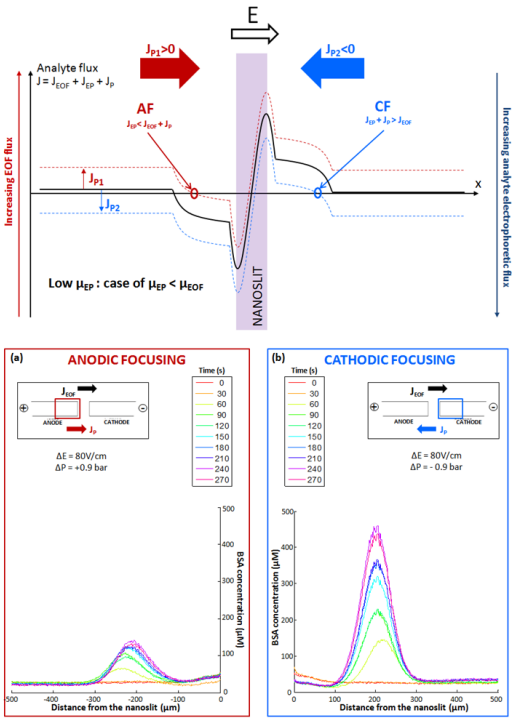

Figure 2: Two types of preconcentration for BSA: (a) Anodic Focusing (AF) when voltage and pressure are applied in the same way corresponding to an "anodic pressure" and (b) Cathodic Focusing (CF) when the two flows are opposite (case of a "cathodic pressure"). ΔE=80V/cm

Keywords: Electrophoretic flow, electroosmotic flow, ionic transport, electropreconcentration, nanochannel, nanofluidics.

References:

Zangle, T. A., Mani, A., Santiago, J. G. (2009), On the Propagation of Concentration Polarization from Microchannel-Nanochannel Interfaces Part II: Numerical and Experimental Study, *Langmuir*, 25, 3909-3916.

Plecis, A., Nanteuil, C., Haghiri-Gosnet, A. M., Chen, Y. (2008), Electropreconcentration with Charge-Selective Nanochannels, *Analytical Chemistry*, 80, 9542-9550.

Louër, A-C., Plecis, A., Pallandre, A., Galas, J-C., Estevez-Torres, A., Haghiri-Gosnet, A-M. (2013), Pressure-assisted selective preconcentration in a straight nanochannel, *Analytical Chemistry*, 85, 7948-7956.

Controlled Insulator to Metal transition in SiO_2 –TiO_2 nanocomposite containing silver nanoparticles

Tapajyoti Das Gupta1 , Joelle Corde1 , Sandrine Perruchas1 , Jean-Pierre Boilot1 , Alistair Charles Rowe1 ,Thierry Gacoin1

Ecole Polytechnique, Palaiseau, France

Abstract: Titanium dioxide is a well known semiconductor compound with exceptional dielectric, electronic and physico-chemical surface properties. These properties have been exploited in many applications such as white pigments, solar cells and photocatalysis, the latter being extensively studied for practical applications in decontamination or self cleaning devices [1]. The basic principle relies on the high redox activity of photogenerated carriers and radicals resulting from their reaction with adsorbed species at the surface of theoxide. Recently, our group developed nanostructured photocatalytic films based on the dispersion of preformed colloidal TiO nanoparticles into a surfactant template mesoporous silica binder. Such coatings were shown to exhibit exceptional self-cleaning properties. Recently, we investigated the potentiality of these film for the development of nanostructured metal-dielectric coating[2] obtained by the in-situ photoreduction of silver salts. Tunable silver volumic fraction up to 18% could be obtained by playing on the irradiation dose during the photoreduction process. Saturated films are near homogeneously filled over their entire thickness and exhibit metallic conduction properties with a conductivity of 40 S.cm properties of the nanocomposite films was also investigated, evidencing a critical volume fraction, $\varphi^* \sim 13.1$ %. The effect of mechanical stress on the electrical properties of the nanocomposite films was also investigated, evidencing a critical volume fraction, $\phi^* \sim 13.1$ %, around which the resistance changes by orders of magnitude by applying a mechanical stress. It has long been recognized that the percolative insulator-to-metal in conducting metal composites is of potential use in sensor applications because the resistance of the material changes rapidly by many orders of magnitude with small variations in the conducting particle volume fraction, φ. However, fluctuations in the composite resistance also become large at the so-called critical volume fraction, φ^*, where percolation occurs. Here we show experimentally that, in consequence, the resulting intrinsic signal-to-noise ratio for strain detection is small at φ^*. The maximum signal-to-noise ratio is obtained slightly to the conducting, metallic side of the percolation threshold[3]. Ag/silica
nanocomposites should therefore be considered as a high sensitivity, low cost composite alternative to commercially available strain gages.
Finally, the photochromic properties of these films were investigated usingpost-synthesis irradiation of silver loaded films at different wavelengths [2].

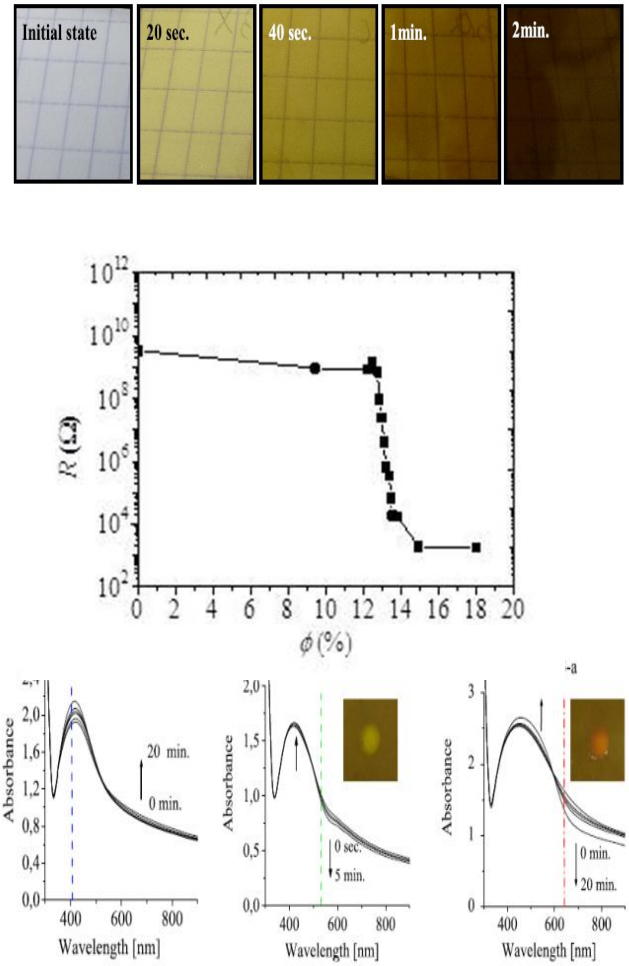

Figure (a).Images of the films subjected to different time of irradiation with UV lamp in the Ag^+ solution (b) Plots for the variation of resistance with volume fraction (c) Absorbance spectra (S1 8.2% vol; S2. 7% vol, S3 11 % vol) irradiated with laser beam at 405 nm, 532 nm and 633 nm respectively[2]

Significant changes in the plasmonic absorption spectra were explained as resulting from a local redistribution of the silver phase through irradiation.

Keywords: nanocomoposite, piezoresisitve material, photocatalysis, in-situ process, photochromic effect

References:

[1] A. Fujishima et al. J. Photochem. Photobiol. C 2000, 1, 1.
[2] J. Corde et al, Nanotechnology 23, 2012
[3] T. Das Gupta et al, Adv Funct Mater , 2014

Surface-Dominated Transport and Enhanced Thermoelectric Figure of Merit in Topological Insulator $Bi_{1.5}Sb_{0.5}Te_{1.7}Se_{1.3}$

Te-Chih Hsiung,[1,2,*] Yang-Yuan Chen [2]
[1] Department of Physics, National Taiwan University, Taipei 106, Taiwan.
[2] Institute of Physics, Academia Sinica, Taipei 11529, Taiwan.

Abstract: The recent discovery of topological insulators (TIs) has provided new route for producing low-dimensional relativistic electronic states. The exotic surface states of TIs have attracted the attention of scientists because of their fascinating physical properties and applicability in thermoelectric (TE) applications (Hsiung *et al.*; 2013, 2015).

Recently, the $Bi_{1.5}Sb_{0.5}Te_{1.7}Se_{1.3}$ (BSTS) system was confirmed to be a high-insulating bulk TI with high bulk resistivity because of the ordered occupation of Te/Se in the quintuple-layer unit, which substantially cancels the bulk carriers. In addition, the low-dimensional nanostructure with a high surface-to-volume ratio enables metallic surface conduction and TE transport properties to be efficiently probed. In this study, we selected BSTS nanowires as our target specimens and expect to observe the novel transport and TE properties therein.

We report an observation of an order of magnitude enhancement of the thermoelectric figure of merit (ZT=0.36) in topological insulator $Bi_{1.5}Sb_{0.5}Te_{1.7}Se_{1.3}$ nanowires at 300 K as compared with its bulk specimen (ZT=0.028). The enhancement was primarily due to an order of magnitude increase of electrical conductivity of the surface-dominated transport and thermally activated charge carriers in the nanowires. Magnetoresistance analysis revealed the presence of Dirac electrons and determined the Fermi level near the conduction band edge. This might be the first thermoelectric measurement of samples with a chemical potential in the gap of topological insulator without gate tuning and provides an opportunity to study the contribution of surface states to Seebeck coefficient and resistivity without concern for the complex effect of band bending.

Keywords: Topological insulators, thermoelectrics, nanowires, power factor, Shubnikov-de Haas oscillations

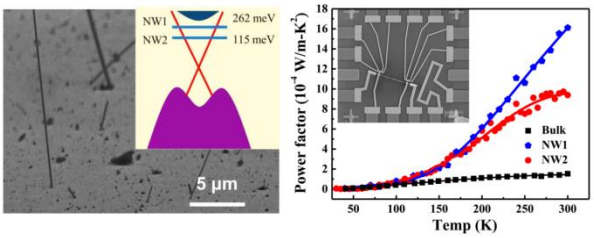

Figure 1: Thermoelectric transport measurements of topological insulator $Bi_{1.5}Sb_{0.5}Te_{1.7}Se_{1.3}$ nanowires reveal an enhancement of the thermoelectric figure of merit as compared with its bulk specimen.

References:

Hsiung, T. C., Chen, D. Y., Zhao, L., Lin, Y. H., Mou, C. Y., Lee, T. K., Wu, M. K., Chen, Y. Y. (2013) Enhanced surface mobility and quantum oscillations in topological insulator $Bi_{1.5}Sb_{0.5}Te_{1.7}Se_{1.3}$ nanoflakes, *Appl. Phys. Lett.* **103**, 163111

Hsiung, T. C., Mou, C. Y., Lee, T. K., Chen, Y. Y. (2015) Surface-Dominated Transport and Enhanced Thermoelectric Figure of Merit in Topological Insulator $Bi_{1.5}Sb_{0.5}Te_{1.7}Se_{1.3}$, *Nanoscale*, **7**, 518-523

Side-jump scattering in nanogranular Bi thin films

C. Christides,[1,*] P. Athanasopoulos,[1]
[1]Department of Computer Engineering & Informatics., University of Patras, Rion Patras 26504, Greece

Abstract: Nanogranular thin films of Bismuth with nominal thicknesses 15nm and 50nm were deposited by magnetron sputtering on Si(100)/SiN_x(100nm) substrates. Hall effect measurements between 5K and 300K reveal two conduction channels, and the observed curves (Fig.1a) of Hall resistivity $\rho_H(B)$ can be formulated as:

$$\rho_H(B) = \rho_H^{Surf} + R_\infty^{Bulk} \cdot B$$

where ρ_H^{Surf} is the intersection point with ρ_H-axis and R_∞^{Bulk} is the slope of $\rho_H(B)$ curve for B>3T, that is assigned to a bulk Hall coefficient: R_∞^{Bulk}~$(e \cdot n_{eff})^{-1}$, with n_{eff} an effective carrier concentration. The temperature dependence (Fig.1b) of film resistivity ρ_{xx}(T,B=0) varies according a fitting function:

$$\rho_{xx}(T,B=0)=\rho_{xx}(5K,B=0)e^{-(\lambda T)^n}$$

that is related to a phase coherence length $L_\Phi(T)$~T^{-n}. Fig.1b shows the fitting curves and parameters to experimental data. A connection has been revealed among $\rho_H^{Surf}(T)$, $\rho_{xx}(T,B=0)$ and $R_\infty^{Bulk}(T)$, indicating that:

$$\rho_H^{Surf}(T,B=0) \sim \rho_{xx}^2(T,B=0) \sim R_\infty^{Bulk}(T) \sim (n_{eff})^{-1}$$

Fig.1c shows a scaling relationship: $\rho_H^{Surf} = a\rho_{xx} + \beta\rho_{xx}^2 = R_S$, that is expected in case of anomalous Hall coefficient R_S. Most important is the contribution of the side-jump term: $\rho_H^{Surf} \sim \rho_{xx}^2$, that is unlikely to be due to intrinsic mechanism inside non-magnetic Bi. The origin of a: $\rho_H^{Surf} \sim \rho_{xx}^2$, term can be attributed to extrinsic contribution from a combination of surface roughness plus electronic confinement inside grains (Zhou *et al.*; 2015), and metallic edge states (Takayama *et al.*; 2015) in nanogranular structure of Bi(15nm) and Bi(50nm) films.

Keywords: granular films, Hall effect, side-jump scattering, semimetallic conductance, surface states.

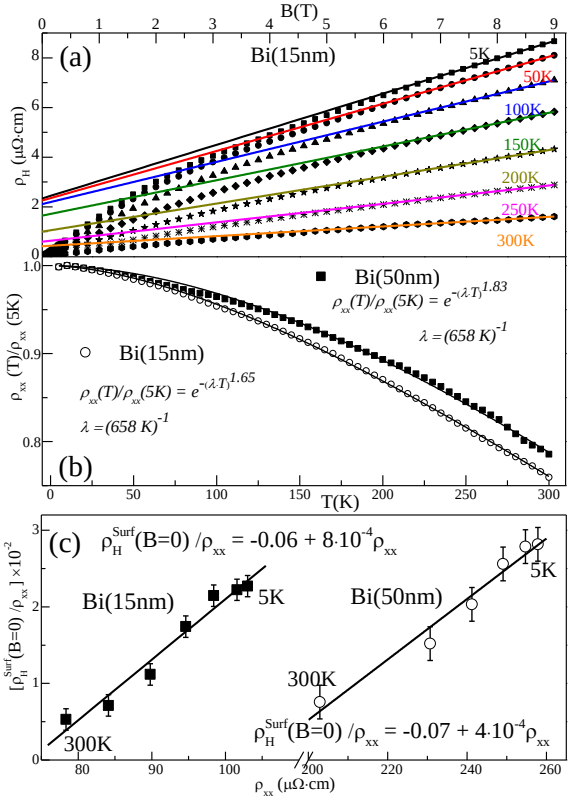

Figure 1: (a) Hall resistivity ρ_H(B) in Bi(15nm) film. (b) Normalized resistivity ρ_{xx}(B=0). (c) Scaling relationship between ρ_H(B=0) and ρ_{xx}(B=0):

The observed analogy (not shown here) of intersection points ρ_H^{Surf} (Fig.1a) and $\rho_{xx}^2(T,B=0)$ values (Fig.1b) to high-field slope values $R_\infty^{Bulk}(T)$ in $\rho_H(B)$ curves (Fig. 1a) is quite unusual and shows that the observed side-jump term cannot be attributed to magnetic susceptibility contributions that is reported in paramagnetic amorphous metals (Rhie *et al.*; 1993).

References:

Zhou, L., Grigoryan, V.L., Maekawa, S., Wang, X., Xiao, J., (2015) Spin Hall effect by surface roughness, *Phys. Rev. B* 91, 045407.

Takayama, A., Sato, T., Souma, S., Oguchi, T., Takahashi, T., (2015), One-Dimensional Edge States with Giant Spin Splitting in a Bismuth Thin Film, *Phys. Rev. Lett. 114, 066402.*

Rhie, K., Naugle, D.G., O, Beom-hoan, Markert, J.T., (1993) Side-jump effect in paramagnetic amorphous metals, *Phys. Rev. B* 48, 5973-5982.

Single-Molecule Switches Trigerred by Light,Chemical and Electrochemical Stimuli

Nadim Darwish* [a], Albert C. Aragonès, [a] Tamim Darwish, [b] Simone Ciampi [c] and Ismael Díez-Pérez [a]

[a] Departament de Química Física, Universitat de Barcelona, Diagonal 645, 08028 Barcelona, Spain and Institut de Bioenginyeria de Catalunya (IBEC) Baldiri Reixac 15-21, Barcelona, 08028 Spain
[b] Bragg Institute, Australian Nuclear Science and Technology Organisation (ANSTO), Locked Bag 2001 Kirrawee DC NSW 2232, Australia
[c] Intelligent Polymer Research Institute, University of Wollongong, Northfields Avenue, Wollongong, NSW 2522, Australia

Abstract: The concoction of chemistry, nanotechnology and electronics initiated what is known today as the field of Molecular Electronics, an intense emerging field that offers promise of replacing the current inorganic micro-sized electronics with nanoscale electronic platforms bearing active molecular components. In addition to their advantages in miniaturization, molecular electronic components provide enormous versatility to tune the electronic properties by the plethora of synthetic tailoring. Reversible single-molecule conductivity switching in response to external stimuli currently represents a major aim encouraged by the highly tunable switching capabilities offered by chemical backbones. Herin, we will present mutli-responsive single-molecule electrical switches based on incorporating phtochromic molecules between two metal electrodes using the scanning tunneling micrsocopy break-junction technique. A light pointer and/or a chemical signal can rapidly and reversibly induce the isomerization of bifunctional spiropyran derivatives in the bulk reservoir and consequently switch the electrical conductivity of the single-molecule device between a low and a high level.[1] In addition, we will present electrochemical switching of single anthraquinone molecules trigerred by electrochemical gating.[2] These studies contribute to the next limit of miniaturization of electronic components which is the realization of single-molecule electronics.

Keywords: molecular electronics, nano-scale electrical devices, single-molecule conductance, electrochemical gating, multi-responsive molecular switches, phot- and chemo-switches

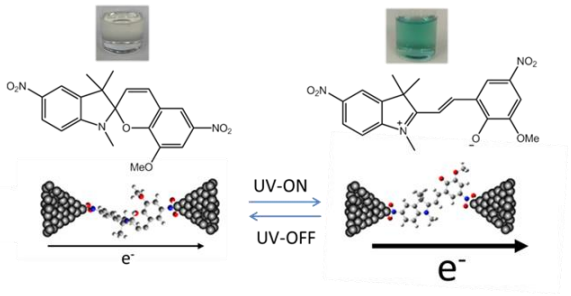

Figure 1: Figure illustrating an example of a single-molecule switching device based on the irradiation of UV-light[1].

References:

1- Darwish, N.; Aragones, A. C.; Darwish, T. A.; Ciampi, S.; Díez-Pérez, I.. Nano Letters 2014. DOI: 10.1021/nl5034599
2- Darwish, N.; Paddon-Row, M. N.; Gooding, J. J., Acc. Chem. Res. 2013, 47, 385-395.

Light emission coupling from Carbon nanotubes in silicon photonic structures

C. Alonso-Ramos[1], A. Noury[1α], E. Durán-Valdeiglesias [1], W. Zhang[1] , F. Sarti[2,3], Federico La China[2,3], H.C. Hoang[1], X. Le Roux[1], H. Yang[5], E. Cassan[1], N. Izard[1*], A. Filoramo[4], V. Bezugly[5],M. Gurioli[2,3] , L. Vivien[1+]

[1]Univ Paris 11, CNRS UMR 8622, Inst Elect Fondamentale (IEF), F-91405 Orsay, France
[2]Department of Physics, University of Florence, 50019 Sesto Fiorentino (FI), Italy
[3]European Laboratory for Non-linear Spectroscopy, 50019 Sesto Fiorentino (FI), Italy
[4] CEA Saclay, IRAMIS, NIMBE (UMR 3685), LICSEN, Bat. 125, F-91191 Gif-sur-Yvette, France
[5]Technische Universitaet Dresden, Institute for Materials Science, Dresden, Germany
[+] *Corresponding author: Laurent.vivien@u-psud.fr*

Abstract: The use of optics in microelectronic circuits to overcome the limitation of metallic interconnects is more and more considered as a viable solution. Numerous photonic building blocks compatible with CMOS fabrication tools have been developed. However, the integration of all these building blocks in the same chip is very complex and is not cost-effective due to the various materials used: Ge, Si and III-V. This drawback could be significantly overcome with the use of carbon nanotubes (CNTs). Indeed, CNTs are nanomaterials of particular interest in photonics thanks to their fundamental optical properties to emit, modulate and detect light in the wavelength range of silicon transparency. Here, we report on the comparison of the light emission coupling from CNTs into optical resonators including strip and slot ring resonators, photonic crystals and micro-disk. A theoretical and experimental analysis of the light interaction of CNTs according to the optical waveguide configurations will be carried out.

First, silicon waveguides were fabricated using classical Si process. CNTs embedded into a polymer layer were then deposited on the top of the waveguide. Figure 1 presents a theoretical comparison of the interaction between light and the strip and slot waveguide geometries, respectively.

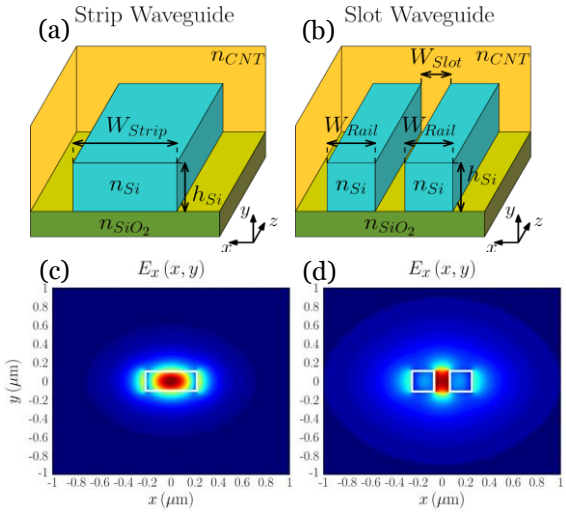

Fig. 1: Schematic views of strip waveguide (a) and slot waveguide (b). TE mode (Electric field E_x)of strip (c) and slot (d) waveguide.

As it can been seen, the optical mode in the slot waveguide is much more localized outside silicon (i.e. in the CNT layer), while for strip waveguide the mode is nearly confined inside silicon. In terms of light interaction with the CNT layer, slot waveguides are thus more promising to enhance the light coupling from CNTs. However, in terms of propagation loss, strip waveguides exhibit lower loss which induces better resonator behavior (i.e. higher Q-factors).

In conclusion, CNTs have some remarkable optical properties which could be exploited to develop a new kind of hybrid phtonics on silicon platform for a large range of applications including on-chip optical communications. We will present the latest results on the experimental demonstration of the light coupling from CNTs photoluminescence into a slot waveguide and its comparison under the same measurement conditions with a strip waveguide.

Acknowledgments
A. Noury acknowledges the Ministry of Higher Education and Research (France) for scholarship. This work has been supported by the European project FET CARTOON and by the ANR JCJC project "Ca (Re-) Lase !". The fabrication of the device was performed at the nano-center CTU-IEF-Minerve, which is partially funded by the 'Conseil Général de l'Essonne'. This work was partly supported by the French RENATECH network.

Keywords: Carbon nanotubes, silicon photonics, light emission, CMOS fabrication

Synthesis of IV-VI Transition Metal Carbide and Nitride Nanoparticles using a Reactive Mesoporous Template for Electrochemical Hydrogen Evolution

Nawal S. H. Alhajri[a], Dalaver H. Anjum[b], M. N. Hedhili[b] and Kazuhiro Takanabe[a,*]

[a] *Division of Physical Sciences and Engineering, KAUST Catalysis Center (KCC), King Abdullah University of Science and Technology (KAUST), 4700 KAUST, Thuwal, 23955-6900 Saudi Arabia.*
[b] *Advanced Nanofabrication, Imaging and Characterization core lab, King Abdullah University of Science and Technology (KAUST), 4700 KAUST, Thuwal, 23955-6900 Saudi Arabia.*

Abstract: Interstitial carbides and nitrides of early transition metals in Groups IV-VI exhibit platinum-like behavior which make them promising candidate to replace noble metals in a wide variety of reactions in particular electrocatalysis. Most synthetic methods used to prepare these materials lead to bulk or micron size powder which limit their use in catalytic applications. Attempts toward production of transition metal carbide and nitride nanoparticles in sustainable, simple and cheap manner have been rapidly increasing. In this paper we present a new approach to prepare nano-scale transition metal carbides and nitrides of group IV-VI by utilizing mesoporous graphitic carbon nitride (mpg-C_3N_4) that not only provides confined spaces for nanoparticles formation but also acts as a chemical source of nitrogen and carbon. In addition, our study shows that a whole class of transition metal carbide and nitride (IV-VI) nanoparticles with a size of 3 nm can be obtained in similar way directly through the reaction of mpg C_3N_4 with transition metal precursors under flow of N_2 at different temperatures while keeping the weight ratio constant at 1:1. The produced nanoparticles were characterized by XRD, CHN elemental analyses, TGA, nitrogen sorption, XPS, and TEM. These results confirmed that as moving from left to right (IV-VI) the transition metals have the tendency to form carbide rather than nitride.structure. The electrocatalytic activities of the produced samples were tested for hydrogen evolution reaction in acid media and the results demonstrated that molybdenum carbide nanoparticles exhibited the highest and most stable HER current in acidic media, with an onset potential of -100 mV vs. RHE, among the samples prepared in this study. This result is attributed to the sufficiently small particle size (8 nm on average) and accordingly high surface area (308 m^2 g^{-1}). The graphitized carbon layer on its surface formed by this synthesis may also function as an electronic bridge which will accordingly enhance the electronic conductivity and improve electron transfer reaction at the surface.

Keywords: transition metal carbide; transition metal nitride; nanoparticles; carbon nitride.

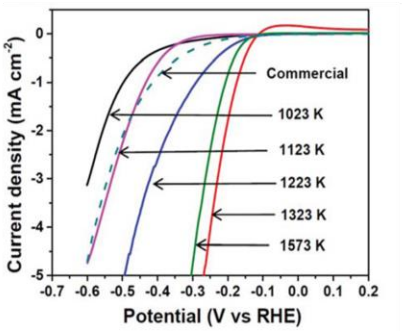

Figure 1: HER voltammograms of molybdenum carbide-carbon nanocomposites synthesized under different temperatures under N_2 flow and commercial Mo_2C.

References:

- Alhajri, N. S.; Yoshida, H.; Anjum, D. H.; Garcia-Esparza, A. T.; Kubota, J.; Domen, K.; Takanabe, K. *Journal of Materials Chemistry A* **2013**, *1*, 12606.
- Alhajri, N. S.; Anjum, D. H.; Takanabe, K. *Journal of Materials Chemistry A* **2014**, *2*, 10548.
- Garcia-Esparza, A. T.; Cha, D.; Ou, Y.; Kubota, J.; Domen, K.; Takanabe, K. *ChemSusChem* **2013**, *6*, 168.

Zinc doped InP colloidal quantum dots

N. Mordvinova[*1], A. Vinokurov[1], T Kuznetsova[1], S. Dorofeev[1], O. Lebedev[2]
[1] Lomonosov Moscow State University, Moscow, Russia
[2] CRISMAT, UMR 6508, CNRS-ENSICAEN-UCBN, 14050 Caen, France

Abstract: Quantum dots (QDs) have very wide scope of applications: in biomedicine, for the construction of photodetectors, solar cells, and electroluminescent devices among them the most interesting QD-LED displays. The II-VI QDs, for example CdSe and CdS, have been studied extensively, however have serious disadvantage – high toxicity of material, that's why another systems, such as A^3B^5-system, should be investigated. InP is a promising material for the creation of eco-friendly materials because it is more stable than II-VI materials and does not contain toxic elements, such as Cd, Hg, or Se. One of the ways to produce InP QDs is phosphine synthetic route, which allows to obtain QDs with narrow size distribution and good crystallinity but quite low photoluminescence intensity (Mordvinova *et al.*; 2014). This work is devoted to doping of InP QDs with zinc using gaseous phosphine as phosphorous precursor and myristic acid as stabylizer. We demonstrate how zinc affects the optical properties of QDs. We report the influence of different parameters (zinc amount, stabilizer, temperature and duration of synthesis) on luminescence wavelength and intensity. In addition we show that doping with zinc is accompanied with zinc-shell covering and is an effective way to improve optical properties of InP QDs.

Keywords: semiconductor nanocrystals, InP quantum dots, phosphine synthetic route, zinc doping, photoluminescence.

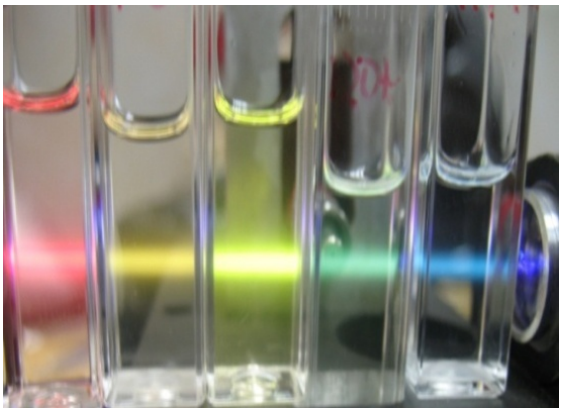

Figure 1: Luminescence of QDs with different mean diameters after postsyntetical treatment.

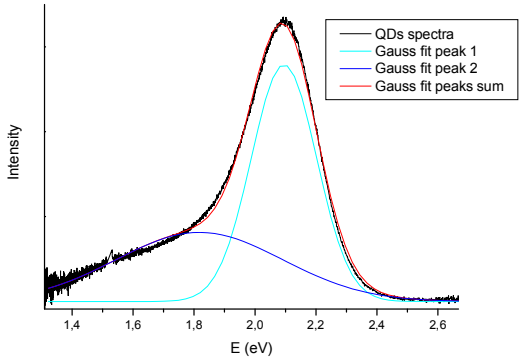

Figure 2: Typical luminescence spectra of Zn-doped QDs and its Gauss fitting.

References:

Natalia Mordvinova, Alexander Vinokurov, Sergey Dorofeev, Tatiana Kuznetsova, Konstantin Znamenkov, (2014), Phosphine synthetic route features and postsynthetic treatment of InP quantum dots, *Journal of Alloys and Compounds*, 582, 43–49.

Performance study of Phase Change Memory in Different Crossbar Architechtures

Nemat H. El-Hassan, T. Nandha Kumar and Haider A.F.Almurib
Department of Electrical and Electronic Eng.,
The University of Nottingham
Selangor, Malaysia.

Abstract: Resistive nonvolatile memories such as memristors, Magnetic Torque Junctions (MTJs) and Phase Change Memorys (PCMs) among others are considered as potentiall candidates for storage class memory, which is a new memory class presented to bridge the gab between high speed volatile memory and low dense power consuming nonvolatile memories. This class is expected to capture the desired qualities from both previous types to fulfill the growing demands of consumer electronics markt. PCM in particular poses most of desirable properties; including high density and scalabily, high operating speed, endurance and full CMOS compatibility (Nemat H. El-Hassan *et al.* 2014). Non-volatility of PCMs comes from the fact that the material exhibits a thermally induced phace change between at least two resistive states, and that the phase does not spontaneously reverse; therefore the material resistance is considered a memory element, and by placing a PCM in a crossbar architecture a very high density memory system can be achieved. Although the standard crossbar structure (Figure 1) offers high density, the sneak path (leakage) current issue effect the operation of PCM units, this effect is measured and compared between a standard nano-wire crossbar architecture and a new architechture suggested to mitigate sneak pathleakage current effects (T. Kumar *et al.* 2014). The leakage effects include operation delay, power loss and programming errors.
In this work we quantify the effects of sneak path current on a PCM based standard crossbar architechure and compare them to the modified architecture of (T. Kumar et al. 2014), in terms of; area overhead, power dissipation, delay time and reliability by using extensive simulation results and the PCM model presented by (Nemat H. El-Hassan et al. 2014)

Keywords: Phase Change; Chalcogenide; Non-Volatile Memory; Joule Heat, Crossbar, Leakage

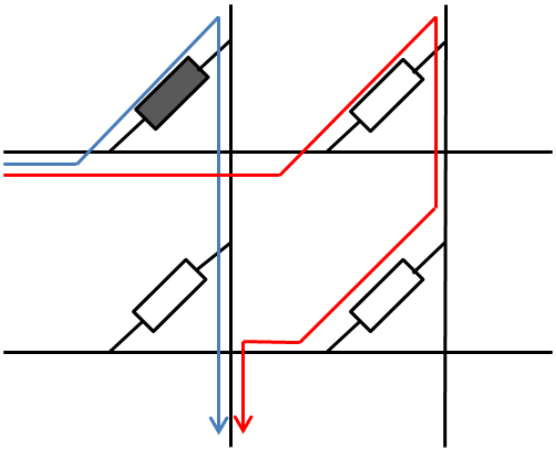

Figure 1 : Leakage currents in a crossbar architechture, the blue line is the current passing through the targeted cell (shaded), the red line is a possible leakage current path.

References:

T. Nandha Kumar, Haider A.F Almurib, Fabrizio Lombardi. (2014), A Novel Design of a Memristor-Based Look-Up Table (LUT) for FPGA In: *IEEE Asia Pacific Conference on Circuits & Systems*, 703-706.

Nemat H. El-Hassan, T. Nandha Kumar, and Haider Abbas F. Almurib. (2014), Improved SPICE Model for Phase Change Memory Cell, *5th IEEE International Conference on Intelligent and Advanced Systems*, 1- 6.

Micellar and Colloidal Dispersions of Conjugated Polymer Nanoparticles for Photoinduced Electron Transfer Applications

S. Wang, and G. Redmond,[1,]
[1]University College Dublin, School of Chemistry & Chemical Biology, Dublin, Ireland.

Abstract: We report on the preparation of aqueous dispersions of conjugated polymer nanoparticles based on poly(2-methoxy-5(2'-ethyl) hexoxy-phenylenevinylene) (MEH-PPV) by solubilisation of the polymer in the hydrophobic cores of F-127 micelles. As-prepared MEH-PPV micelles exhibit an average hydrodynamic diameter of 21 nm. Absorption, and photoluminescence excitation and emission spectral changes are observed on transfer of the conjugated polymer from a non-aqueous solvent to an aqueous micellar environment and are attributed to increased inter-chain interactions due to conjugated polymer chain collapse during encapsulation in the hydrophobic micellar cores; see Figure at right. When prepared in water, the micelles aggregate significantly over time. However, when prepared in buffer solution, the micelles exhibit good long-term collodial stability. When the MEH-PPV micelles are doped by the addition of controlled amounts of PCBM, the observed correspondence of photoluminescence emission quenching, quantum yield decreases, and emission lifetime shortening with increasing PCBM concentration indicates efficient photo-induced donor-to-acceptor charge transfer between MEH-PPV and the fullerenes in the cores of the micelles. This assignment is confirmed by transient absorption spectroscopic measurements that demonstrate that the MEH-PPV:PCBM micelles act as spatially confined donor-acceptor systems capable of successfully facilitating photo-induced charge carrier separation.

Also, we report on the preparation of aqueous dispersions of conjugated polymer nanoparticles based on the low band gap polymers APFO-3 and PCDTBT using a re-precipitation method in the absence of any surfactant additives. The resulting nanoparticle suspensions are stable over time, optically clear (not turbid), and present a characteristic purple colour associated with light absorption by the conjugated polymers. Dynamic light scattering measurements indicate average hydrodynamic diameters for the nanoparticles of approximately 36 nm (APFO-3) and 42 nm (PCDTBT). While polymer absorption and photoluminescence excitation spectra vary little on transfer from solvent solution to nanoparticle dispersion, the photoluminescence emission spectra of the nanoparticles are found to be significantly red-shifted and broadened, characteristic of increased inter-chain interactions due to conjugated polymer chain collapse in water during nanoparticle formation, resulting in the formation of a fraction of red-shifted aggregate species with energetic disorder. Likewise,

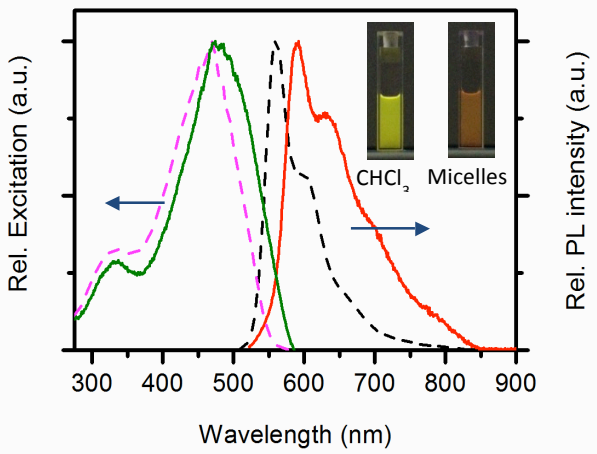

Figure: Fluorescence excitation and emission spectra acquired for MEH-PPV polymer chains dissolved in a good solvent ($CHCl_3$) and dispersed in an aqueous micellar format.

photoluminescence quantum yields and emission lifetimes decrease in the nanoparticle format, consistent with increased inter-polymer chain interactions in the nanoparticles providing more pathways for non-radiative decay of polymer excited states. Ensemble photobleaching studies indicate that the particles exhibit excellent photostabilities with nanoparticle death numbers being several orders of magnitude larger than those of typical organic dyes. Complementary single nanoparticle photoluminescence emission imaging studies highlight the multi-chromophoric nature of the polymer nanoparticles and confirm the favourable photostabilities associated with both the APFO-3 and PCDTBT nanoparticles. Finally, when the nanoparticles are doped by the addition of controlled amounts of PCBM, the observed correspondence of photoluminescence emission quenching, quantum yield decreases, and emission lifetime shortening with increasing PCBM concentration suggests efficient photo-induced donor-to-acceptor charge transfer between the conjugated polymers and the fullerenes dopants co-localised in the cores of the micelles illustrating the potential of these novel materials for application in future nanostructured bulk hetero-junction organic photovoltaic devices or in photocatalytic systems.

Keywords: nanoparticles, conjugated polymers, fullerenes, colloidal dispersions, optical spectroscopy, fluorescence, quenching, transient absorption, electron transfer, photovoltaics, photocatalysis.

Coupling between plasmonic response of supported gold particles and changes on TiO_2 band gap

S. R. Islas,[1*] R. Zanella,[1] J. M. Saniger ,[1]
[1]Materiales y Nanotecnología, Centro de Ciencias Aplicadas y Desarrollo Tecnologíco, UNAM, México, D.F.

Abstract: The supported gold nanoparticles in the visible light region exhibit a localized surface plasmon resonance (LSPR), and this defines the collective movement of conduction band electrons which is stimulated by irradiation of visible light (Garcia, 2012). Among the many factors that influence the LSPR of the Au NPs supported on TiO_2, and consequently its optical spectrum, those with higher relevance for this work are the size and shape of the NPs, the dielectric function of the surrounding NPs host and, more importantly, the gold NPs-support interactions.

The response plasmonic of the gold nanoparticles only has been used to study the metallic gold like the "ready to use" catalytic system (Zanella et al., 2004), while disregarding the influence of the activation process conditions on the final catalytic behavior. On the contrary, less studied how the nature of the gas used for thermal treatments can affect the metal-support interaction.

We study the processes of formation of gold nanoparticles *in situ* by means diffuse reflectance UV-visible spectroscopy. This study shown that this formation process in general is similar when is carried out in different atmospheres like Ar, N_2, H_2 and O_2, but the onset temperatures and final position of the plasmon band depends of the interaction between the atmosphere with the support. Moreover, it is possible attachment the changes in the band gap of the TiO_2 with the process of formation of plasmon absorption band of the gold nanoparticles. Both processes are coupled, probably mediated by charge transfer (Pacchioni G 2013, and Wang, Y.-G. et al. 2013).

Keywords: gold nanoparticles, resonance plasmon band, band gap, diffuse reflectance UV-Visible spectroscopy.

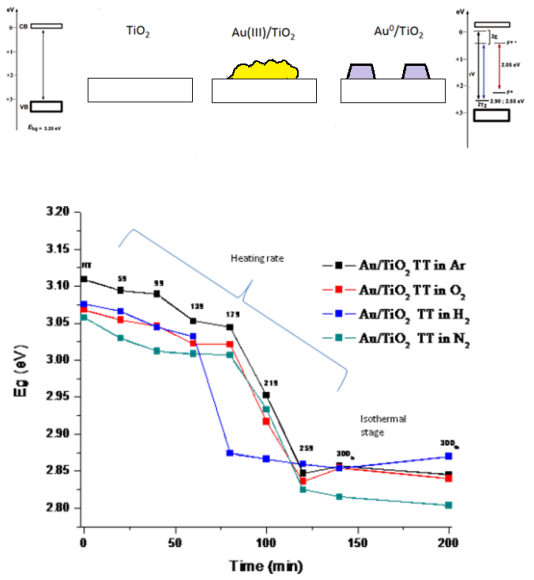

Figure 1: Figure illustrating as the changes on the supports band gap are attachment with the interaction between the gold nanoparticles and the conditions on the thermal treatment, which is by means of charger transfer process.

References:

Garcia, M. A. (**2012**), Surface Plasmons in Metallic Nanoparticles: Fundamentals and Applications. *J. Phys. D. Appl. Phys.*, *45*, 389501.

Zanella, R.; Giorgio, S.; Shin, C.; Henry, C. R.; Louis, C.,(**2004),** Characterization and Reactivity in CO Oxidation of Gold Nanoparticles Supported on TiO_2 Prepared by Deposition-Precipitation with NaOH and Urea., *222*, 357–367.

Pacchioni, G. (**2013)**, Electronic Interactions and Charge Transfers of Metal Atoms and Clusters on Oxide Surfaces. *Phys. Chem. Chem. Phys.*, *15*, 1737–1757.

Wang, Y.-G.; Yoon, Y.; Glezakou, V.-A.; Li, J.; Rousseau, R. (**2013)**, The Role of Reducible Oxide-Metal Cluster Charge Transfer in Catalytic Processes: New Insights on the Catalytic Mechanism of CO Oxidation on Au/TiO2 from Ab Initio Molecular Dynamics. *J. Am. Chem. Soc.*, *135*, 10673–10683.

Nanoplasmonics in Inorganic Nanoparticles

T. Teranishi*
Kyoto University, Institute for Chemical Research, Uji, Kyoto, Japan

Abstract: Localized surface plasmon polaritons, which are referred to simply as localized surface plasmons, are collective free carrier oscillations in nanoparticles (NPs) that are excited by incident light waves. At the NP surface, the localized surface plasmons exhibit enhanced near-field amplitudes, which are highly localized at the NP surface and decay rapidly in the dielectric surroundings. A very important aspect of localized surface plasmons is the localization of an enhanced electromagnetic field around the NPs with very high spatial resolution (subwavelength) as well as the generation of hot electrons (Teranishi *et al.*, 2011; Yang *et al.*, 2010; He *et al.*, 2012). Here I present the unique plasmonic properties of indium tin oxide (ITO) NPs (Kanehara *et al.*, 2009; Furube *et al.*, 2012) and non-stoichiometric copper sulfide nanodisks (Kanehara *et al.*, 2012; Chen *et al.*, 2015) in the near IR (NIR) region by changing the carrier (free electron or hole) density and structural anisotropy (Figure 1). In addition, as an example of plasmon-induced hot electron application, the visible-to-NIR plasmon-enhanced catalytic activity of palladium hexagonal nanoplates for the Suzuki coupling reactions is presented (Trinh *et al.*, submitted).

Keywords: localized surface plasmon, carrier density, electromagnetic field, hot electron injection, indium tin oxide, copper sulfide, palladium hexagonal nanoplate.

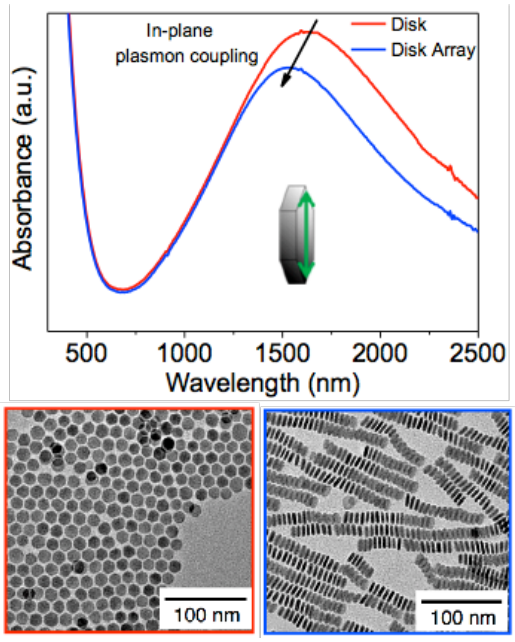

Figure 1: Change in localized surface plasmon resonance peak by aligning the Cu_7S_4 nanodisks in one dimension in $CHCl_3$

References:

Teranishi, T., Eguchi, M., Kanehara, M., Gwo, S. (2011) Controlled Localized Surface Plasmon Resonance Wavelength for Conductive Nanoparticles over the Ultraviolet to Near-Infrared Region, *J. Mater. Chem.,* 21, 10238-10242.

Yang, S., Kobori, H., He, C.; Lin, M.; Chen, H.; Li, C.; Kanehara, M., Teranishi, T., Gwo, S. (2010), Plasmon Hybridization in Individual Gold Nanocrystal Dimers: Direct Observation of Bright and Dark Modes, *Nano Lett.*, 10, 632-637.

He, C., Chen, H., Wang, C., Lin, M., Mitsui, D., Eguchi, M., Teranishi, T., Gwo, S. (2011), Far-Field Optical Imaging of a Linear Array of Coupled Gold Nanocubes at Visible Wavelengths: Direct Visualization of Dark Plasmon Modes, *ACS Nano*, 5, 8223-8229.

Kanehara, M., Koike, H., Yoshinaga, T., Teranishi, T. (2009), Indium Tin Oxide Nanoparticles with Compositionally Tunable Surface Plasmon Resonance Frequencies in the Near IR Region, *J. Am. Chem. Soc.*, 131, 17736-17737.

Furube, A., Yoshinaga, T., Kanehara, M., Eguchi, M., Teranishi, T. (2012), Electric Field Enhancement in NIR Two-Photon Absorption by Indium Tin Oxide Nanoparticle Film, *Angew. Chem. Int. Ed.*, 134, 816-819.

Kanehara, M., Arakawa, H., Honda, T., Saruyama, M., Teranishi, T. (2012), Large-Scale Synthesis of High-Quality Metal Sulfide Semiconductor Quantum Dots with Tunable Surface-Plasmon Resonance Frequencies, *Chem. Eur. J.*, 18, 9230-9238.

Chen, L., Sakamoto, M., Sato, R., Teranishi, T. (2015), Determination of a Localized Surface Plasmon Resonance Mode of Cu_7S_4 Nanodisks by Plasmon Coupling, *Faraday Dicuss.*, in press.

Trinh, T. T., Sato, R., Fujiyoshi, Y., Haruta, M., Kurata, H., Teranishi, T., Visible to Near-Infrared Plasmon-Enhanced Catalytic Activity of Pd Hexagonal Nanoplates for the Suzuki Coupling Reaction, submitted.

MoS_2 Transistors with Electrografted Organic Ultrathin Film as Efficient Gate Dielectric

H. Casademont,[1] L. Fillaud,[1] X. Lefevre,[1] R. Cornut,[1] B. Jousselme,[1] V. Derycke[1,*]
[1]CEA Saclay, IRAMIS / NIMBE (UMR 3685) / LICSEN, F-91191 Gif sur Yvette, France

Abstract: Two dimensional layered semiconductors, and in particular transition metal dichalcogenides such as molybdenum disulfide (MoS_2), have recently received increasing attention due to the combination of their unique electronic properties with their atomically thin geometry. Contrary to graphene, MoS_2 has a finite band gap of 1.2-1.9 eV (depending on the number of layers), thus complying with the requirements of digital electronic applications. To maximize the potential of MoS_2 as channel material in field effect transistors, it must be associated with an efficient gate dielectric.
Beside the mainstream CMOS technology, other fields such as large-area and/or printable electronics, sensors and display technologies could also benefit from the combination of 2D materials and new dielectrics, especially if these dielectrics present additional advantages in terms of mechanical flexibility, low temperature processes, conformability to structured substrates, cost and simplicity of equipment and processes, etc. In this respect, the development of *robust organic* nano-dielectrics and their combination with new semiconductors represent a high potential route.

In this context, we developed new dielectrics based on electrografted organic thin films on metallic electrodes. These dielectrics are produced at room temperature and under mild conditions. The process yields uniform films of nanometer thickness (4-8 nm range). In this work [1], we demonstrated the first transistors combining MoS_2 as channel material and an electrografted organic ultrathin film as gate dielectric. The transistors exhibit high I_{ON}/I_{OFF} ratio together with steep subthreshold slope as low as 110 mV/decade (Figure 1). Besides, the transfer characteristics of these transistors have no-hysteresis due to the hydrophobic and trap-free nature of our electrografted dielectric. The transistors reported in [1] were fabricated on rigid substrates and using mechanically exfoliated MoS_2. Their potential in large scale (based on CVD MoS_2) and flexible electronics will be discussed on the basis of our latest results.

Keywords: MoS_2 transistors, organic dielectrics, fluorinated diazonium salt, electrografting.

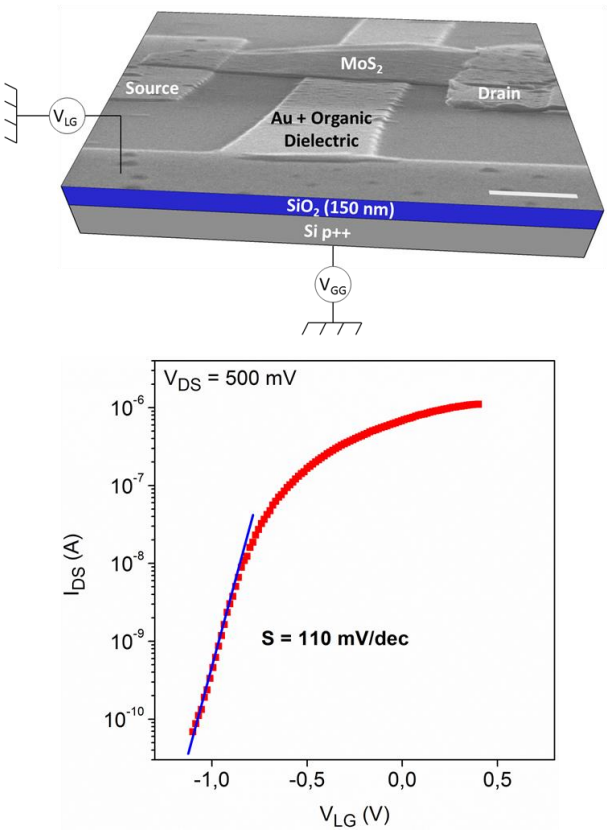

Figure 1: On top: Schematic representation and SEM image (scale bar = 500 nm) of a MoS_2 FET with an electrografted local-gate electrode. At the bottom: Transfer characteristic $I_D(V_{LG})$ measured at V_{DS} = 0.5 V and V_{GG} = 40 V of a MoS_2 FET with an organic dielectric thickness of 4 nm.

References:

[1] H. Casademont, L. Fillaud, X. Lefèvre, B. Jousselme, V. Derycke, submitted.

Nanoscale Magnetic Materials and Magnetic Nanodots for Spintronic Applications

Santanu Ghosh

Nanostech Laboratory, Indian Institute of Technology Delhi, New Delhi-16, India

Abstract: After the discovery of electron in 1911 by Robert Milikan in his famous 'Oil drop experiment', a new technology named 'Electronics' has changed the face of human civilisation. It will not be an exaggeration if the science and technology of the last century is named as an 'Era of electronics'. Starting with simple battery, galvanometer, vacuum diodes etc., now in almost all devices, equipments and home appliances, we have semiconductor based integrated electronic circuits. The saga continues till today. The entire electronics is based on a small physical quantity named as 'charge' of electron and its motion. The electron has another degree of freedom named as 'spin', which is basically an intrinsic angular momentum of an elementary particle. Although this physical entity was also discovered in early 20th century by Davisson and Germer, and theoretically interpreted by P. A. M. Dirac, we had to wait till 1986 to manipulate this in the motion of electron. This was possible because of a constant endeavour of materials scientists to grow low dimensional materials, down to few nm metallic multilayers. A concept of spin based electronics or 'Spintronics' has started with the discovery of giant magnetoresistance (GMR) by A. Fert and P. Grünberg in 1987. Since that, the scientist and technologists have realized this concept in various spin based devices, like 'spin valve', 'spin FET', 'magnetic RAM', GMR based data storage etc.

With the above introduction, and after depicting a short road map of spintronics, the following materials aspects, essential for spintronics will be addressed in this talk.

(A) Microstructure controlled RT-FM in Ni-ZnO films: Search for room temperature ferromagnetism (RT-FM) in wide band gap semiconductors has emerged as an important area of research from fundamental physics and possible applications in future spintronic devices. Room temperature ferromagnetism is observed in 200keV Ni^{+2} ions implanted with fluences of 6×10^{15} (2 % Ni) 8 $\times 10^{15}$ (3% Ni) and 2 $\times 10^{16}$ ions/cm^2 (7% Ni) on ZnO films grown on Si (100) substrate by vapour phase transport process. Experiments on this material indicate that exchange interaction between the charge carriers generated due to thermal effects of ion implantation and the localized spins of Ni is considered as main reason behind RT-FM.

(B) Extra ordinary Hall effect (EHE) and tunnelling magnetoresistance (TMR) in nanogranular films: Magnetic metal nanoparticles (NPs) embedded in dielectric media is another important material to realize spin dynamics in a controlled manner. Size, shape, uniformity of NPs is the key issues in designing devices based on these materials. In this talk, a large hall coefficient based on anomalous Hall effect in Ni NPs embedded in thin SiO_2 matrix will presented. This will be followed by tunnelling magnetoresistance effect and role of Coulomb blockade in FeCo nanoparticles in thin SiO_2 matrix. Tailoring of nanoparticles shape by ion irradiation and a novel observation on electron emission from NPs will be discussed at the end.

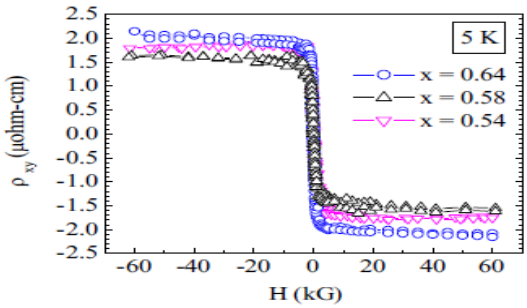

Figure 1: Extraordinary Hall effect of Ni nanoparticles embedded in thin silica matrix for highly sensitive magnetic field sensor

Keywords: (i) Magnetic semiconductor, (ii) Exchange interaction, (iii) Microstructure, (iv) Transparent ferromagnetism, (v) Extra ordinary Hall effect, (vi) Tunneling magnetoresistance.

References:

J. App. Phys. 113, 183708 (2013), (ii) J. Appl. Phys. 111 (2012) 013715, (iii) Nanoscale Research Letter (NANO EXPRESS), 2011, 6: 155, (iv) J. Appl. Phys, 109 (2011), 073914, (v) J. Appl. Phys. 107 (2010), 113913, (vi) J. Appl. Phys. 107 (2010) 023901, (vii) J. Appl. Phys. 105 (2009) 033909, (viii) Vacuum 85 (2010) 139, (ix) Rad. Eff. And def. Sol. 163, (2008) 215.

Polymer-Based Nanowires and Nanotubes: nanosources, wave-guiding

J.L. Duvail,[1,*] A. Garreau,[1] J. Bigeon,[2] N. Huby,[2] B. Bêche,[2] F. Massuyeau,[1] A. Désert,[1] S. Cordier,[3] Y. Molard,[3] E. Faulques[1]

[1]Institut des Matériaux Jean Rouxel, UMR 6502 CNRS Université de Nantes, France

[2]Institut de Physique de Rennes, UMR 6251 CNRS Univeristé de Rennes-1, France

[3]Institut des Sciences Chimiques de Rennes, UMR 6226 CNRS Université de Rennes-1, France

Abstract: One-dimensional polymer-based nanostructures such as nanowires (NWs) and nanotubes (NTs) are nowadays intensively investigated since they promote enhanced properties, as well as new paradigms for electronic, optical, optoelectronic, and photonic devices (Garreau *et al.*, 2014).

Here, we propose a review of recent developments achieved in our group with collaborations on polymer-based nanowires and nanotubes. Various polymer-based NWs and NTs were synthesized by template strategies with advanced architectures designed for improving their functionality (waveguiding, color control of photoluminescence, photoconductivity and mechanical reinforcement,…). Both conjugated polymers (CPs) and photoresists containing photoactive species (transition metal compound clusters, single-walled-carbon nanotubes SWCNTs) were involved. The focus is made on the emerging strategies for understanding and controlling the behavior of charges, excitons and photons, as well as light propagation in sub-wavelength nanostructures.

First, an original design was realized to control accurately the color of photoluminescence in organic nanostructures (Garreau *et al.*, 2013). It consists in minimizing the role of charge and energy transfer mechanisms between two types of luminophores. This was achieved by an optimized spatial separation at the nanoscale with nanowires in a coaxial geometry: a green polymeric emitter shell (poly-paraphenylene-vinylene PPV) and a red phosphorescent emitter core ($[Mo_6Br_8F_6]^{2-}$ clusters@poly(methyl methacrylate) PMMA). In addition, the choice of luminophores was motivated to get a spectral separation, i.e. distinct color of PL emission, as well as no overlapping of their absorption and emission spectral range. Thus, it is possible to anticipate and to control simply the color of the emitted light on the chromaticity diagram as an interpolation of the CIE coordinates of each luminophore. This design make possible to reach a very sharp color change within 10 nm scale. Additionally, unique proportion equal typically to 1:1 for the green and red luminophores are required.

Second, we report light injection and sub-wavelength propagation in nanotubes made of SU-8, a photoresist used for integrated photonics. Nanotubes have been rarely investigated as waveguides. However, it is a very promising geometry for highly integrated photonic devices, as shown by theoretical simulation by finite domain time-dependent (FDTD) method (Bigeon *et al.*, 2014). The features of direct light injection and subwavelength propagation regime within nanotubes were determined. The injection into nanotubes of SU8 was successfully achieved by using polymer microlensed fibers with sub-micronic radius of curvature. The propagation losses into single SU8 nanotube were determined. The attenuation coefficient has been evaluated at 1.25 dB/mm by a cut-back method transposed to such nanostructures. The mechanisms responsible for losses in nanotubes were identified in view of FDTD theoretical support.

These recent advances in polymeric based NWs and NTs contribute to open new ways for the next generation of optoelectronic and photonic integrated devices.

Keywords: Nanowires, Nanotubes, Polymer, Nano-optoelectronics, Nanophotonics.

References:

Garreau, A. Duvail, J.L., (2014), Recent advances in optically-active polymer-based nanowires and nanotubes *Advanced Optical Materials*, 2, 1122-1140

Garreau, A., Massuyeau, F., Cordier, S., Molard, Y., Gautron, E., Bertoncini, P., Faulques, E., Wéry, J., Humbert, B., Bulou, A., Duvail, J.L. (2013), Color control in coaxial two-luminophore nanowires *ACS Nano* 7, 2977–2987

Bigeon, J., Huby, N., Duvail, J.L., Bêche, B., (2014), Injection and waveguiding properties in SU8 nanotubes for subwavelength regime propagation and nanophotonics integration *Nanoscale* 6, 5309-5314

3D Simulation of DG-FinFET transistor with different channel materials and gate dielectrics

N. Boukortt[1,2,*], B. Hadri[1], L. Torrisi[2], S. Patanè[2], A. Caddemi[3], and G. Crupi[3]
[1]Department of Electrical Engineering, University of Mostaganem, 27000 Mostaganem, Algeria.
[2]Dipartimento di Fisica e Scienze della Terra, University of Messina, 98166 Messina, Italy
[3]DICIEAMA Department, University of Messina, 98166 Messina, Italy.

Abstract:

This work investigates two different structures of double gate n-FinFET in 3-D with 8 nm gate length using SiGe and 3C-SiC in the channel region, respectively. In this work, the numerical simulation tool Atlas Silvaco was used to extract novel results concerning the electrical characteristics of the device. The influence of the gate work function and the gate dielectric on threshold voltage, subthreshold slope, transconductance, DIBL, leakage current, on current, and On/Off current ratio has been investigated. This study has been performed for four different gate dielectrics which are SiO_2, Si_3N_4, Al_2O_3, and ZrO_2. We observed that the best results are obtained when ZrO_2 is used as a gate oxide material.

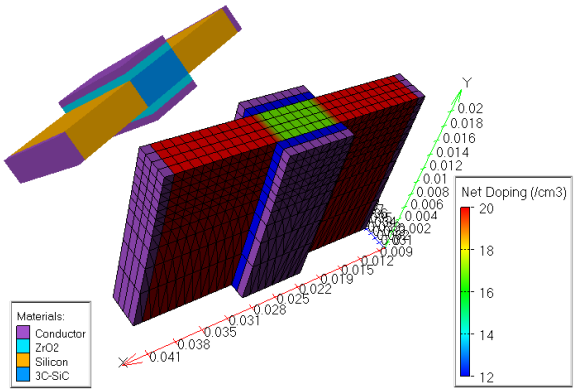

This figure illustrates the schematic structure used for our simulation. The FinFET technology is characterized by vertical silicon fins, fin length (L_g), fin height (H_{FIN}), and the silicon thickness (W_{FIN}) as shown in the figure. This study will also permit us to discuss about new multi-gate transistors (MuGFET) which enhance the performances of advanced microprocessors such as Intel Core new generation technology.

Keywords: Device scaling, Double gate MOSFET, FinFETs, High-k dielectric materials, 3C-SiC, Gate work function, Leakage current, Silvaco Software.

References:

Yakimova, R. Vasiliauskas, R. Eriksson, J. Syväjärvi, M. (2012), Progress in 3C-SiC growth and novel applications, *Mater S Forum*., 711, 3-10.

Raja, P. S. Joseph Daniel, R. Bino, N. (2012), Silicon Nanowire Based MOSFET Parameter Analysis, *IOSR-JECE.*, 3, 35-43.

Raja, P.S. Joseph Daniel, R. (2012), Effect of gate dielectric on threshold voltage of Nanoscale MOSFETS, *Int. J. Eng Res Dev*., 5, 93-104.

Shashank, N. Basak, S. Nahar, R. K. (2010), Design and Simulation of Nano Scale High-k Based MOSFETs with Poly Silicon and Metal Gate Electrodes, *Int.J. Adv Tech*., 1, 252-261.

Mohapatra, S. K. Pradhan, K. P. Sahu, P. K. (2014), Influence of High-k Gate Dielectric on Nanoscale DG-MOSFET, *Int. J. AST*., 65, 19-26.

Wong, H. Iwai, H. (2006), On the scaling issues and high-k replacement of ultrathin gate dielectrics for nanoscale MOS transistors, *Microelectron Eng*., 83, 1867-1904.

Kumar, M. Dubey, S. Kumar Tiwari, P. Jit, S. (2013), Analytical modeling and simulation of subthreshold characteristics of back-gated SSGOI and SSOI MOSFETs: A comparative study, *Curr. Appl. Phys*., 13, 1778-1786.

Lee, C. Ferain, I. Afzalian, A. Yan, R. Dehdashti Akhavan, N. Razavi, P. Colinge, J.-P. (2010), Performance estimation of junctionless multigate transistors, *Solid State Electron*., 54, 97-103.

Pradhan, K.P. Mohapatra, S.K. Sahu, P.K. Behera, D.K. (2014), Impact of high-k gate dielectric on analog and RF performance of nanoscale DG-MOSFET, *Microelectron. J*., 45, 144-151.

Rahimian, M. Orouji, A.-A. (2011), Nanoscale SiGe-on-insulator (SGOI) MOSFET with graded doping channel for improving leakage current and hot-carrier degradation, *Superlattices Microstruct*., 50, 667-679.

Key Variable Components for Enhancing Charge Transfer at PbS Quantum Dots/Porphyrin Interfaces: From Quantum Confinement to Electrostatic Interaction

A. O. El-Ballouli, E. Alarousu, O. M. Bakr and O. F. Mohammed

Solar and Photovoltaics Engineering Research Center, Division of Physical Sciences and Engineering, King Abdullah University of Science and Technology (KAUST), Thuwal, Kingdom of Saudi Arabia

Abstract: Quantum dot (QD) solar cells have emerged as a promising low-cost alternative to existing photovoltaic technologies (Pan *et al.*, 2013; Kamat *et al.*, 2013). Accordingly, understanding the interfacial charge transfer dynamics at different QD/electron-transporting material systems is necessary to optimize the solar cell performance by ensuring fast injection and separation processes, along with a long-lived charge separation state. Very recently, we have shown that only small-sized PbS QDs with a bandgap (E_g) > 1 eV can efficiently transfer electrons to phenyl-C_{61}-butyric acid methyl ester (PCBM) upon light absorption; as inferred from the ultrafast formation of the anionic species of PCBM (El-Ballouli *et al*., 2014). Nevertheless, it remains essential also to utilize larger-sized QDs efficiently for engineering multi-junction cells with broader energy harvesting capabilities; which cannot be achieved using PCBM as an electron accepting component. In this case, searching for an alternative electron accepting unit is crucial to harvest the light by large-sized PbS QDs. Here, we investigate the charge transfer and separation at PbS QDs/porphyrin interfaces using a combination of femto- and nanosecond broadband transient absorption (TA) spectroscopy and steady-state photoluminescence quenching measurements. Our results demonstrate that the ultrafast interfacial charge transfer between PbS QDs and porphyrin can be tuned by quantum confinement due to driving force variations, while maintaining the whole QD size range (E_g = 1.45-0.83 eV) effective for the electron transfer. Additionally, the charge transfer is tunable by the interfacial electrostatic interaction between the positively charged *meso* unit of porphyrin and negatively charged ligands capping the QDs. The work presented here will provide new key components to control the charge transfer processes at QD interfaces, and will thus advance both the design and the understanding of QD interfaces for solar energy technology and for other potential applications that principally rely on the interfacial dynamics such as light-emitting diodes and photocatalysis.

Keywords: semiconductor quantum dots, photovoltaics, interfacial charge transfer, ultrafast transient absorption spectroscopy.

References:

Pan, J.; El-Ballouli, A.; Rollny, L.; Voznyy, O.; Burlakov, V.; Goriely, A.; Sargent, E.; Bakr, O. (2013), Automated synthesis of photovoltaic-quality colloidal quantum dots using separate nucleation and growth stages, *ACS Nano*, 7, 10158–10166.

Kamat, P. (2013), Quantum dot solar cells: The next big thing in photovoltaics. *J. Phys. Chem. Lett.*, 4, 908-918.

El-Ballouli, A.; Alarousu, E.; Bernardi, M.; Aly, S.; Lagrow, A. P.; Bakr, O.; Mohammed, O. (2014), Quantum confinement-tunable ultrafast charge transfer at the PbS quantum dot and phenyl-C61-butyric acid methyl ester interface. *J. Am. Chem. Soc.*, 136, 6952-6959.

Room Temperature Synthesis and Characterization of Stable, Highly Luminescent PbS/CdS Core-Shell Quantum Dots with Emission Below 1100 nm

E. Durmusoglu,[1,*] P. Dagtepe,[2] Y. Turker,[3] H. Yagci Acar,[1]
[1] Koc University, Graduate School of Materials Science and Engineering, Rumelifeneri Yolu, Sarıyer, 34450 Istanbul, Turkey
[2] Kuantag A.Ş., Kısıklı Mahallesi Sarıgazi Caddesi No:65, Üsküdar, 34692 Istanbul, Turkey
[3] Koc University, Department of Chemistry, Rumelifeneri Yolu, Sarıyer, 34450 Istanbul, Turkey

Abstract: Semiconductor PbS and PbS/CdS core-shell quantum dots (QDs) have attracted a great attention due strong absorbance in the visible and emission in the near Infrared (NIR) region, mostly between 700-1600 nm. These optical properties make them a good candidate for applications such as luminescent tagging, sensors, photovoltaics and bio-imaging. Detectors used for the luminescence measurement or signal detection are actually important in terms of the sensitivity range, availability and cost. Relatively cheap and widely available silicon detectors work quite well up until 1100 nm. But, small size PbS QDs with emission below 1100 nm are scarce and are suffer from quenching. We successfully synthesized PbS QDs emitting below 1100 nm by using both lead oxide-thioacetamide and lead chloride-elemental sulfur precursor pairs with modifications to the most widely used Hines-Scholes (Hines *et al*.; 2006) and Cademartiri (Cademartiri et al.; 2006) methods.

In order to enhance the luminescence stability, we have grown a CdS shell around these small PbS crystals. Cation-exchange at room temperature was performed followed by annealing at higher temperatures for the formation of CdS shell and improvement of luminesence stability and intensity. CdS shell growth increased the luminescence intensity, stability over-time by reducing non-radiative events and reducing the surface defects. Moreover, blue shift in the emission maxima is observed with CdS deposition of the PbS which fits the emission to the sensitive range of Si-detectors.

We will discuss the influence of variables source of the PbS on the particle properties of PbS/CdS nanoparticles.

Keywords: NIR emission, lead sulfide, leadsulfide/cadmiumsulfide core-shell ,quantum dot, shell growth

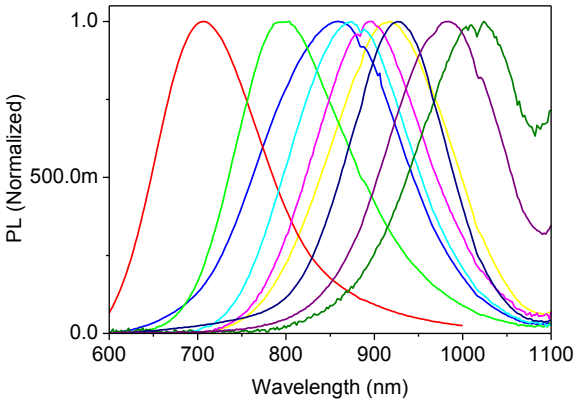

Figure 1: Emission spectrum of Different PbS/CdS quantum dots

References:

Hines, M.A., Scholes G.D., (2006). Synthesis of colloidal PbS nanocrystals with size tunable NIR emission, *Google Patents*, US 7118627 B2

Cademartiri, L., Bertolotti, J., Sapienza, R., Wiersma, D. S., von Freymann, G., & Ozin, G. a. (2006). Multigram scale, solventless, and diffusion-controlled route to highly monodisperse PbS nanocrystals. *The Journal of Physical Chemistry. B*, *110*(2), 671–3.

PANI deposited carbon cloth as binder-free electrode for symmetric supercapacitor application

M.V. Astakhov, R.R. Galimzyanov, A.A. Klimont, I.S. Krechetov, S.V. Stakhanova, O. V. Uryupina, M. Kundu*
National University of Science and Technology "MISIS", Moscow 119049, Russia

Abstract: In view of the current energy scenario and pursuit of alternative energy sources, supercapacitors (SCs) with excellent power density and superior cycling durability has positioned itself as the smartest choice for clean and efficient back up power sources and energy storage devices. The electrode material is one of the key components of a SC and to a large extent determines a SC's performance. Recently, in many reports, using nano-sized PANI with different microstructure deposited on carbon cloth a high value of gravimetric capacitance (F g^{-1}) with good cycle life has been reported (He *et al*.; 2013, and Bian *et al*.; 2012). In most of these cases, electrodes with low amounts PANI loading achieve very high gravimetric capacitance values with poor area-normalized capacitance values. But for real applications, achieving high gravimetric as well as area-normalized capacitance values is most crucial for their commercial success.

In this study, nano-structured PANI containing composite electrode based on Busofit T-040 carbon cloth (CC) with high specific surface area (900 m^2 g^{-1}) have been developed for symmetric supercapacitor devices by cost effective one step chemical polymerization of aniline. The carbon cloth consist of individual fibers of 7-8 μm diameter which are sufficiently tightly packed with random orientation (Fig. 1a). Such porous structure of carbon cloth is expected to facilitate the diffusion of electrolyte into the electrode material as well as to provide more channels for rapid ion transport. PANI uniformly deposited on the carbon surface as an individual granules whose diameter is about 30-50 nm (Fig. 1b).

The capacitive performance of CC as well as PANI/CC were characterized by the cyclic voltammetry (CV) and the galvanostatic charge-discharge in two-electrode configuration. PANI/CC demonstrates good electrochemical performance over carbon cloth in terms of weight-normalized and area-normalized specific capacitance. The weight-normalized and area-normalized specific capacitances for PANI/CC are 222 F g^{-1} and 6.66 F cm^{-2} respectively. Where as for CC these values are 120 F g^{-1} and 3.14 F cm^{-2}. The technological simplicity, easy to scale up and electrochemical performance of the PANI/CC demonstrate the significance of this work for industrial application.

Keywords: Supercapacitor, two electrode system, specific capacitance, chemical polymerization, polyaniline, carbon cloth.

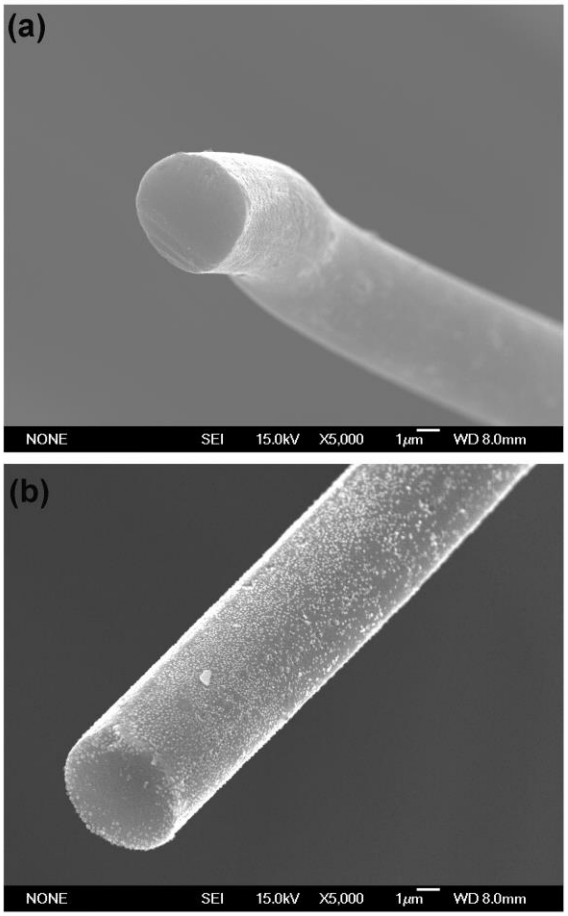

Figure 1: SEM images of CC (a) PANI/CC (b)

References:

He X., Gao B., Wang G., Wei J., Zhao C. (2013) A new nanocomposite: Carbon cloth based polyaniline for an electrochemical supercapacitor, Electrochim. Acta, 111, 210–215.

Bian L. J., Luan F., Liu S. S., Liu X. X. (2012) Self-doped polyaniline on functionalized carbon cloth as electroactive materials for supercapacitor, Electrochim. Acta, 64, 17–22.

High performance photoconductive device for UV region fabricated using graphene- n-GaN nanowire hybrid structure on Si substrate

San Kang,[1] Arjun Mandal,[1] Jae Hwan Chu,[2] Ji-Hyeon Park,[1] Soon-Yong Kwon,[2] and Cheul-Ro Lee [1]
[1]Semiconductor Materials Process Laboratory, School of Advanced Materials Engineering, Engineering College, Research Center for Advanced Materials Development (RCAMD), Chonbuk National University, Baekje-daero 567, Jeonju 561-756, Republic of Korea
[2]School of Materials Science and Engineering, Low Dimensional Carbon Materials Center, Ulsan National Institute of Science and Technology (UNIST), UNIST-gil 50, Ulsan 689-798, Republic of Korea

Abstract: This study demonstrates high performance photoconductive device to be operated in ultraviolet (UV) region consisting of graphene-n-GaN nanowire (NW) hybrid structure grown on silicon substrate with metal organic chemical vapor deposition (MOCVD) process. Raman spectroscopy and high-resolution transmission electron microscopy (HR-TEM) images confirmed the presence of monolayer graphene in the hybrid structure (Chu *et al.*, 2014). The graphene layer was not damaged after it was integrated with n-GaN NWs. The graphene layer had not only influenced the growth of defect-free, highly dense GaN NWs but also improved its material and crystalline qualities as confirmed from photoluminescence and X-ray diffraction (XRD) analyses. As a result, the graphene-n-GaN NWs hybrid structure under study represented a superior photoconductive channel with trap density much less than that of previously reported graphene-based photoconductive channels (Lee *et al.*, 2012). There was noticeable improvement in the photocurrent and photoresponsivity of the hybrid structure. Moreover, growth of the hybrid structure directly on silicon substrate and growth of n-GaN NWs without using metal-catalyst or droplet seeds added special importance to this study. Such simple, cost-effective and efficient photoconductive device involving graphene-n-GaN NW hybrid structure and utilizing the excellent electrical properties of graphene is undoubtedly a new proposal for GaN-based optoelectronics industry.

Keywords: GaN nanowires, graphene, photocurrent, photoresponsivity, ultraviolet photoconductive devices, metal organic chemical vapor deposition.

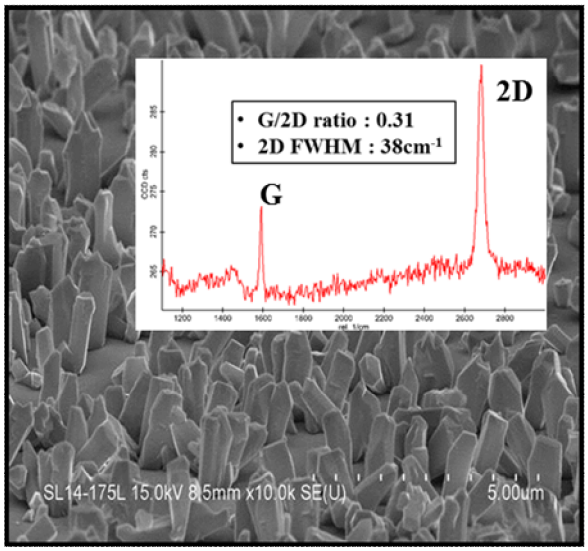

Figure 1: Field emission scanning electron microscopy (FE-SEM) image of graphene-n-GaN NW hybrid structure. FE-SEM image shows highly dense n-GaN NWs. Inset shows Raman spectroscopy of the underlying graphene layer.

References:

Chu, J. H., Kwak, J. S., Kim, S. D., Lee, M. J., Kim, J. J., Park, S. D., Choi, J. K., Ryu, G. H., Park, K. B., Kim, S. Y., Kim, J. H., Lee, Z. H., Kim, Y. W., Kwan, S. Y. (2014), Monolithic graphene oxide sheets with controllable composition, *Nat. Comm.*, 5, 3383.

Lee, H. W., Heo, K., Park, J. S., Park, Y. G., Noh, S. G., Kim, K. S., Lee, C. H., Hong, B. H., Jian, J., Hong, S. H. (2012), Graphene–nanowire hybrid structures for high-performance photoconductive devices, *J. Mater. Chem.*, 22, 8372-8376.

Transparent and flexible electrodes based on metallic nanowire networks: New nanomaterials and operating stability.

A. Cabos[1], C. Celle[1], A. Carella[1], J-P. Simonato[1]
[1]CEA-LITEN / DTNM / SEN / LSIN, 17 rue des Martyrs, 38054 Grenoble, France.
Corresponding author: anthony.cabos@cea.fr

Abstract: Transparent conductive thin films are widely used in technologies like solar cells, light-emitting diodes, and display technologies. The fabrication of transparent conductive films is currently realized with thin films of transparent conductive oxides (TCOs), and in particular indium tin oxide (ITO). The as-made ITO transparent conductors suffer from limitations like costly fabrication process and brittleness. The use of solution-processable nanomaterials, and especially metallic nanowires, appears as a promising alternative since it affords a large random two dimensional nanowire area, low-cost deposition method with high performances [1]. Among metals, silver is the more mature process, copper has merely the same properties, with another advantage, price and abundance of its.

Thanks to polyol (or hydrothermal for copper) process, metallic nanowire are synthesized in our laboratory, silver nanowire have a mean length of 10µm and a mean diameter of 60nm and copper nanowire a mean length of 128 µm and a mean diameter of 166nm (Figure 1) [2].Their dimension confers them a high aspect ratio and dispersed randomly in a substrate, threshold of percolation can be reached. Dispersed nanowires lead to a transparent and flexible electrode. Many printing techniques are available to make those electrodes in order to integrate into devices such as thermal film heater, thermochromics display or touch sensor [3] [4]. Thanks to the use of spray coating, flexible electrodes have excellent performance (i.e. $R\square<20\Omega/\square$ at T>90%), and moreover infrared go also through the electrode [1].

Figure 1: SEM pictures of silver nanowire networks for transparent flexible electrode.

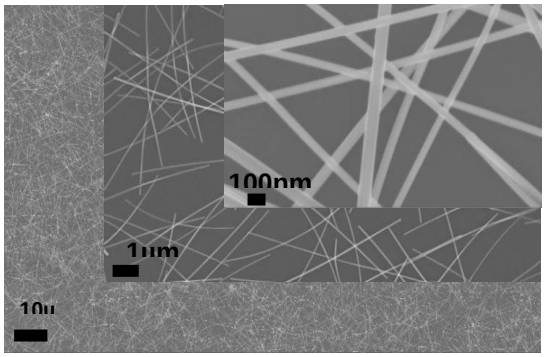

The study will be focused on stability of electrode under various stresses (electrical, environmental). Results are very promising because after three years, electrodes are stable under ambient air. More details will be given on the stability of those electrodes in operating conditions and their reaction at different stresses. Part of the study will also deal with other nanomaterials, synthesis, their performance and their stability under different environments.

Keywords: Organic, flexible and printed electronics / metallic nanowire/ transparent electrode

References:

[1] D. Langley, G.Giusti, C. Mayousse, C. Celle, D. Bellet, J.-P. Simonato, Nanotechnology, 24, 452001 (2013)
[2] C. Mayousse, C. Celle, A. Carella , J.-P. Simonato, Nano Research, 7(3) : 315-324 (2014)
[3] Celle, C., Mayousse, C., Moreau, E., Basti, H., Carella, A., & Simonato, J.-P. Nano Research, 5(6), 427–433. (2012)
[4] Mayousse, C., Celle, C., Moreau, E., Mainguet, J.-F., Carella, A., & Simonato, J.-P. (2013) 24(21), 215501.

On Low Temperature Photoluminescence of Zinc-blende CdS and Au-CdS Nanocrystals

Shital V. Kahane,[1] V. Sudarsan,[2] Shailaja Mahamuni[1]
[1]Department of Physics, SP Pune University, Ganeshkhind, Pune, India
[2]Chemistry Division, Mod Labs, Bhabha Atomic Research Centre, Trombay, Mumbai, India

Abstract: Optical studies are carried out on chemically prepared (Lin *et al*., 2006) zinc-blende CdS and core-shell Au-CdS nanocrystals (NCs) using low temperature photoluminescence (PL) spectroscopy. Contrary to the reported literature primarily discussing defect related emission in CdS, the enhancement in band edge photoluminescence intensity by 1.5 times is observed in Au-CdS core-shell NCs compared to bare CdS. Low temperature photoluminescence spectroscopic measurements reveal splitting of band edge luminescence into very sharp and narrow lines (Figure 1). PL features, as expected, clearly reveal red-shift with an increase in the temperature. Measured energy values of narrow lines fit well with the empirical Varshni equation (Hoang *et al*., 2006) revealing bulk like temperature dependence of the band gap and an intrinsic nature of CdS. The feature located at 2.96 eV (Fx), and having the highest intensity is attributed to the near band edge emission or free exciton. The feature 2.91 eV (difference of 50 meV) is due to optical phonon replica (Fx-LO) of free exciton while the one at 2.86 eV (difference of 100 meV) is Fx-2LO replica. Feature A (3.02 eV) represents the emission from second excited state ($1P_{3/2}$-$1p_e$) of CdS while B (3.10 eV) is the emission from third excited state ($1S_{1/2}$-$1s_e$) (Kim *et al.,* 2013). Shell of zinc-blende CdS on cubic Au NCs was formed. Core-shell Au-CdS NCs are studied with the aid of low temperature PL measurements. Emission from second ($1P_{3/2}$-$1p_e$) and third ($1S_{1/2}$-$1s_e$) excited state remains unaffected, while phonon replicas are perturbed in Au-CdS NCs due to change in lattice parameter along with electron-phonon interaction.

Keywords: Zinc-blende CdS nanocrystals, Au-CdS core shell nanocrystals, chemical method, low temperature photoluminescence, splitting of band edge emission, Varshni equation, optical phonons.

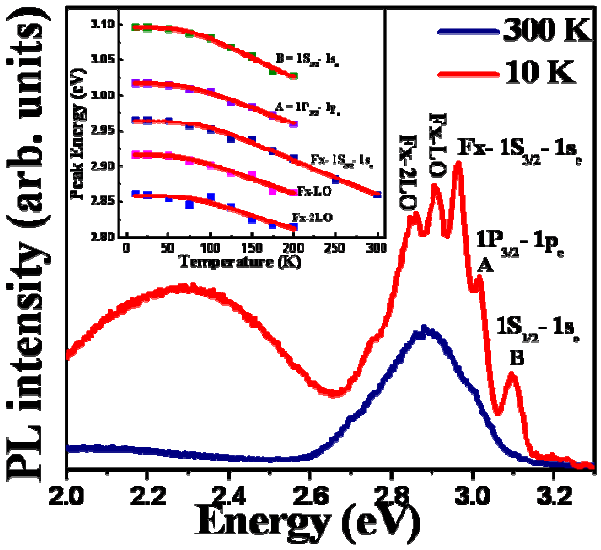

Figure 1: Room and low temperature (10 K) photoluminescnec spectra of CdS nanocrystals. Inset shows temperature dependence PL emission peaks of CdS QDs. Solid squares indicates experimental data while curve indicates calculated result using Varshni equation.

References:

Lin, H., Chen, Y., Wu, J., Wang, D., Chen, C. (2006) Carrier transfer induced photoluminescence change in metalsemiconductor core-shell nanostructures, *Appl. Phys. Lett.,* 88, 161911-3.

Hoang, T., Titova, L., Jackson, H., Smith, L., Yarrison-Rice, J., Lensch, J., Lauhon, L. (2006) Temperature dependent photoluminescence of single CdS nanowires, *Appl. Phys. Lett.*, 89, 123123-3.

Kim, Y., Jang, D. (2013) Direct observation of valence band splitting using room temperature photoluminescence of CdSnhollow submicrospheres *Chem. Commun.,* 49, 8940-8942.

Session IV : Nanotech in Life Sciences & Medicine